TÉCNICO LISBOA

Kinetic mechanism reduction methodology for secondary gas phase reactions in biomass gasification

António Rodrigues Martins

Thesis to obtain the Master of Science Degree in

Mechanical Engineering

Supervisors: Prof. Miguel Abreu Almeida Mendes
Dr. Raquel Inês Segurado Correia Lopes da Silva

Examination Committee

Chairperson: Prof. José Manuel da Silva Chaves Ribeiro Pereira
Supervisor: Prof. Miguel Abreu de Almeida Mendes
Members of the Committee: Prof. Luís António da Cruz Tarelho
Eng. Ana Isabel Marques Ferreiro

October 2021

ACKNOWLEDGEMENT

Agradeço ao Professor Miguel Mendes, à Mestre Ana Isabel Ferreiro e à Doutora Raquel Segurado por todo o apoio, a compreensão e o ambiente positivo que me proporcionaram ao longo dos últimos meses na minha jornada final para me tornar mestre em engenharia mecânica.

Em particular, gostaria de deixar um agradecimento muito especial à Mestre Isabel Ferreiro, que foi de facto uma mentora excecional e sem a qual este meu percurso teria sido com certeza menos proveitoso. Foi sem dúvida um pilar no meu trabalho e aprendizagem, mostrou sempre uma abertura para discutir os temas em questão e sempre com boa disposição e com uma abordagem fantástica que me deram forças para ultrapassar naturais obstáculos que se apresentaram durante este meu trabalho. Foi claramente, para mim, a criação de um laço de amizade que é das coisas que mais valorizo. Por tudo isto, e mais uma vez, um grande e sentido obrigado Isabel.

Também uma palavra de agradecimento particular também para o Professor Miguel Mendes e para a Doutora Raquel Segurado, que sempre me ajudaram a alcançar os resultados pretendidos e até a ir mais além. As vossas orientações, sempre serenas e clarividentes, foram importantíssimos durante o meu percurso, sendo que a boa disposição nas nossas reuniões me ajudaram também a apreender os conhecimentos que me passaram de uma forma bastante produtiva. Muito obrigado por toda a vossa ajuda.

Gostaria ainda de agradecer aos meus amigos Manuel Domingues, Dário Antunes, Nuno Sousa, Tiago Azevedo, Tiago Ferreira, João Marques, João Verdasca, Diogo Lucas, Tiago Costa, Joaquim Verdasca, João Abreu e Armando Henrique por todo o convívio e momentos fantásticos que tive convosco nestes últimos anos. Sem vocês até podia ter alcançado os meus objetivos neste percurso escolar, mas a jornada nunca teria sido tão boa.

Em último lugar, gostaria de agradecer aos meus pais, que me proporcionaram a oportunidade de estudar e tirar um curso superior, e também por todo o seu apoio e carinho. Tive a sorte de ter um pai e uma mãe fantásticos que me educaram, que me proporcionaram muitas experiências e me transmitiram valores fundamentais para poder percorrer tranquilamente esta minha jornada escolar. A vocês, um obrigado de um filho sortudo.

RESUMO

A gasificação da biomassa é um processo de geração de energia amplamente reconhecido como uma tecnologia eficiente e sustentável, representando uma alternativa viável à queima de combustíveis fósseis. No entanto, a formação de alcatrões e impurezas durante a gasificação da biomassa levanta a necessidade de aprimorar o processo de gasificação a fim de eliminar esses produtos indesejados e melhorar a eficiência do processo. A modelação numérica é uma solução atrativa para realizar análises detalhadas do processo de gasificação a fim de encontrar possíveis soluções para este problema. Apenas um número reduzido de estudos disponíveis na literatura apresenta mecanismos altamente detalhados que são capazes de prever com precisão o comportamento cinético da gasificação. No entanto, esses modelos são extremamente complexos e envolvem longos tempos computacionais. O principal objetivo deste trabalho é propor um mecanismo reduzido que seja capaz de prever as reações secundárias da fase gasosa durante a gasificação da biomassa. Um método de busca e uma técnica de eliminação de espécies e reações baseada em estimação de erros são aplicados a um mecanismo detalhado que simula as reações secundárias de gasificação com 134 espécies e 4533 reações, mantendo suas características essenciais. Finalmente, o mecanismo reduzido selecionado é validado comparando os resultados obtidos com os dados do mecanismo original. O método de redução aplicado neste trabalho conseguiu obter mecanismos reduzidos capazes de prever com precisão a fração de gás nos produtos finais, a composição final do gás e as curvas de libertação de H_2, CO e CO_2 do mecanismo inicial detalhado, juntamente com o tempo de computação significativamente reduzido. Um mecanismo com 89 espécies e 476 reações é um dos mecanismos obtidos no processo de redução que possui as características mencionadas na frase anterior, com uma redução no tempo computacional de 52,91%. A análise de sensibilidade realizada aos componentes da biomassa provou que este mecanismo reduzido pode ser utilizado para vários tipos de biomassa.

Palavras-Chave: gasificação de biomassa, reações secundárias de fase gasosa, modelação cinética, redução de mecanismos.

ABSTRACT

Biomass gasification is an energy-generating process widely recognized as an efficient and sustainable technology, representing a viable alternative to the burning of fossil fuels. However, the formation of tars and impurities during biomass gasification raises the necessity of enhancing the gasification process in order to eliminate these unwanted products and improve the efficiency of the process. Numerical modelling is an attractive solution to perform detailed analysis to the gasification process in order to find possible solutions for this problem. A few studies available in the literature present highly detailed mechanisms that are able to accurately predict the gasification kinetic behavior. However, these models are extremely complex and comprise long computational times. The main objective of this work is to propose a reduced mechanism that is able to predict the secondary gas-phase reactions during biomass gasification. A scanning method and an error-based species and reactions elimination technique are applied to a detailed secondary gas-phase mechanism with 134 species and 4533 reactions, maintaining its essential characteristics. Finally, the selected reduced mechanism is validated by comparing the obtained results with the data from the original mechanism. The reduction method applied in this work is found to effectively obtain reduced mechanisms capable of accurately predicting the gas yield, final gas composition and H_2, CO and CO_2 release rate curves of the initial detailed mechanism together with significantly reduced computation time. A mechanism with 89 species and 476 reactions is one of the mechanisms obtained from the reduction process that has the characteristics mentioned in the previous statement, with a computational time reduction of 52.91%. The sensitivity analysis carried out on the biomass components proved that this reduced mechanism can be used for a wide range of biomass fuels.

Keywords: biomass gasification, secondary gas-phase reactions, kinetic modeling, mechanism reduction.

TABLE OF CONTENTS

LIST OF FIGURES

LIST OF TABLES

NOMENCLATURE

Symbols

A	Pre-exponential factor (s^{-1})
A_p	Particle Area (m^2)
C_D	Drag Coefficient
c_p	specific heat (J/kg.K)
d	diameter (m)
E	Activation Energy (cal/mol)
g	gravity (9.8 m^2/s)
H	Hydrogen
k	reaction rate (s^{-1})
m	mass (kg)
N	Number of error contributions
N	Nitrogen
n_m	mole (mol)
n	reaction order
O	Oxygen
P	Pressure (Pa)
p	particle
$\dot{Q}$	Heat generated (W)
R	Ideal Gas Constant (8.314 J/mol.K)
S	Sulfur
S/B	Steam to biomass ratio
T	Temperature (ºC)
t	time (s)
U	Fraction
V	Volume (m^3)
v	velocity (m/s)
X	Char conversion (wt.%)
Y	Mass fraction
M_w	Molecular weight (kg/kmol)
ΔH	Heat of reaction (kJ/Kmol)

Greek Letters

β	Temperature exponent in the Arrhenius Law
δ	Error
ε	Emissivity
λ	Thermal conductivity (W/m.k)

λ	Excess air coefficient
μ	Dynamic viscosity (kg/m.s)
σ	Stefan-Boltzmann constant (5.67x 10^{-8} J/s.m^2.K^4)
ρ	Density (kg/m^3)
ω	Net mole production (kmol/m^3)

Acronyms

3PM	Three parallel model
CCE	Carbon conversion efficiency (%)
CELL	Cellulose
CS	Carbon in syngas
CV	Calorific value (MJ/Nm^3)
daf	dry, ash free
db	dry basis
DP	Degree of polymerization
gas	Gasification
gen	generated
GY	Gas yield
HAB	Herbaceous and agricultural biomass
HAS	Herbaceous and agricultural straws
HCE	Hemicellulose
LHV	Low heating value (MJ/Nm^3)
LIG	Lignin
MPFA	Path flux analysis with multi generations
MPFASA	Path flux analysis with multi generations and sensitivity analysis
Nu	Nusselt number
pyr	pyrolysis
Re	Reynolds number
rx	reaction
SA	Sensitivity analysis
sp	Specie
TANN	Tannins
TGL	Triglycerides
UT	Unconverted tars
VP	Volumetric percentage
WS	Wheat straw
WWB	Wood and woody biomass

1. INTRODUCTION

1.1. MOTIVATION

The increased awareness of the risks of burning fossil fuels and their potential devastating consequences has turned the world's attention to alternative, renewable and clean energy sources such as wind, solar, geothermal and bioenergy [1]. Bioenergy is the energy that is generated from organic matter, known as biomass. It is considered that both biomass and its respective biofuels do not contribute to enhance greenhouse effect, as the released carbon dioxide originated from the thermochemistry processing of the biomass is balanced with the absorption of that same carbon dioxide during the flora live span [2]. Therefore, the focus on bioenergy has been increasing over the last years, as it is a valuable means to face global warming. However, the growing worldwide use of bioenergy does not come without significant risks. An uncontrolled and unsustainable acquirement of the bioenergy primary energy sources (biomass, biofuel) can lead to degradation of land and ecosystems, reduce food security and actually increase the greenhouse gas emissions. A general perspective of a sustainable bioenergy usage is presented in Figure 1. A viable means to support the implementation of these sustainable politics regarding bioenergy is to enhance biomass-to-energy conversion techniques, which can be achieved by increasing the efficiency of thermochemical conversion processes [3].

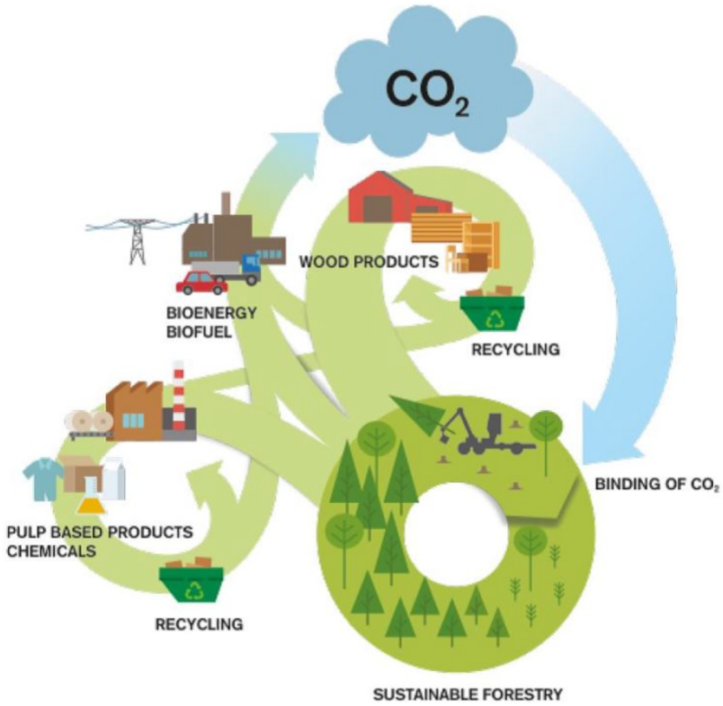

Figure 1.1. Sustainable bioenergy usage [4].

Gasification is a thermochemical process that is able to convert solid biomass into gaseous products (producer gas) that can be further used in energy-generating processes or

synthesized into other value-added chemicals [5]. Gasification is a multistage process that includes different stages, i.e., drying, pyrolysis, partial oxidation or combustion, cracking and char reduction. In particular, pyrolysis, that has great importance in gasification, is a thermal treatment that decomposes organic materials into liquid, solid (char) and gaseous (light permanent and combustible gases) forms in the absence of oxygen [6]. The liquids released from biomass pyrolysis include H_2O, low weight molecular species and tars. Tars are heavy hydrocarbons that represent one of the utmost challenges in industrialization of biomass gasification infrastructures, since these components are often converted into impurities/particles [7] that lead do the necessity of producer gas (syngas) treatment after the gasification process, as represented in Figure 1.2. An efficient way to mitigate these occurrences is enhancing the gasification processes, where tars can be reformed under the presence of oxidizing atmospheres. It is still a challenge to operate gasifiers using biomass as feedstock and often suboptimal results are delivered. In this sense, numerical modelling is a very attractive solution to overcome these barriers [8].

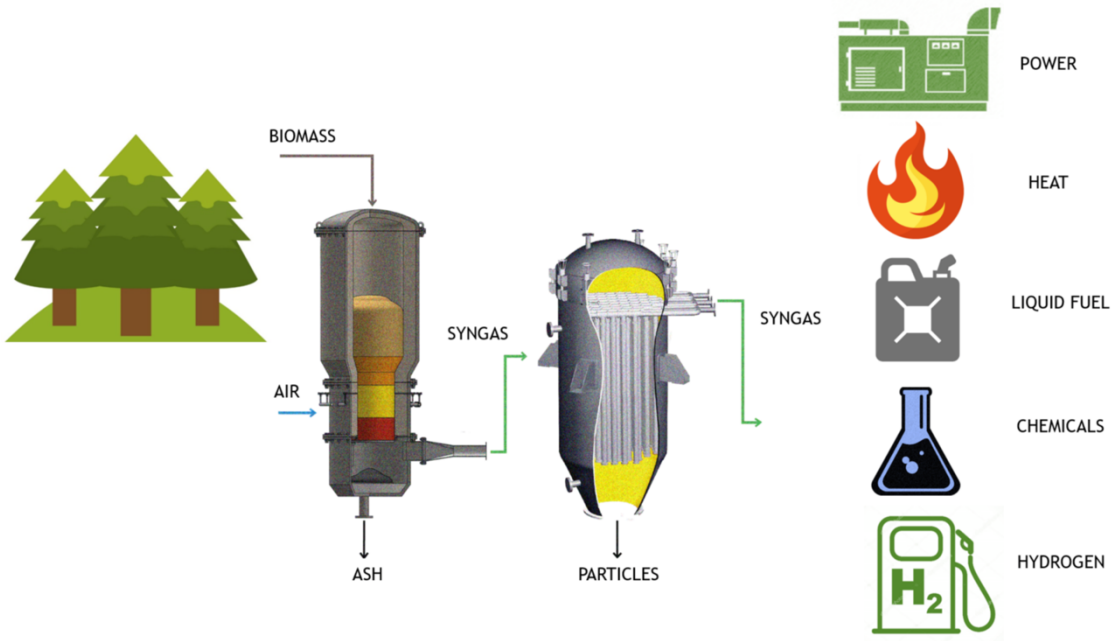

Figure 1.2. Energy flow in gasification process [9].

Gasification modeling is a highly complex process that can include variables such as reactor characteristics, kinetic mechanisms (involving primary and secondary reactions) and feedstock properties [10]. Kinetic mechanism schemes of biomass gasification are crucial to define the progress of the decomposition-reaction paths and to evaluate the dependence of the rate of progression on process parameters [11]. A few studies have considered very detailed mechanisms that are able to predict release rate curves, product yields and product speciation under different gasification uses [11–14]. However, these models often comprise long computational times and chemical stiffness. Within this perspective, applying reduction

methodologies is highly recommended to reduce detailed kinetic mechanisms while keeping their essential features [15].

1.2. PREVIOUS STUDIES

A number of studies regarding reduction methods that present promising results are already present in the available literature [16–18]. A summary of those studies is presented in Table 1.2. Although the general approach implemented in the different studies is significantly different, the mathematical tools used in each case are fairly similar. These tools cover sensitivity analysis, path flux analysis and scanning methods on both species and reactions, in order to obtain their importance in the mechanism. Chang et al. [16] implemented a hierarchical approach based on the global sensitivity analysis of reaction classes and sub-mechanisms present in the initial detailed mechanism, also using the path sensitivity analysis in multiple steps along the reduction process of a detailed iso-cetane mechanism. The dominant sub-mechanisms and the most important reaction classes, which are the ones that have a larger impact (larger sensitivity coefficient) in the behavior of the mechanism, are firstly identified. Afterwards, reactions in the unimportant sub-mechanism and isomers of the dominant classes in fuel-specific sub-mechanisms are lumped and the less important reactions are eliminated. Lastly, an optimization procedure was implemented to widen the range of temperatures on which the final reduced mechanism can be successfully applied. Wang et al. [17], used both a path flux and sensitivity analysis to efficiently reduce two highly detailed mechanisms: GRI-Mech 3.0, used to simulate methane combustion and an n-heptane combustion mechanism, focusing on species elimination (elimination of all reactions where a specie was a product and/or a reactant) rather than direct reaction elimination. Starting with a group of pre-selected species established as essential to the detailed mechanism, a path flux analysis was used to assess the relation between each specie in the mechanism and the pre-selected ones. Through this method, less important species were identified and eliminated, and an initial skeletal mechanism was obtained. Afterwards, a sensitivity analysis was carried out to identify the redundant species present in the skeletal mechanism, reducing it even further. The final skeletal mechanism was successfully validated for a wide range of operating conditions. Petzold et al. [18], used a scanning method as the main approach for the mechanism reduction. The two highly detailed mechanisms used to test the validity of the reduction methodology were the GRI-Mech 1.2, which accurately simulates methane combustion, and the Exxon model, which contains a detailed set of gas-phase radical reactions. Firstly, the scanning method is applied to the species. This method consists of deleting the species one by one and comparing the resultant solution without the eliminated specie with the one obtained with the reference mechanism. Species with smaller errors are eliminated and a reduced mechanism is created. Afterwards, the same method is applied to the reactions and a further reduced mechanism is obtained. As mechanisms often present a larger number of reactions than of species, the scanning method is firstly applied to the species as it is less computationally expensive than applying it firstly to the reactions. Finally, an optimization process is conducted

for the reduced mechanism in order to reduced it further to its final form. The reduced mechanism was expected to give accurate results for a limited range of initial conditions.

The reduction methodology presented by Chang et al. [16] was found extremely efficient. However, it is highly complex and does not contain in its methodology direct elimination of species, which is simple and effective means of drastically reducing the computational time. On the other hand, the approach used by Wang et al. [17] focused only on species reduction, without single/direct reaction elimination, since the tools used in the study required significant computational cost if applied to the reactions, which limits the number of reactions that can be eliminated. Finally, Petzold et al. [18] presented a simple and effective reduction methodology capable of significantly reducing large detailed mechanisms while keeping their initial features. However, a major drawback of this method is that the reduced model obtained is expected to work only for operating conditions close to the ones used in the reduction process, which significantly limits the utility of the reduced mechanism.

The gasification of biomass is a process that can take place within a wide range of operating conditions regarding the type of biomass, temperature, type and quantity of gasifying agent and residence time [19–24]. Ku et al. [24] found that the type of gasifying agent chosen greatly affects the outcome of the gasification process (Table 1.2). It was found that the ideal values of excess air (ratio between the introduced air and the stoichiometric air) were typically between 0.33 and 0.63 for temperatures between 900-1500 K, according to Jangsawang et al. [25]. These ideal points are obtained from the analysis of the cross over points between the amount of CO and CO_2 present in the reactor during the gasification process. The cross over point, also called carbon boundary point, represents the point where the fuel has reacted with the exact amount of oxygen so that gasification is complete and no solid carbon formation occurs [26], as shown in Figure 1.3. According to the literature (Table 1.2), the range of temperature values considered for biomass gasification is set between 700 ºC and 1400 ºC, whereas the steam to biomass ratio values studied vary from 0 to 2.

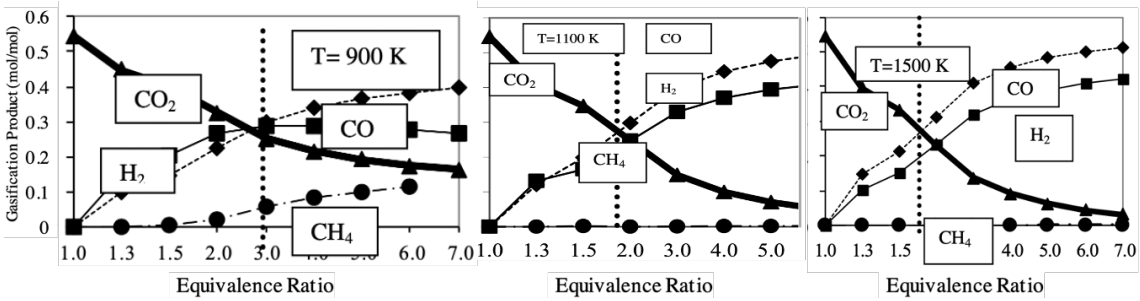

Figure 1.3. Gasification products as a function of the equivalence ratio in biomass gasification (adapted from [25]).

1.3. OBJECTIVES

In the given context, the main objective of this work is to implement a numerical tool that is able to reduce the CRECK-S-BIO mechanism [12], which is used to simulate the process of biomass gasification, while keeping its characteristic features. The reduced mechanism should be able to accurately predict the behavior of the initial detailed mechanism in a macroscopic point of view, comprising less computational time. Within this aim, reduction techniques will be applied to both species and reactions to obtain a reduced mechanism. A parametric study will also be incorporated in the reduction process in order to obtain reduced mechanisms able to predict the detailed mechanism's selected characteristic features in a wide range of temperatures and steam to biomass ratios. Since the two ultimate goals of this work are the presentation of the reduction methodology and the validation of the method, only two operating parameters (temperature and S/B) were selected to be part of the parametric study. Focus will be given to the gasification of wheat straw (agricultural residue) in a drop tube furnace (DTF) considering the typical range of gasification operation conditions. Additionally, the performance of the reduced mechanism is also accessed for the different biomass components.

Table 1.1. Summary of most relevant previous studies on biomass gasification.

Reference	Reactor	Conditions studied	Evaluated parameters	Important info
Zhao et al. (2010) [19]	Entrained-flow reactor	• Temperature (700-1000 ºC) • Residence time • Excess air ratio (0.22-0.34)	• Producer gas low heating value (LHV) • Fuel gas production • Carbon conversion efficiency • Cold gas efficiency	• Main components produced are CO, CO2 and H2, with hydrocarbons such as CH4 and C2H4 being in lower quantities; • Optimal reaction temperature is 800 ºC and optimal excess air ratio is 0.28, condition in which the low heating value of the produced gas, cold gas efficiency and carbon conversion present their maximum values; • Gasification process is finished within 1.3-1.6 seconds when gasification temperature is 700-900 ºC; • Gasification is faster at higher temperatures.
Hernandez et al. (2010) [20]	Entrained - flow reactor	• Temperature (700-1200 ºC) • Space Residence time • Types of fuels	• Producer gas LHV • Fuel conversion • H2/CO • Cold gas efficiency	• Reduction of the fuel particle size leads to a significant improvement of the gasification parameters; • All evaluated gasification parameters significantly benefit from longer space residence times; • Combined effect of higher values of space residence time and temperature has a positive effect on the gasification process, leading to improved gas composition and gasification efficiencies; • Biomass fuels presented a better gasification behavior when compared to coal-coke.
Qin et al. (2012) [21]	Entrained drop tube furnace	• Residence time • Feeder Air flow • Oxygen concentration • Excess air ratio (0.25-0.30) • Steam/Carbon ratio • Temperature (1000-1400ºC) • Biomass types	• Soot formation • Producer gas composition	• Lower soot yield in gasification when compared to pyrolysis; • Studies with 5% and 21% of oxygen concentrations revealed that at high temperatures and with steam addition the soot yield was reduced while increasing the H2 and CO yields; • With temperatures >1200 ºC the process of entrained flow air/ steam gasification achieves a high carbon conversion within a few seconds and a high-quality syngas with a low soot yield, very low hydrocarbon content and without tars; • Increasing the feeder air flow, residence time and excess air ratio will reduce the amount of soot in syngas,

Hernandez et al. (2012) [22]	Entrained - flow reactor	• Steam content in gasifying agent • Steam to biomass ratio (0.64-3.19) • Operating temperature (750-1150 ºC)	• Producer gas: - Composition - Heating Value • Gas yield • Cold gas efficiency • Product gas ratios and production	• Optimal range of steam content in gasifying agent is 40-70%; • Addition of steam proved to be positive for the biomass gasification performance; • Producer gas low heating value rises with the temperature increase; • Increase steam to biomass ratio promotes char and CH_4 steam reforming, also promoting the water-gas shift reaction.
Billaud et al. (2015) [23]	Entrained - flow reactor	• Steam and CO2 addition • Excess air ratio (0-0.61) • Temperature (800-1400)	• Producer gas composition • Soot and tar yields • Carbon distribution	• H2O or CO2 addition has no influence on gasification product yields at 800 and 1000 °C for the tested conditions; • Char gasification is enhanced for temperatures between 1200-1400ºC with soot formation being inhibited; • Char and soot formation decrease as soot formation increases; • Steam to biomass ratio studied between values 0-0.64.
Ku et al. (2019) [24]	Entrained - flow reactor	• Gasifying agent • Biomass type • Reactor structure	• Gas composition • Gas yield • Steam decomposition • Cold gas efficiency • Carbon conversion • LHV	• Introduction of oxygen improves the CO production and carbon conversion. However, an excessive use will lead to lower values of combustible gas yield, steam decomposition and cold gas efficiency; • Using CO2 as gasifying agent increases the CO yield, carbon conversion and cold gas efficiency while reducing the steam decomposition; • The steam addition to the gasification process causes the H2 production, carbon conversion and lower heating value go up while the steam decomposition declines; • Steam-carbon dioxide composite gasification is better than both pure carbon dioxide gasification and steam gasification in syngas yield, carbon conversion and lower heating value. However, there is a decline in steam decomposition; • Biomass samples with a low moisture, high volatile or fixed carbon content can generate a higher combustible gas production.

Table 1.2. Summary of most relevant studies on mechanism reduction.

Reference	Mechanisms	Nº sp Nº rx	Mathematical Tools	Reduction targets	Conditions studied	Important info
Chang et al. (2019) [16]	Iso-cetane mechanism	sp =1107 rx = 4469	• Morris method • Global sensitivity analysis • Path sensitivity analysis	• Ignition delay • CO2 mole fraction • CO mole fraction • Iso-cetane mole fraction	• Temperature • Equivalence ratio • Pressure	• Hierarchical approach based on reaction classes and sub-mechanisms • Reactions with low sensitivity coefficients but high rate of production are considered in this study; • Iso-cetane mechanism with 56 species and 131 reactions is obtained with results indicating that the reduced mechanism retains the characteristics of the detailed mechanism; • It is concluded that the method proposed can be employed in the reduction of detailed mechanisms of related fuels.
Petzold et al. (1999) [18]	GRI-Mech 1.2	sp = 32 rx = 177	• Scanning method on species • Scanning method on reactions • Continuous optimization method • Greedy method	• CO2 mole fraction • CO mole fraction • CH4 mole fraction • H2O mole fraction • O2 mole fraction • temperature	-----	• Results obtained only expected to be valid in some, limited domain of initial and operating conditions for a limited interval of time; • Sensitivity analysis determines the change in the species concentration for small perturbations of the rate constants; • Sequential reduction process: first scanning of the species, secondly scanning of the reactions and lastly optimization; • Mechanisms often present a significantly larger number of reactions than species, therefore scanning species firstly is less expensive; • Reduced mechanism of GRI-Mech 1.2 with final 17 species and 38 reactions and reduced mechanism of Exxon model with 31 species and 42 reactions are obtained with very close results compared with original mechanisms .
	Exxon model	sp = 116 rx = 447				
Wang et al. (2017) [17]	GRI-Mech 3.0	sp = 53 rx = 325	• MPFA method (multi generations path flux analysis) • SA method (sensitivity analysis)	• Temperature • O2 mole fraction • OH mole fraction • O mole fraction • Ignition delay	• Initial Temperature • Initial Pressure • Equivalence ratio	• Study focuses on species reduction rather than direct reaction reduction • MPFA identifies and eliminates unimportant species, while the SA method can further identify redundant species with great computational cost; • MPFASA (combination of the two methods) is able to identify more species with less effect on specific numerical features of the detailed mechanism than its precursors; • GRI-Mech 3.0 reduced mechanism with 21 species and a n-heptane mechanism with 121 species are obtained with satisfying results.
	n- heptane mechanism	sp = 469 rx = 1221				

2. THEORETICAL FOUNDATIONS

2.1. BIOMASS: DEFINITION AND CHARACTERIZATION

Biomass is a renewable and complex biogenic organic–inorganic solid product generated by natural and human-induced processes [2]. Its natural constituents can be originated from both land and water-based flora through photosynthesis or generated via animal and human food digestion, whereas its anthropogenic products are obtained through the processing of the natural constituents previously mentioned [2,5].

As a solid fuel resource, biomass can be divided into 6 different groups regarding its biodiversity, source and origin: (1) Wood and woody biomass; (2) Herbaceous and agricultural biomass; (3) Aquatic biomass; (4) Animal and human biomass wastes; (5) Contaminated biomass and industrial biomass wastes (semi-biomass); and (6) Biomass mixtures, which are mixtures of the types previously mentioned. These groups are divided into multiple sub-groups, with different structural and chemical properties, and therefore a different behavior when subjected to a thermochemical conversion process [2,5]. From the referred types of biomass, non-woody agricultural wastes are worth focusing on due to their large abundance, fast growth, high availability and low cost. On the other hand, these wastes are identified as low density and low-quality solid fuels, whose disposal can involve substantial costs due to its lignin and high ash content [2,27,28]. Therefore, enhancing the energy conversion efficiency of non-woody agricultural wastes remains an absolute necessity and a critical challenge [7].

The analysis of the chemical composition of biomass is of the greatest importance for the work developed in the research of energy-generating processes from this resource. Through a proximate analysis, multiple variables can be obtained, such as fixed carbon, volatile matter and moisture and ash content, whereas from an ultimate analysis elemental data can be obtained. These results enable the unveiling of the initial biomass composition. Biomass is commonly composed mainly by Carbon (C), oxygen (O), hydrogen (H), nitrogen (N), calcium (Ca) and potassium (K), and also by minor elements which include silica (Si), magnesium (Ma), aluminum (Al), sulfur (S), iron (Fe), phosphorus (P), chloride (Cl) and sodium (Na), with trace elements such as manganese (Mn) and titanium (Ti). There is a high variability in biomass chemical composition as well as in ash components, not only due to the many different types of biomass, but also because of the high variations of moisture, ash yield and inorganic matter found in it [2,5].

The phase composition of biomass divides the biomass into three types of components: organic matter, inorganic matter and fluid matter. The major organic components are the structural organic components (cellulose, hemicellulose, lignin), which are presented in Figure 2.1, and the extractives [2,5].

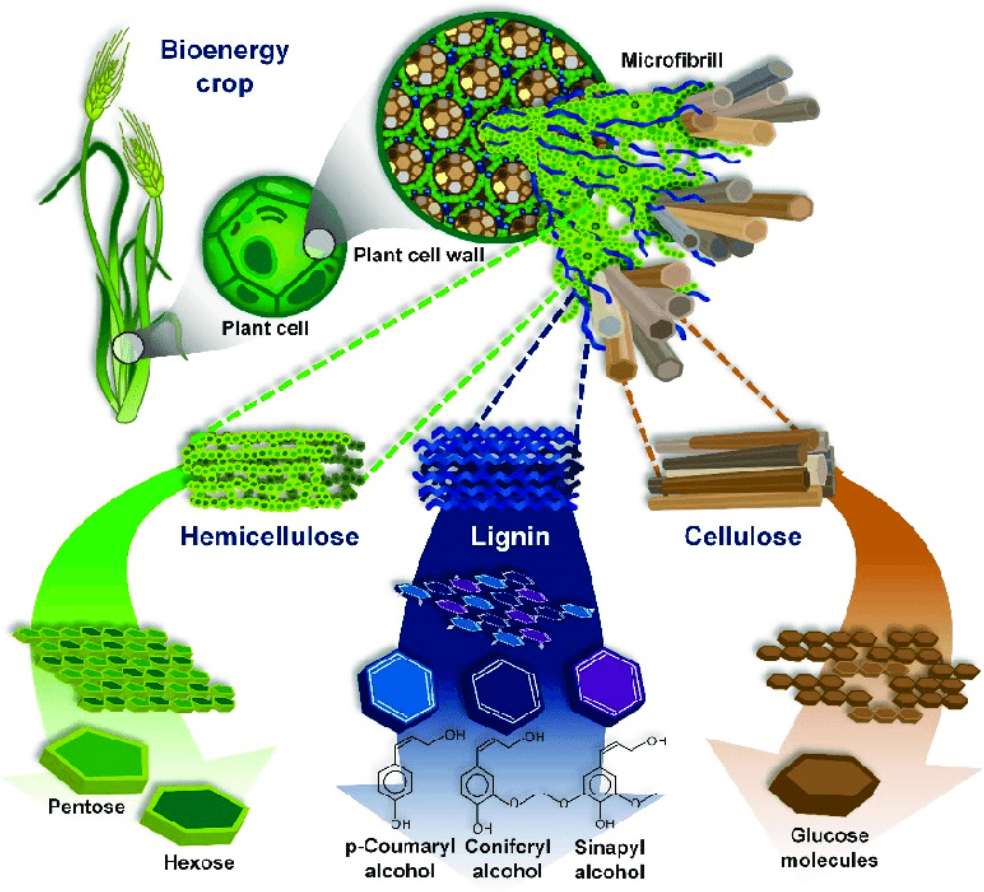

Figure 2.1. Structure of lignocellulosic biomass and its polymers [29].

Cellulose is a linear polysaccharide, and it is the most abundant polysaccharide in plant cell walls. It is composed by glucose, which is a six membered ring cyclic sugar. Multiple units of glucose link themselves through glycosidic bonds and form non-branched chains, with a high degree of polymerization (DP = 10-15 thousand) that link between themselves through strong interchain hydrogen bonds. This structural bonding configuration of cellulose provides it with high resistance towards hydrolysis and enzyme activity [6], as well as with high thermal stability [30]. Hemicellulose is an heterogeneous complex polysaccharide, formed by a complex mixture of multiple hexose and pentose monosaccharide units (xylose, galactose, mannose, glucose and arabinose), and with a low degree of polymerization when compared with cellulose (DP= 70-200), and are closely bonded with cellulose by noncovalent linkages, which originates a microfibril network [6]. It has a branched and amorphous structure, and a low thermal stability, with branches being easily removed from the main chain by volatiles at low temperatures [30]. Lignin is three-dimensional polymer, formed by aromatic polymers (not sugars) with a branched and amorphous structure, being responsible for reinforcing cell walls through covalent linkage to hemicellulose [6]. Extractives are nonstructural substances produced by plants that can be divided into two groups: (1) hydrophobic resins, which are mainly formed by terpenes and fat acids and (2) phenolic compounds, which are hydrophilic species mainly composed by sugars, aromatics, acids, tannins and flavonoids [6].

The inorganic matter that is part of biomass is composed by crystalline structures (silicates, oxyhydroxides, sulphates, phosphates, carbonates, chlorides, nitrates), semi-crystalline structures (silicates, phosphates, hydroxides, chlorides) and amorphous constituents (glasses and silicates). The fluid matter accounts with both organic and inorganic origins of moisture, gas and gas-liquid components found in biomass [2,5]. Table 2.1 shows the chemical characteristics and the structural components composition for three different types of biomass.

Table 2.1. Chemical characteristics and structural components composition of various biomass groups and sub-groups (WWB - Wood and woody biomass; HAB - Herbaceous and agricultural biomass; HAS - Herbaceous and agricultural straws) [27].

Biomass	WWB	mean	HAB	mean	HAS	mean
Proximate analysis (wt.%, ar)						
Moisture	4.7 – 62.9	19.3	4.7 – 62.9	19.3	7.4 – 16.8	10.2
Volatile Matter	30.4 – 79.7	62.9	41.5 – 76.6	66.0	58.0 – 73.9	66.7
Fixed Carbon	6.5 – 24.1	15.1	9.1 – 35.3	16.9	12.5 – 17.8	15.3
Ash	0.1 – 8.4	2.7	0.1 – 8.4	2.7	4.3 – 18.6	7.8
Ultimate analysis (wt.%, daf)						
C	48.7 – 57.0	52.1	42.2 – 58.4	49.9	48.5 – 50.6	49.4
O	32.0 – 45.3	41.2	34.2 – 49.0	42.6	40.1 – 44.6	43.2
H	5.4 – 10.2	6.2	3.2 – 9.2	6.2	5.6 – 6.4	6.1
N	0.1 – 0.7	0.4	0.1 – 3.4	1.2	0.5 – 2.8	1.2
S	0.01 – 0.42	0.08	0.01 – 0.60	0.15	0.08 – 0.28	0.15
Structural components (wt.%, daf)						
Cellulose	12.4 – 65.5	39.5	23.7 – 87.5	46.1	18 – 54.8	45.4
Hemicellulose	6.7 – 65.6	34.5	12.3 – 54.5	30.2	18 – 39	31.5
Lignin	10.2 – 44.5	26.0	0.0 – 54.3	23.7	14.9 – 35.3	23.1
Extractives (wt.%, daf)	1.0 – 9.9	3.1	1.2 – 86.8	13.7	3.8 – 21.7	13.6
Ash analysis (wt.%, db)						
Cl	0.01 – 0.05	0.02	0.04 – 0.83	0.21	0.03 – 0.64	0.41
SiO_2	1.86 – 68.18	22.22	8.73 – 84.92	46.18	7.87 – 77.2	43.94
CaO	5.79 – 83.46	43.03	2.98 – 44.32	11.23	2.46 – 30.68	14.13
K_2O	2.19 – 31.99	10.75	2.93 – 53.38	24.59	12.59 – 38.14	24.49
P_2O_5	0.66 – 13.01	3.48	3.14 – 20.33	6.62	0.98 – 10.38	4.13
Al_2O_3	0.12 – 15.12	5.09	0.67 – 2.59	1.39	0.1 – 5.57	2.71
MgO	1.1 – 14.57	6.07	1.42 – 8.64	4.02	1.67 – 14.1	4.66
Fe_2O_3	0.37 – 9.54	3.44	0.58 – 1.73	0.98	0.41 – 2.82	1.42
SO_3	0.36 – 11.66	2.78	0.83 – 9.89	3.66	1.18 – 4.93	3.01
Na_2O	0.22 – 29.82	2.85	0.09 – 6.2	1.25	0.16 – 3.52	1.35

TiO_2	0.06 – 1.2	0.29	0.01 – 0.28	0.08	0.02 – 0.33	0.16
Mn (ppm)	775 – 35740	13160	–	3100	155 – 2790	865

* am – as measured, daf – dry ash free basis

2.2. GASIFICATION

Gasification is a multistage and complex process, divided into 5 different stages that overlap themselves. However, Safarian et al [8] proposed the following thermochemical order: drying, pyrolysis, combustion (partial oxidation), cracking and reduction (char gasification).

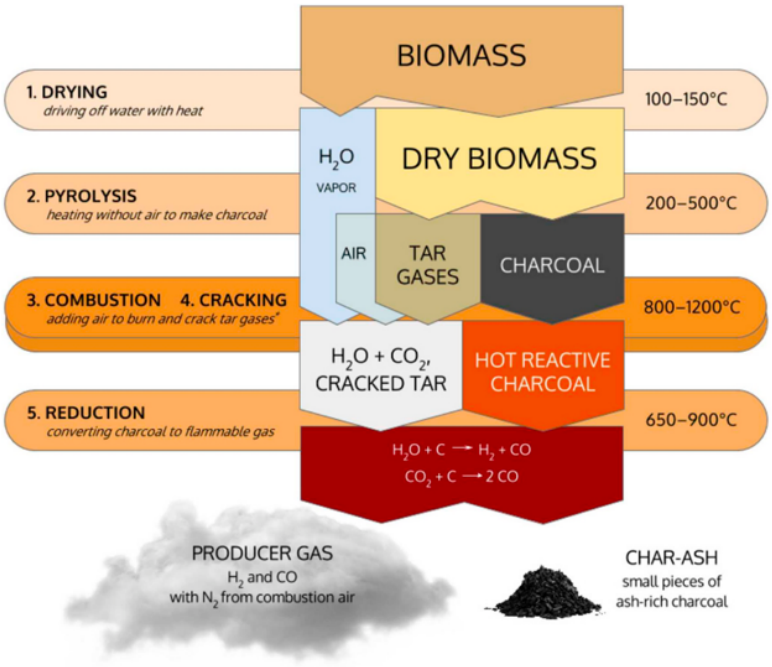

Figure 2.2. Gasification process steps [8].

Drying consists of the removal of the moisture content from biomass, reducing it from the average 5-35 % to less than 5%, and it occurs due to the heat released in the combustion phase that is used to evaporate the moisture, producing water vapor and dry biomass. The dry biomass is then driven to the pyrolysis phase, where it is heated to temperatures in between 200-700Cº in an oxygen-free atmosphere and primary reactions occur, which consist in the decomposition of the matrix carbonaceous materials into different primary products: gas, tar and char, with water vapor also being produced. The volatile gas contains hydrogen (H2), carbon monoxide (CO), methane (CH4), carbon dioxide (CO2) and light hydrocarbons [8,31,32]. The term tars refer to condensable heavy aromatic hydrocarbons that are in the liquid state at ambient temperature but in a form of vapor at gasification temperature. The tars produced during the pyrolysis phase consists of oxygenated organic compounds (alcohols, carbon acid, aldehydes, ketones, etc.) [32]. Char consists in the devolatilized solid matter that remains after drying and pyrolysis, composed by unconverted organic matter and ash (carbon rich structure that also includes inert materials) [32].

The admission of air into the reactor triggers the combustion and cracking phases. The combustion phase is the reaction of the oxygen present in the admitted air with the combustible substances (char and volatiles) [8] resulting from the pyrolysis phase, producing mainly CO2, H2O and most importantly heat (exothermic reactions), which is of the outmost importance for the entire gasification process, as it is used to preserve the operating temperature necessary for the process, since heat is absorbed by the multiple endothermic processes present in the gasification process: in the drying phase, with energy necessary to evaporate the water; in the pyrolysis phase, where heat is used for the devolatilization of the dry biomass; in the tar cracking processes, which occur mainly at elevated temperatures (> 500ºC [32]) and the heating of the char/charcoal, which will lead to the reduction phase. The cracking phase consists on the thermal cracking of the tars where, due to the elevated temperatures, the heavy hydrocarbons break into light permanent and combustible gases. Together with the cracking process, polymerization (endothermic) reactions also occur, rearranging the tars and forming polycyclic aromatic hydrocarbons (PAHs) which through sub-sequent processes (nucleation, surface growth) lead to the formation of soot, which are particles that represent unwanted impurities in the gasification process [7,33], with their formation process being presented in Figure 2.3. Finally, the reduction phase consists mainly in reactions between the gas products such as CO2 and H2O and the hot reactive charcoal releasing flammable gases (H_2 and CO) and originating the final syngas [8,32].

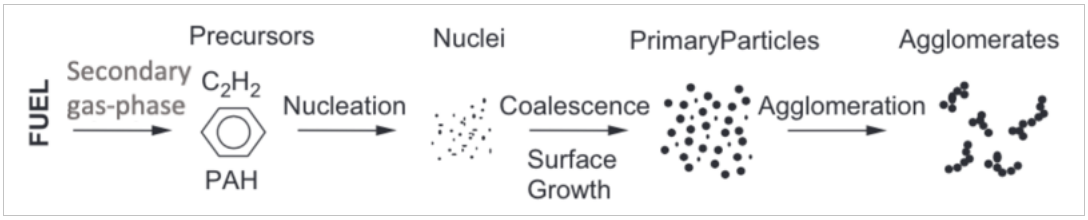

Figure 2.3. Soot formation stages (adapted from [33]).

From this entire multistage process, there are three types of products originated: synthetic gas (syngas), liquid and char-ash. The syngas is mainly composed by the hydrogen (H_2), carbon monoxide (CO), carbon dioxide (CO_2), methane (CH_4) and light hydrocarbons, along with other non-condensable gases [32]. The syngas can be used for multiple downstream applications such as power or heat generation, hydrogen (H_2) and methanol (CH_4) production, liquid fuel synthesis, synthetic natural gas and town gas (coal gas) production. The liquids are a mixture of water, low weight molecular species and unconverted tars. These unconverted tars, which are in their liquid phase in an ambient temperature-pressure environment [32], are described by Safarian et al. [8] as a black, viscous and corrosive liquid mainly composed by heavy organic and inorganic molecular structures. Lastly, the char-ash is a product that consists in inert solid matter and the charcoal (mainly carbon) that did not react in the reduction phase [8].

The efficiency of the gasification process can be assessed by the analysis of the syngas it produces. Several factors contribute to such analysis: gas yield, presence of uncracked tars, composition (H_2/CO ratio), low heating value (LHV) and carbon conversion efficiency [34–36]. The gas yield represents the fraction of gas in the final gasification products (gas, liquid and solid), it is used to assess the quantity of gas produced in a specific gasification process and it is calculated as follows:

$$GY = \frac{V_{gas}}{V_{prod}} \quad \text{(Eq. 1)}$$

with V_{gas} representing the volume of gas and V_{prod} the total volume (m^3) of the products resulting from the gasification process. The H_2/CO ratio is used to assess the quality of the syngas and it represents the ratio between the fractions of hydrogen and carbon monoxide in the final gas composition, which in this work consists of H_2, CO, CO_2 and CH_4, as these species are the most abundant in the final syngas. For example, synthetic gases with H_2/CO ratios between 1 and 2 are generally applied to major synthesis-gas-based chemicals production, while values of H_2/CO ratio higher than two potentiate the syngas to be used in a wider range of applications such as gas to liquid processes, fuel cells and transportation fuels [37,38]. This value of the H_2/CO is calculated in the following way:

$$H2/CO = \frac{V_{H2}}{V_{CO}} \quad \text{(Eq. 2)}$$

with V_{H2} and V_{CO} representing volumes (m^3) hydrogen and carbon monoxide, respectively. The low heating value represents the energy released throughout the combustion process of a specific gas and it is calculated as demonstrated in equation 3. The syngas low heating value is calculated through the sum of the heating values of the flammable species present in that same syngas. In Table 2.2 are presented the calorific values of the mentioned flammable species.

$$LHV_{sp} = CV_{sp} \times \frac{VP_{sp}}{100} \quad [\frac{MJ}{Nm^3}] \quad \text{(Eq. 3)}$$

$$LHV_{gas} = \sum LHV_{sp} \quad \text{(Eq. 4)}$$

The term CV_{sp} represents the calorific value (MJ/Nm^3) and the VP_{sp} the volumetric percentage (%).

Table 2.2. Calorific values of energy valuable of the main flammable species present in the syngas [39].

Species	H_2	CO	CH_4
Calorific Value (MJ/Nm^3)	10.798	12.636	35.818

The uncracked tars are the tars that did not undergo the cracking process and that turn into impurities undesired in the gasification process, and it is quantified as the ratio between the mass of tars m_{tars} (kg) and the mass of biomass m_{Bio} (kg):

$$UT = \frac{m_{tars}}{m_{bio}} \quad \text{(Eq. 5)}$$

Finally, the carbon conversion efficiency is defined as the ratio between the amount of carbon in the syngas and the amount of carbon in the feedstock (fuel) [19] and it calculated as follows:

$$CCE = 100 * \frac{12 \times \dot{n}_{m,CS}}{U_c \times \dot{m_{bio}}} \ [\%] \qquad \text{(Eq. 6)}$$

with $\dot{n}_{m,CS}$ representing the molar flow rate of carbon present in the syngas (mol/s), U_c representing the fraction of carbon in the initial biomass sample and $\dot{m_{bio}}$ the mass flow rate of biomass into the reactor (kg/s)

2.3. DROP TUBE FURNACE

In this work, the developed numerical tool uses a reactor model that simulates biomass gasification in a drop tube furnace (DTF), represented in Figure 2.4. A drop tube furnace is simple system that is able to reproduce with a fair accuracy the operating characteristics of an entrained flow reactor [40]. In a DTF, the fuel and the carrier gas are injected in co-current with and the gasifying agent, near the top of the system in a central pipe, with a pneumatic feeding system used to deliver the fuel (in form of solid powder). The particles of biomass injected in the DTF must have very small dimensions due to the short residence time, along with very high heating rate values verified to make viable the application of this type of reactors [41]. The products of the several phases of the gasification process move from the top to the bottom of a nonporous mullite tube where the gasification takes place, with the walls of that tube ideally at a uniform temperature [40]. The particles (char and soot) remaining at the end of the gasification process are then collected by a particle collection system, with the syngas being carried out of the system with the aid of pumps for downstream analysis [7,32,40]. This reactor was selected to be used in this work due to three main reasons: fuel flexibility, enabling the enhancement of the reduction process using different types of biomass; good ability to control the process operating parameters and scalability, which allows the use of the developed numerical tool for mechanism reduction in a larger range of applications without having to modify the reactor model used [32].

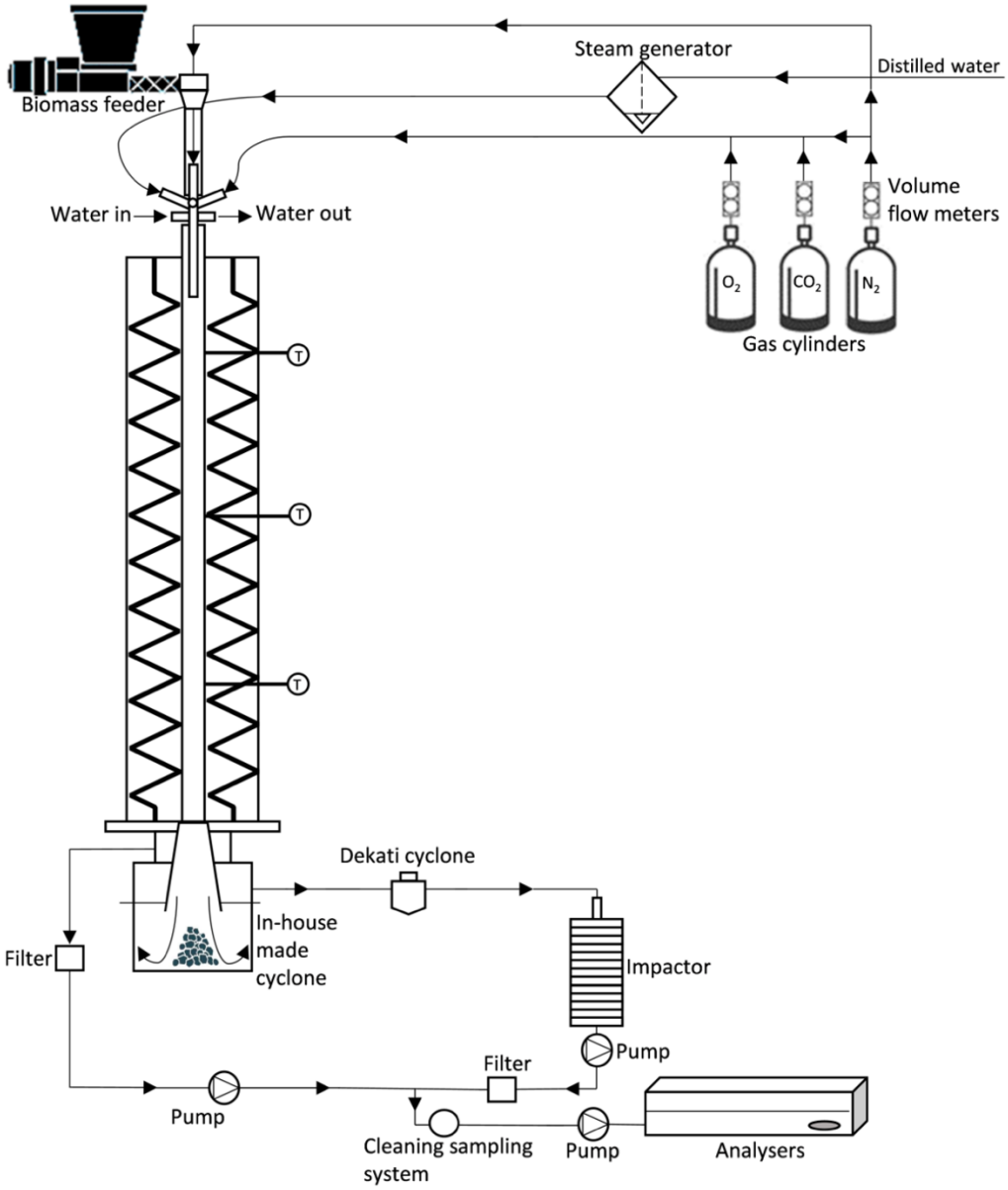

Figure 2.4. Scheme of the DTF [7].

2.4. KINETIC MECHANISMS

Debiagi et al. [12] proposed a very detailed mechanism that is able to describe biomass pyrolysis behavior and secondary gas-phase reactions under gasification conditions, taking into account 161 species and 4561 reactions (pyrolysis: 52 species and 28 reactions; secondary gas-phase mechanism: 134 species and 4533 reactions) . This mechanism named CRECK-S-BIO and presented in Figure 2.7 considers that biomass is constituted by seven reference components: cellulose (CELL), hemicellulose (HCE), three structures of lignin identified as LIGH, LIGO, and LIGC rich in hydrogen, oxygen, and carbon, respectively, and hydrophobic (TGL) and hydrophilic (TANN) extractives, with their chemical constitution being presented if Figure 2.5 [6,11]. In this mechanism, pyrolysis takes place through the decomposition of the seven solid biomass components [6]. After the pyrolysis phase, the

secondary gas phase reactions take place, where the partial oxidation of the released volatiles occurs, with tars also undergoing thermal cracking.

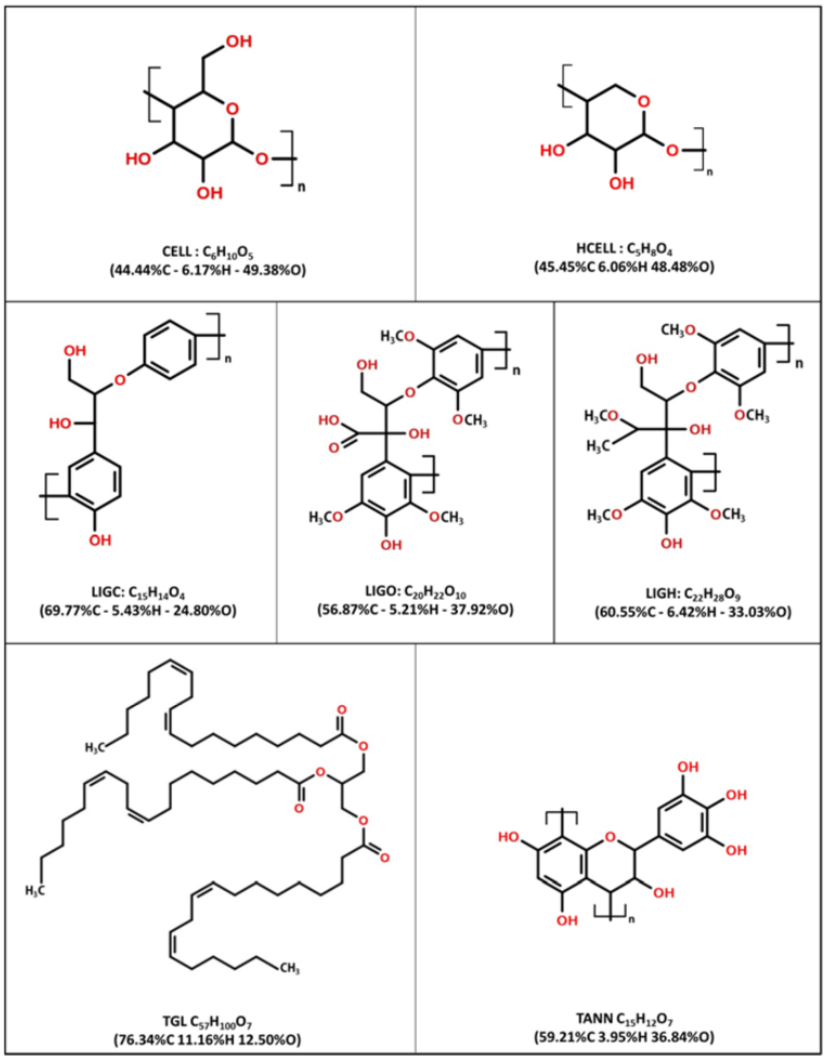

Figure 2.5. Chemical structure of all the components [6].

In order to assess the performance of the entire gasification process (LHV, gas yield, amount of uncracked tars, CCE and H2/CO), reactions of char gasification (R34 to R37 from Table 2.3) and soot reactions (R29 to R33 from Table 2.3) are added to the CRECK-S-BIO mechanism, with the phenomena behind these reactions shown in Figure 2.6. During char gasification, the reactive gas molecules, which are present in the surrounding atmosphere, reach the surface particle and penetrate through the pores of the char particles where the oxidation and reduction reactions take place. H_2O, CO_2 and O_2 react with carbon, promoting the release of H_2 and CO. The products from such reactions leave the pores in the opposite way of the gasifying molecules entering the particle, with the gas flow inside the particle being a consequence of a mass diffusion phenomena. The soot gasification is identical to the char gasification process, with the difference that the mass diffusion occurs between the sphere particles that form the soot, due to impossibility of penetration in those very small sized spherules. As a consequence, soot

gasification occurs in the surface of the particles that form it [42]. The reactions involving soot and char are presented in Table 2.3 together with the 28 reactions that take place during the pyrolysis phase.

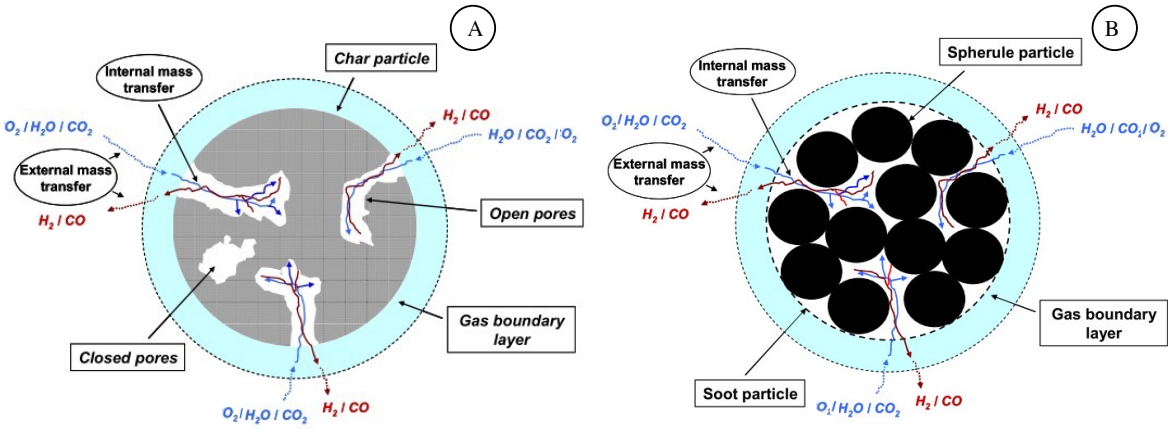

Figure 2.6. a) Char and b) soot oxidation and reduction [42].

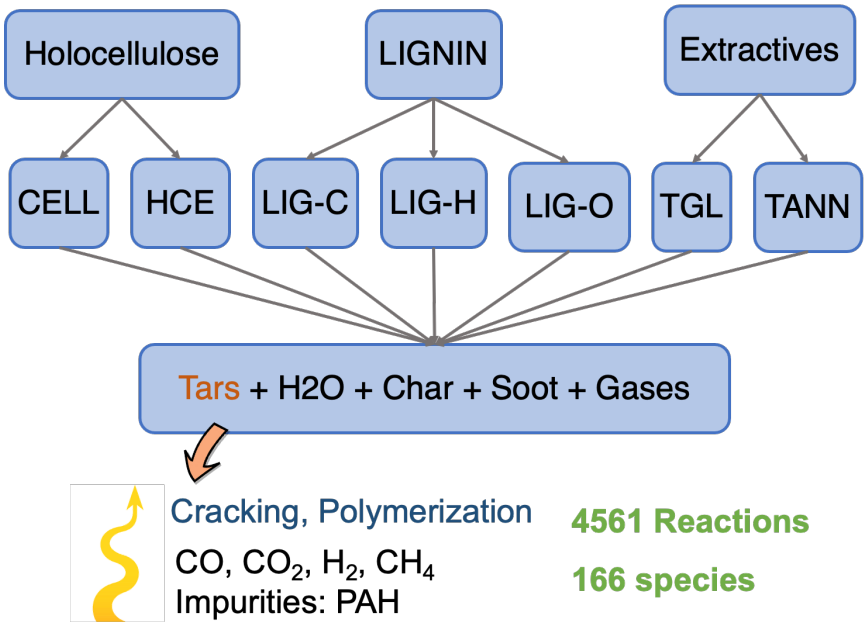

Figure 2.7. Biomass gasification kinetic mechanism (CRECK-S-BIO).

Table 2.3. Drying, pyrolysis, char and soot reactions in the CRECK-S-BIO mechanism [7,12].

Process	Reaction	Reaction
Water Evaporation	AQUA $\rightarrow$ H_2O	R1
Pyrolysis	CELL $\rightarrow$ CELLA	R2
	CELLA $\rightarrow$ 0.4 $C_2H_4O_2$ + 0.05 $C_2H_2O_2$ + 0.15 CH_3CHO + 0.25 $C_6H_6O_3$ + 0.35 C_3H_6O + 0.15 CH_3OH + 0.3 CH_2O + 0.61 CO + 0.36 CO_2 + 0.05 H_2 + 0.93 H_2O + 0.02 HCOOH + 0.05 $C_3H_6O_2$ + 0.05 GCH_4 + 0.2 GH_2 + 0.61 Char	R3
	CELLA $\rightarrow$ $C_6H_{10}O_5$	R4
	CELL $\rightarrow$ 5 H_2O + 6 Char	R5
	HCE $\rightarrow$ 0.35 HCE1 + 0.65 HCE2	R6
	HCE1 $\rightarrow$ 0.6 $C_5H_8O_4$ + 0.2 $C_3H_6O_2$ + 0.12 $C_2H_2O_2$ + 0.2 $C_5H_4O_2$ + 0.4 H_2O + 0.08 GH_2 + 0.16 CO	R7
	HCE1 $\rightarrow$ 0.4 H_2O + 0.79 CO_2 + 0.05 HCOOH + 0.69 CO + 0.01 GCO + 0.01 GCO_2 + 0.35 GH_2 + 0.3 CH_2O + 0.9 $GCOH_2$ + 0.625 GCH_4 + 0.375 GC_2H_4 + 0.875 Char	R8
	HCE2 $\rightarrow$ 0.2 H_2O + 0.275 CO + 0.275 CO_2 + 0.4 CH_2O + 0.1 C_2H_5OH + 0.05 $C_2H_4O_2$ + 0.35 CH_3COOH + 0.025 HCOOH + 0.25 GCH_4 + 0.3 GCH_3OH + 0.225 GC_2H_4 + 0.3 GCO_2 + 0.725 $GCOH_2$ + 1 Char	R9
	LIGC $\rightarrow$ 0.35 LIGCC + 0.1 $C_9H_{10}O_2$ + 0.08 C_6H_5OH + 0.41 C_2H_4 + 1 H_2O + 0.7 $GCOH_2$ + 0.3 CH_2O + 0.32 CO + 0.495 GCH_4 + 5.735 Char	R10
	LIGH $\rightarrow$ 1 LIGOH + 0.5 C_3H_6O + 0.5 C_2H_4 + 0.2 $C_2H_4O_2$ + 0.1 CO + 0.1GH_2	R11
	LIGO $\rightarrow$ LIGOH + CO_2	R12
	LIGCC $\rightarrow$ 0.3 $C_9H_{10}O_2$ + 0.2 C_6H_5OH + 0.35 $C_2H_4O_2$ + 0.7 H_2O + 0.65 CH_4 + 0.6 C_2H_4 + 1 H_2 + 1.4 CO + 0.4 GCO + 6.75 Char	R13
	LIGOH $\rightarrow$ 0.9 LIG + 1 H_2O + 0.1 CH_4 + 0.6 CH_3OH + 0.05 GH_2 + 0.3 GCH_3OH + 0.05 CO_2 + 0.65 CO + 0.6 GCO + 0.05 HCOOH + 0.85 $GCOH_2$ + 0.35 GCH_4 + 0.2 GC_2H_4 + 4.25 CHAR + 0.025 HMWL + 0.1 C_2H_3CHO	R14
	LIG $\rightarrow$ 0.7 $C_{11}H_{12}O_4$ + 0.3 $C_6H_5OCH_3$ + 0.3 C0 + 0.3 GCO + 0.3 CH_3CHO	R15
	LIG $\rightarrow$ 0.6 H_2O + 0.4 CO + 0.2 CH_4 + 0.4 CH_2O + 0.2 GCO + 0.4 GCH_4 + 0.5 GC_2H_4 + 0.4 GCH_3OH + 2 $GCOH_2$ + 6 Char	R16
	LIG $\rightarrow$ 0.6 H_2O + 2.6 CO + 1.1 CH_4 + 0.4 CH_2O + 1 C_2H_4 + 0.4 CH_3OH + 4.5 Char	R17
	TGL $\rightarrow$ C_2H_3CHO + 2.5 MLINO + 0.5 U2ME12	R18

	TANN $\rightarrow$ 0.85 C_6H_5OH + 0.15 GC_6H_5OH + GCO + H_2O + ITANN	R19
	ITANN $\rightarrow$ 5 Char + 2 CO + H_2O + $GCOH_2$	R20
	$GCO_2 \rightarrow CO_2$	R21
	GCO $\rightarrow$ CO	R22
	$GCOH_2 \rightarrow$ 0.2 Char + 0.2 H_2O + 0.8 CO + 0.8 H_2	R23
	$GH_2 \rightarrow H_2$	R24
	$GCH_4 \rightarrow CH_4$	R25
	$GCH_3OH \rightarrow CH_3OH$	R26
	$GC_2H_4 \rightarrow C_2H_4$	R27
	$GC_6H_5OH \rightarrow C_6H_5OH$	R28
Soot Inception	$C_2H_2 \rightarrow$ 2 soot + H_2	R29
	$C_nH_m \rightarrow$ n soot + $\frac{m}{2}$ H_2	R30
Soot oxidation	Soot + 0.5 $O_2 \rightarrow$ CO	R31
Soot reforming	Soot + $H_2O \rightarrow$ CO + H_2	R32
Soot reduction	Soot + $CO_2 \rightarrow$ 2 CO	R33
Char oxidation	Char + 0.5 $O_2 \rightarrow$ CO	R34
	Char + $O_2 \rightarrow$ 2 CO	R35
Char reforming	Char + $H_2O \rightarrow$ CO + H_2	R36
Char reduction	Char + $CO_2 \rightarrow$ 2 CO	R37

3. MATERIALS AND METHODS

3.1. BIOMASS COMPOSITION AND OPERATING CONDITIONS

Due to its high availability as an agricultural residue, the biomass considered in this work is wheat straw. Table 3.1 presents the proximate and ultimate analysis for this biomass fuel, while its organic composition is shown in Table 3.2.

Table 3.1. Proximate and ultimate analysis of the biomass fuels studied

Parameter	Wheat straw
Proximate analysis (wt.%, ar)	
Volatile matter (VM)	64.9
Fixed carbon (FC)	11.5
Ash	14.7
Moisture	8.9
Ultimate analysis (wt.%, daf)	
C	51.6
H	6.8
N	0.6
S	< 0.02
O[a]	41.0

[a] Calculated by difference, ar – as received, daf – dry-ash-free

Table 3.2. Wheat straw organic composition (CELL – cellulose; HCE – hemicellulose; LIGH, LIGC, LIGO – lignin rich in hydrogen, carbon and oxygen, respectively; TGL – triglycerides; TANN – tannins).

Species	CELL	HCE	LIGH	LIGC	LIGO	TGL	TANN
Mass fraction (%)	25.7	23.3	0.2	13.4	15.2	4.1	18.0

In this work, all operating conditions are fixed except for the operating temperature and the steam to biomass ratio. The interval of studied temperatures is 900-1200 ºC and it was selected as it represents average values of temperature studied in the literature dedicated to biomass gasification (Table 1.2), whereas the steam to biomass ratio values studied vary from 0 to 1.7. There are studies that present S/B values from 0 to 2, however it has been found that gasification results do not vary significantly between 1.7 and 2, which leads to the selection of the interval of S/B values of 0-1.7 to be studied in this work [24]. The gasifying agent chosen is air with a constant flow rate of 0.5 L/min, the carrier gas is nitrogen with a constant flow of 10 L/min and the residence time is a function of the temperature and pressure of the gasification process. The summary of the operating conditions is presented in Table 3.3. The reduced mechanism will be tested and validated within this range of conditions.

Table 3.3. Gasification operating conditions (S/B = steam to biomass ratio; λ = excess air coefficient).

T(ºC)	S/B	λ
900-1200	0 – 1.7	0.4

3.2. REACTOR MODELLING

Ferreiro et al. [7] developed the kinetic-diffusion controlled model used in this work. This one-dimensional model considers a spherical biomass particle entering the DTF along with a carrier gas, where both are heated through convection and radiation. The release rate of the volatiles and the heat transfer between the particle and its surroundings is calculated along the axial direction of the DTF. Figure 3.1 shows a concept visualization of the adopted model with the specifications of this work regarding the gasifying agent and carrier gas composition:

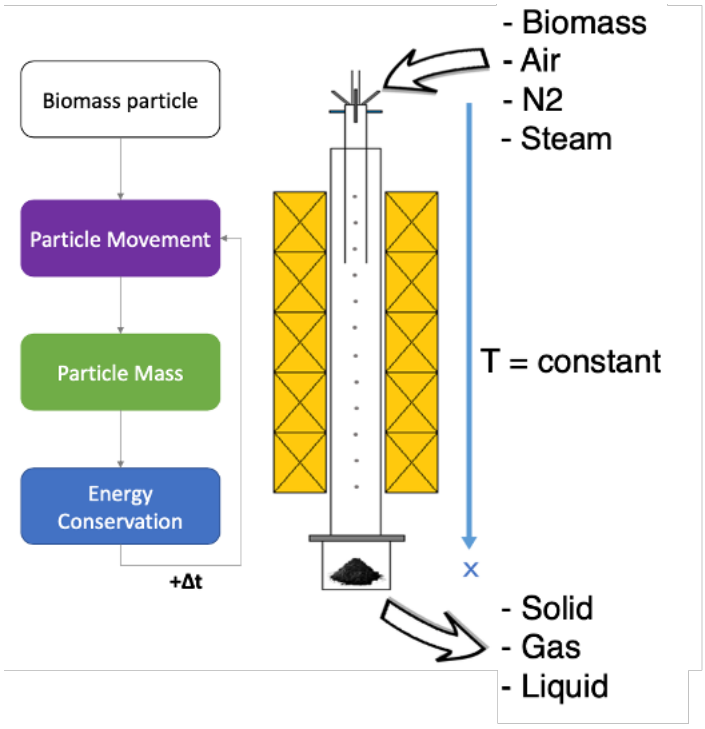

Figure 3.1. Reactor model.

The model inputs are the measured temperature profiles, biomass composition (obtained experimentally in a previous work [43]) and the reactor and mass flow characteristics. In this work in specific, the temperature is assumed to be constant along the entire length of the reactor with values varying accordingly to Table 3.3, the biomass composition is as presented in table 3.2 and the reaction zone of the reactor has 1320 mm. This model comprises three main governing equations: mass balance (Eq.7), energy balance (Eq.10) and particle trajectory (Eq.18), all presented in the scheme on the left in Figure 3.1 [7]. The mass balance is calculated as follows:

$$m_p \frac{dY_{\mathrm{sp}}}{dt} = \dot{m}_{\mathrm{sp,gen}} \quad \text{(Eq. 7)}$$

with

$$\dot{\mathrm{m}}_{\mathrm{sp,gen}} = \dot{\omega} \times \frac{M_{\mathrm{w,sp}}}{\rho_{\mathrm{gas}}} \quad [\frac{kg_{sp}}{kg_{gas} \times s^{-1}}] \quad \text{(Eq. 8)}$$

Where the term m_p relates to the mass of the particle (kg), Y_{sp} to the mass fraction of the species, $\dot{m}_{\mathrm{sp,gen}}$ to the mass flow rate of generation of the considered specie (kg/s), $\dot{\omega}$ to the net mole production rate (kmol/m^3.s), $M_{\mathrm{w,sp}}\ to$ the molecular weight (kg/kmol) and ρ_{gas} to the gas density (kg/m^3). The previous equations result in the following expression that gives the particle mass at each position in the DTF:

$$m_{\mathrm{p}} = m_{\mathrm{p,0}} \times \sum_{\mathrm{sp}} Y_{\mathrm{sp}} \quad [kg] \quad \text{(Eq. 9)}$$

The energy balance equation used in this model is a result of the sum of all energy contributions the are released or absorbed by the biomass particle, and it was constructed as follows:

$$c_{\mathrm{p,p}} m_{\mathrm{p}} \frac{dT}{dt} = \dot{Q}_{\mathrm{in}} - \dot{Q}_{\mathrm{out}} = \dot{Q}_{\mathrm{convection}} + \dot{Q}_{\mathrm{radiation}} - \dot{Q}_{\mathrm{pyrolysis}} - \dot{Q}_{\mathrm{soot}} - \dot{Q}_{\mathrm{gasification}} \quad \text{(Eq. 10)}$$

with:

$$\dot{Q}_{\mathrm{convection}} = \frac{\lambda_{\mathrm{g}}}{d_{\mathrm{p}}} \mathrm{Nu}\, A_{\mathrm{p}} \left(T_{\mathrm{gas}} - T_{\mathrm{p}}\right) \quad [W] \quad \text{(Eq. 11)}$$

$$\dot{Q}_{\mathrm{radiation}} = A_{\mathrm{p}} \varepsilon \sigma \left(T_{\mathrm{wall}}^4 - T_{\mathrm{p}}^4\right) \quad [W] \quad \text{(Eq. 12)}$$

$$\dot{Q}_{\mathrm{pyrolysis}} = \sum_{\mathrm{j=1}}^{\mathrm{rx_{pyr}}} \left(k_{\mathrm{pyr,j}}(T) \Delta H_{\mathrm{j}}\right) dm_{\mathrm{p}} \quad [W] \quad \text{(Eq. 13)}$$

$$\dot{Q}_{\mathrm{soot}} = \sum_{\mathrm{j=1}}^{\mathrm{rx_{soot}}} \left(k_{\mathrm{gas,j}}(T,P) \Delta H_{\mathrm{j}}\right) f(X)_{\mathrm{soot}}\, dm_{\mathrm{p}} \quad [W] \quad \text{(Eq. 14)}$$

$$\dot{Q}_{\mathrm{gasification}} = \sum_{\mathrm{j=1}}^{\mathrm{rx_{gas}}} \left(k_{\mathrm{gas,j}}(T,P) \Delta H_{\mathrm{j}}\right) f(X)_{\mathrm{char}}\, dm_{\mathrm{p}} \quad [W] \quad \text{(Eq. 15)}$$

and:

$$k_{\mathrm{pyr}}(T) = A T_{\mathrm{p}}^{\beta} \exp\left(-\frac{E}{R T_{\mathrm{p}}}\right), \quad k_{\mathrm{gas}}(T,P) = A T_{\mathrm{p}}^{\beta} P_{\mathrm{g}}^{\mathrm{n}} \exp\left(-\frac{E}{R T_{\mathrm{p}}}\right) \quad \text{(Eq. 16)}$$

$$f(X)_{\mathrm{char}} = (1-X)\sqrt{1 - ln(1-X)}\,, \quad f(X)_{\mathrm{soot}} = (1-X) \quad \text{(Eq. 17)}$$

with c_p being the specific heat of the particle (J/kg.k), T the temperature (ºC), $\dot{Q}$ the heat generated (W), λ_{g} the thermal conductivity of the gas (W/m.k), d_p the particle diameter (m), Nu the Nusselt number, A_p the particle area (m^2), ε the emissivity, ΔH the heat of reaction (kJ/kmol), dm_p the derivate of the mass particle with respect to time, k the reaction rate constant, A the pre-exponential factor, β the temperature

exponent in the Arrhenius Law, E the activation energy (cal/mol), P the total gas pressure (Pa), n the reaction order and X the char conversion (wt. %). It should be noted that the heat terms regarding the convection and radiation phenomena have positive signs in Equation 10 as these are absorbed by the particle, whereas the heat terms related to the pyrolysis, soot reactions and gasification have negative signs, since heat is released considering the overall balance of each one of these processes. Lastly, the particle trajectory governing equation, obtained from gravity, buoyancy and drag forces acting on the particle is written as follows:

$$\frac{dv_{\mathrm{p}}}{dt} = \frac{\left(v_{\mathrm{gas}} - v_{\mathrm{p}}\right)}{\frac{4}{3}\frac{\rho_{\mathrm{p}} d_{\mathrm{p}}^2}{C_{\mathrm{D}}\mathrm{Re}\mu_{\mathrm{gas}}}} + \mathrm{g} \qquad \text{(Eq. 18)}$$

With v_p representing the velocity (m/s), g the gravity acceleration (m^2/s), C_D the drag coefficient, Re the Reynolds number and μ_g the gas dynamic viscosity (kg/m.s). The particle initial velocity considered at the exit of the injector being calculated as:

$$v_{\mathrm{p},0} = \frac{d_{\mathrm{p}}^2 \mathrm{g}\left(\rho_{\mathrm{p}} - \rho_{\mathrm{g}}\right)}{18\mu_{\mathrm{g}}}, \ \mathrm{Re} < 2 \qquad [m/s] \qquad \text{(Eq. 19)}$$

In order to solve the previous equations, the species conservation and determine the reaction rates and final product yields, a stiff ordinary differential equation solver (CVODE) [44] is implemented in Python with assistance of the Cantera library [44]. A more detailed description of this model and the above equations can be found in a previous work [7].

3.3. MECHANISM REDUCTION MODELLING

The reduction process is developed in Python as a sub-routine of the numerical tool described above. The mechanism adopted in this work to predict the biomass pyrolysis contains 52 species and 28 reactions [6]. As this mechanism is already fully reduced, it will not take part in the reduction process.

The reduction methodology used in this work is based on the approach used by Petzold et al. [18], with the scanning method presented in this study applied to both species and reactions. However, the optimization step is replaced with a merging step, where reduced mechanisms obtained for multiple specific operation points are merged to form a mechanism with the objective of providing a wider range of operating conditions that the mechanism can be applied to. Figure 3.2 shows the algorithm used in the reduction process. Firstly, the reference mechanism (CRECK-S-BIO) is initialized. The reduction process starts by scanning all species. This method consists in computing the error caused by deleting a single specie from the reference mechanism, repeating this process for each specie. The error represents the difference between the results obtained for the reference mechanism and the ones obtained for the reference mechanism without the specie. Afterwards, the species are ordered according to their associated errors. The goal of the scanning method is to evaluate the importance of each specie

in the secondary gas-phase reactions behavior, with the ones with lower associated errors being the less important to the reference mechanism. The deletion of a specie is achieved by eliminating every reaction where this specie is a product and/or a reactant. In the second stage of the reduction process, a range of error margins is established. Species with lower error magnitude than the applied margin are deleted. Consequently, for each margin, a new mechanism is obtained and the error between the new and the reference mechanisms is estimated. Then, the same reduction techniques (scanning and elimination) are applied to the remaining reactions of the reduced mechanisms previously obtained. New further reduced mechanisms with the same number of eliminated species but with a higher number of eliminated reactions are obtained. A post-processing analysis is performed to the obtained results and a reduced mechanism is selected. The reduction methodology is then applied for a range of typical operating conditions, with a reduced mechanism being selected for each condition. Finally, all the selected mechanisms are merged, originating a final mechanism that contains all the reactions from the unified mechanisms.

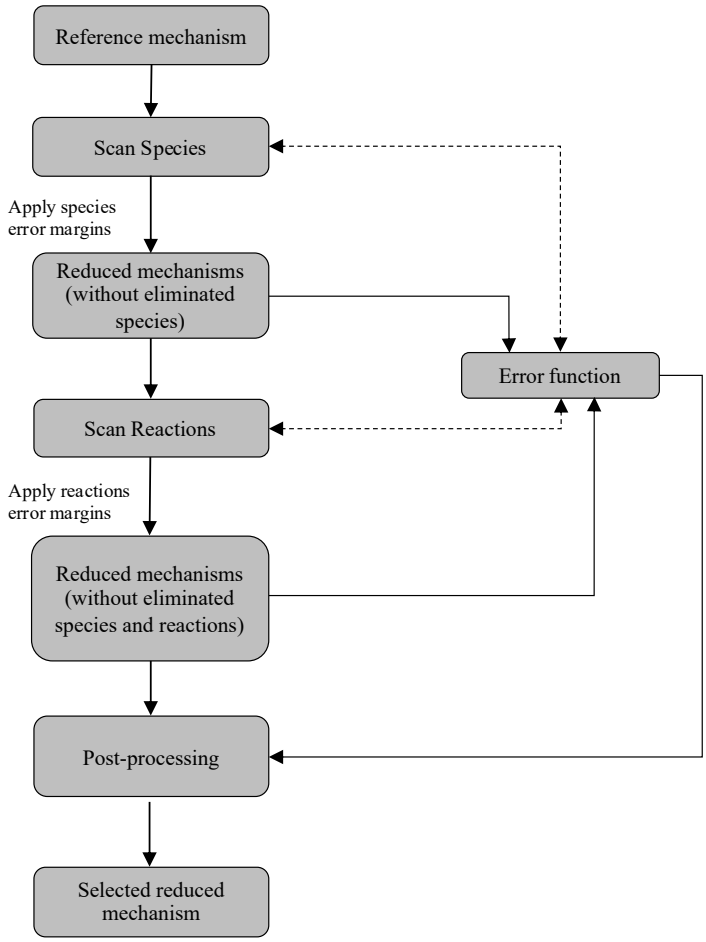

Figure 3.2. Algorithm of the mechanism reduction process

In the present work, the error between the reference and the reduced mechanisms is determined through an error function that is formulated to preserve the behavior and the characteristics of the

reference mechanism. Seven different characteristics are considered: the total gas yield, the H_2, CO and CO_2 yields and release rate peaks. The error associated with the yield parameters represents the difference between the yield values from the reference and reduced mechanisms. The peak error parameters represent the error corresponding to the larger difference between the maximum values (peaks) of the gases release rates (H_2, CO_2 and CO) of the reference mechanism and the values of the release rates points of the reduced mechanism at the same time/position. For each above-mentioned characteristic points, a specific error function, based on the relative error, is defined as:

$$\boldsymbol{\delta_i} = \frac{\left|\boldsymbol{Y_{reference,i}} - \boldsymbol{Y_{reduced,i}}\right|}{\boldsymbol{Y_{reference,i}}} \quad \text{(Eq. 20)}$$

$$\delta = \frac{1}{N}\sum_{i=0}^{N} \delta_i \quad \text{(Eq. 21)}$$

where δ_i represents the error of the ith characteristic point, Y the output value of the evaluated characteristic point. The total error is a result of seven (N) different error contributions, which are important for the analysis of the mechanism's final products and its behavior along the secondary gas-phase reactions of the gasification process. The selected reduced mechanism, as the reference mechanism, will be able to predict the secondary gas-phase reactions that occur during biomass gasification, including mass loss profiles, product speciation, release rates, gas composition and product yields, as function of time/position in a DTF.

4. RESULTS

4.1. REFERENCE MECHANISM

The reduction process was applied to the CRECK-S-BIO mechanism taking into consideration the typical range of gasification working conditions presented in Table 3.3. It is obviously expected that for each condition the results given by the CRECK-S-BIO mechanism are significantly different. An initial study was conducted to assess the results obtained from the gasification process using the CRECK-S-BIO mechanism together with the reactions involving soot and char [7,12,45]. The results from this initial study were then to be compared with the results obtained with the reduced mechanisms. Figure 4.1 shows the results of the syngas low heating value (LHV), final gas yield in volume percentage, the hydrogen to carbon monoxide ratio (H_2/CO ratio), carbon conversion efficiency (CCE) and the amount of unconverted tars for forty-nine different sets of gasification operating conditions. From the analysis of the heatmaps, it is possible to see that the gas yield rises with the rising temperature and with the decreasing value of the steam to biomass ratio. It is also possible to identify a direct relationship between the H_2/CO ratio and the syngas low heating value: the higher the H_2/CO ratio, the lower the syngas LHV, with the LHV decreasing with the decreasing of both temperature and steam to biomass ratio for almost every set of operating conditions presented in Figure 4.1. The H_2/CO ratio increase with the increase of the steam to biomass ratio is related to the significant amount of hydrogen released from the reaction of the steam with the elements present in the mechanism (ex: tar cracking) [46]. Since hydrogen has the lowest heating value of the considered gases that are a part of the syngas, the increase of hydrogen causes a decrease in the LHV. The value of the syngas LHV should present a maximum value around a temperature of 1100ºC which is not verified in Figure 4.1c, which is due to the fact that the char reactions used in this work are not fully optimized [41]. Figure 4.1d shows that the carbon conversion efficiency raises with the increasing temperature and the increase of the steam to biomass ratio, with the temperature being the dominant factor. The increase of the CCE with the S/B is due to the raise in the char destruction [7] and the tar cracking promoting transfer of carbon from the tars and char to the syngas, which also explains the decrease of unconverted tars with the increasing of the S/B [46]. The rise in temperature also promotes the cracking of tars [47] and the char destruction [7] which leads to higher carbon content in the syngas, raising the value of the CCE.

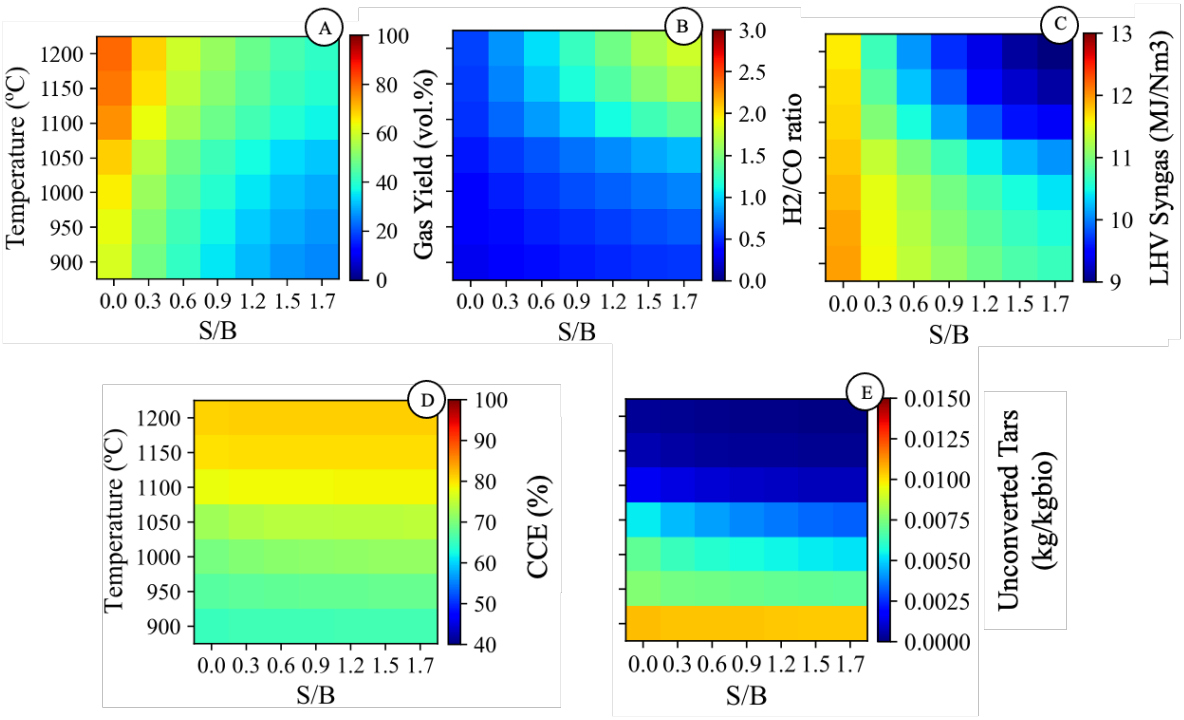

Figure 4.1. a) Gas Yield (vol.%), b) H2/CO ratio, c) syngas LHV, d) CCE (%) and e) amount of unconverted tars predicted values for different sets of typical gasification operating conditions using the reference mechanism.

Figure 4.2 shows five different sets of operating conditions that undergo the reduction process. From each selected condition, a reduced mechanism is obtained and posteriorly merged with the remaining obtained reduced mechanisms, to generate a reduced mechanism that is able to predict the secondary gas-phase reactions of the gasification process in the typical range of biomass gasification operating conditions, for the biomass composition shown in Table 3.2. The selected conditions represent the boundaries of the operating conditions regarding temperature and steam to biomass ratio (red points) and also a set corresponding to the condition equidistant (green central point) from the minimum and maximum boundaries. To assess the importance of the central operating condition in the reduction process, the final reduced mechanism will be obtained using two different methodologies: i) using only the conditions set as the boundaries and ii) adding the central point to the aforementioned conditions.

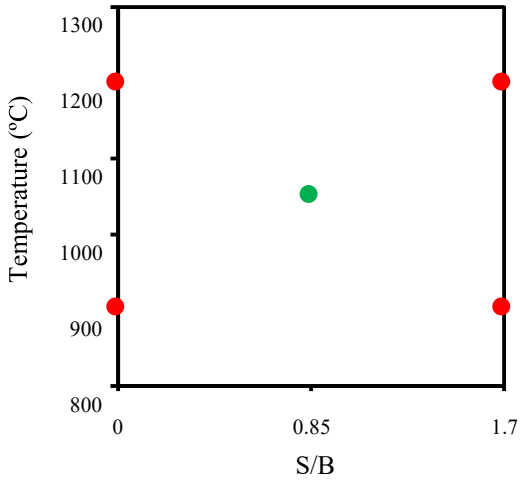

Figure 4.2. Selected operating conditions used in the reduction process.

4.2. REDUCTION AND SELECTION

Figures 4.3 to 4.7 show the data of the reduced mechanisms obtained through the species and reactions reduction steps for each condition presented in Figure 4.2:

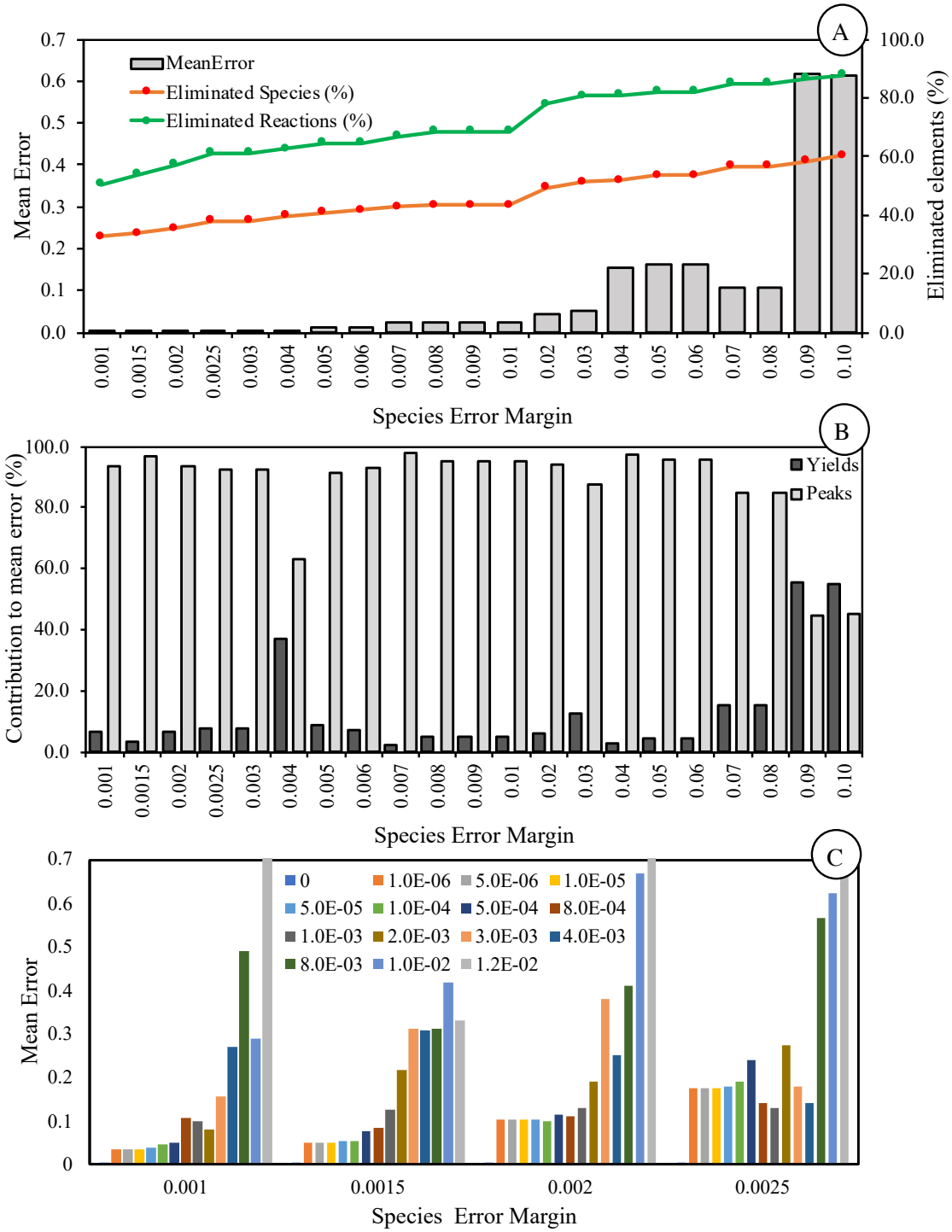

Figure 4.3 a) Mean error for the mechanisms obtained from species reduction, b) Contribution of the peaks and yields errors to the mean error (%) and c) Mean error for mechanisms originated from species and reactions reduction for a temperature of 900 ºC and S/B of 0.

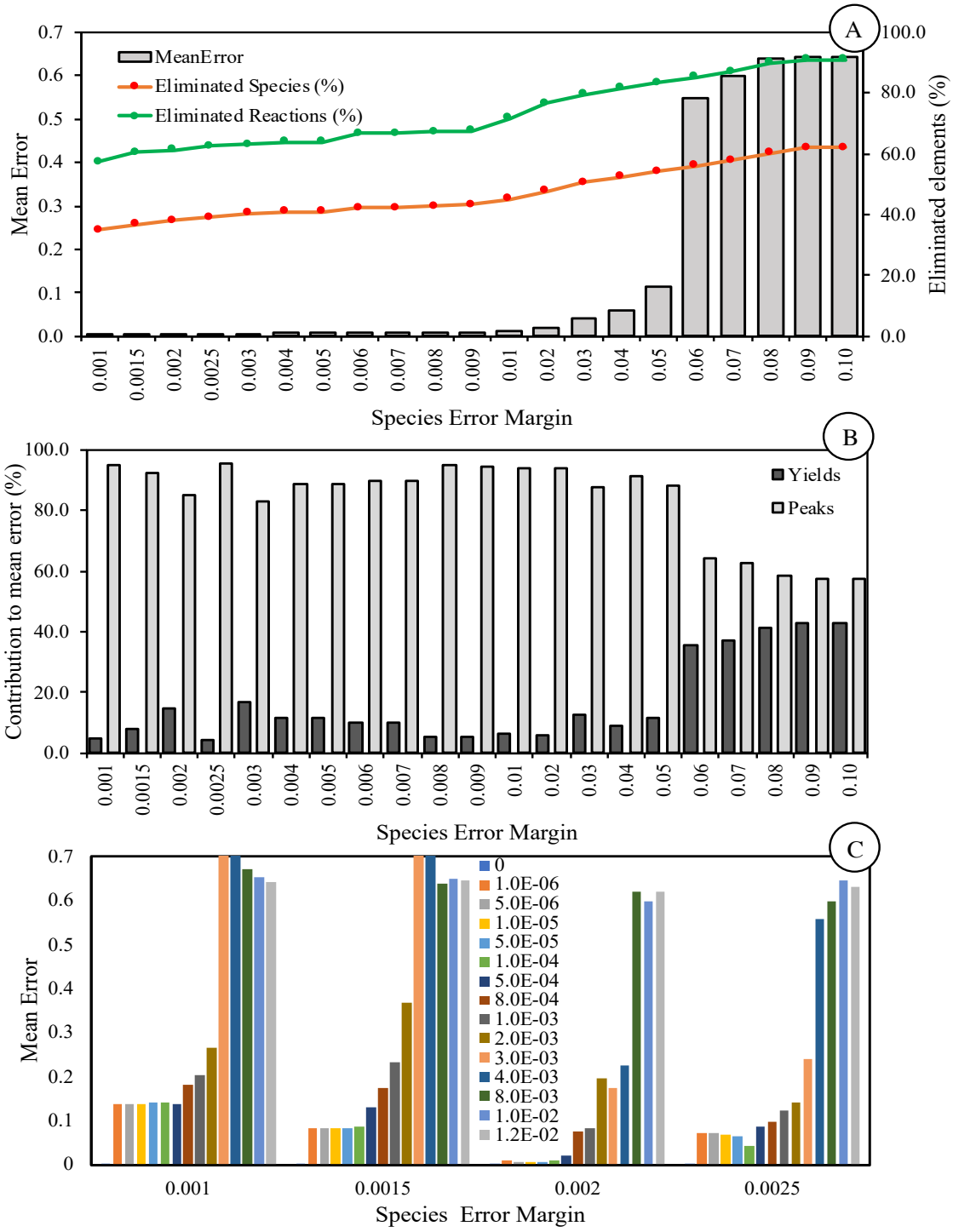

Figure 4.4. a) Mean error for the mechanisms obtained from species reduction, b) Contribution of the peaks and yields errors to the mean error (%) and c) Mean error for mechanisms originated from species and reactions reduction for a temperature of 900 ºC and S/B of 1.7.

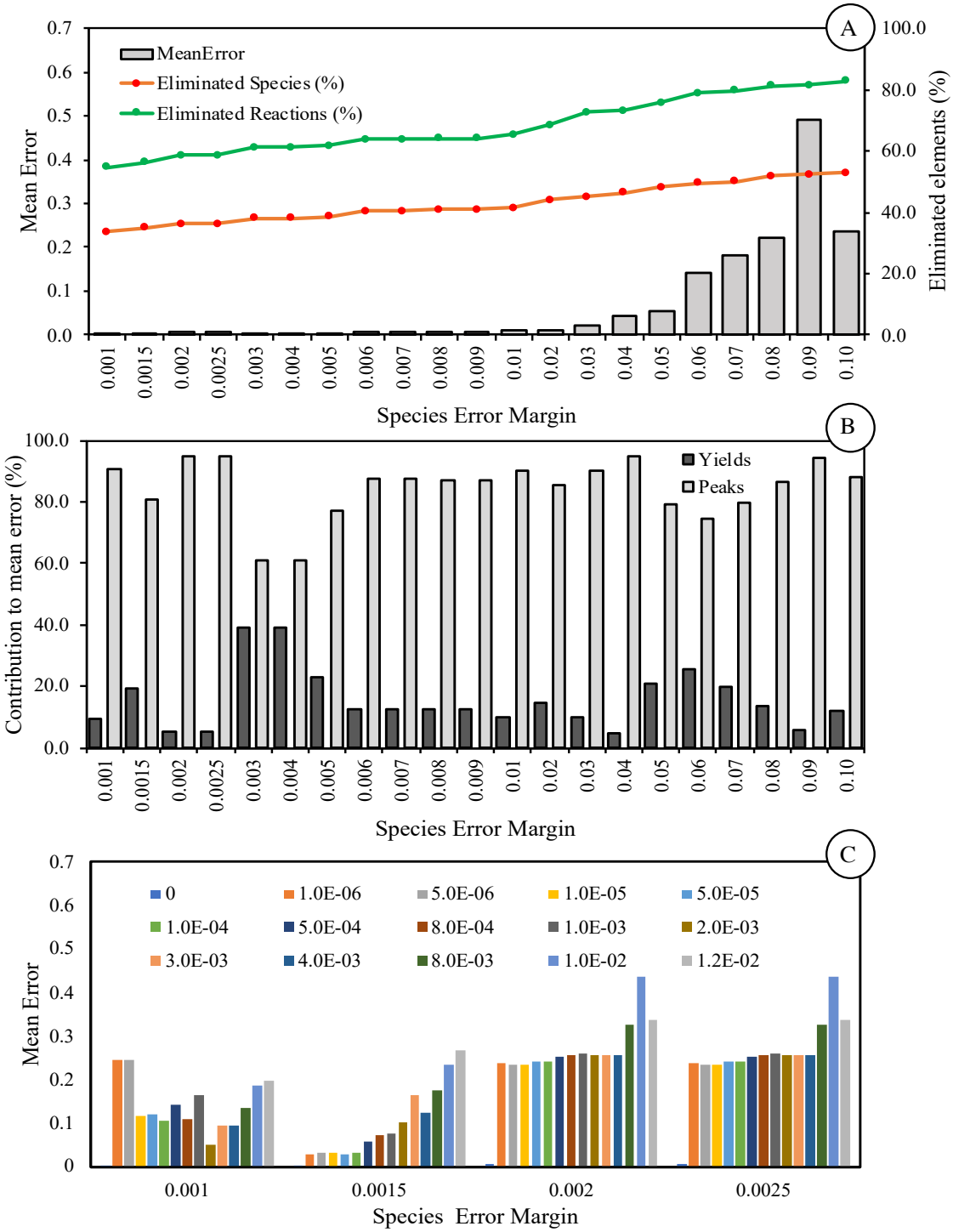

Figure 4.5. a) Mean error for the mechanisms obtained from species reduction, b) Contribution of the peaks and yields errors to the mean error (%) and c) Mean error for mechanisms originated from species and reactions reduction for a temperature of 1050 ºC and S/B of 0.85.

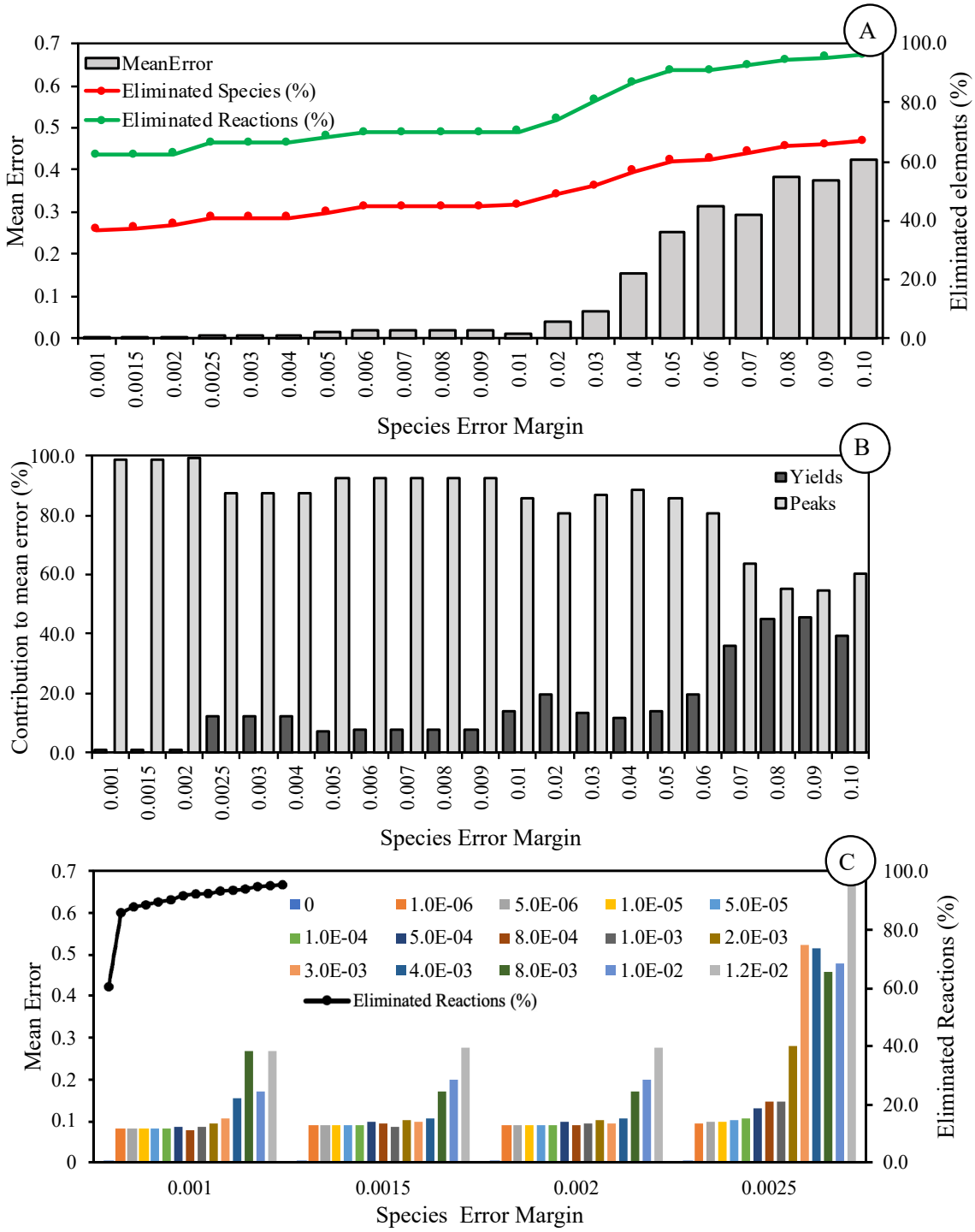

Figure 4.6. a) Mean error for the mechanisms obtained from species reduction, b) Contribution of the peaks and yields errors to the mean error (%) and c) Mean error for mechanisms originated from species and reactions reduction for a temperature of 1200 ºC and S/B of 0.

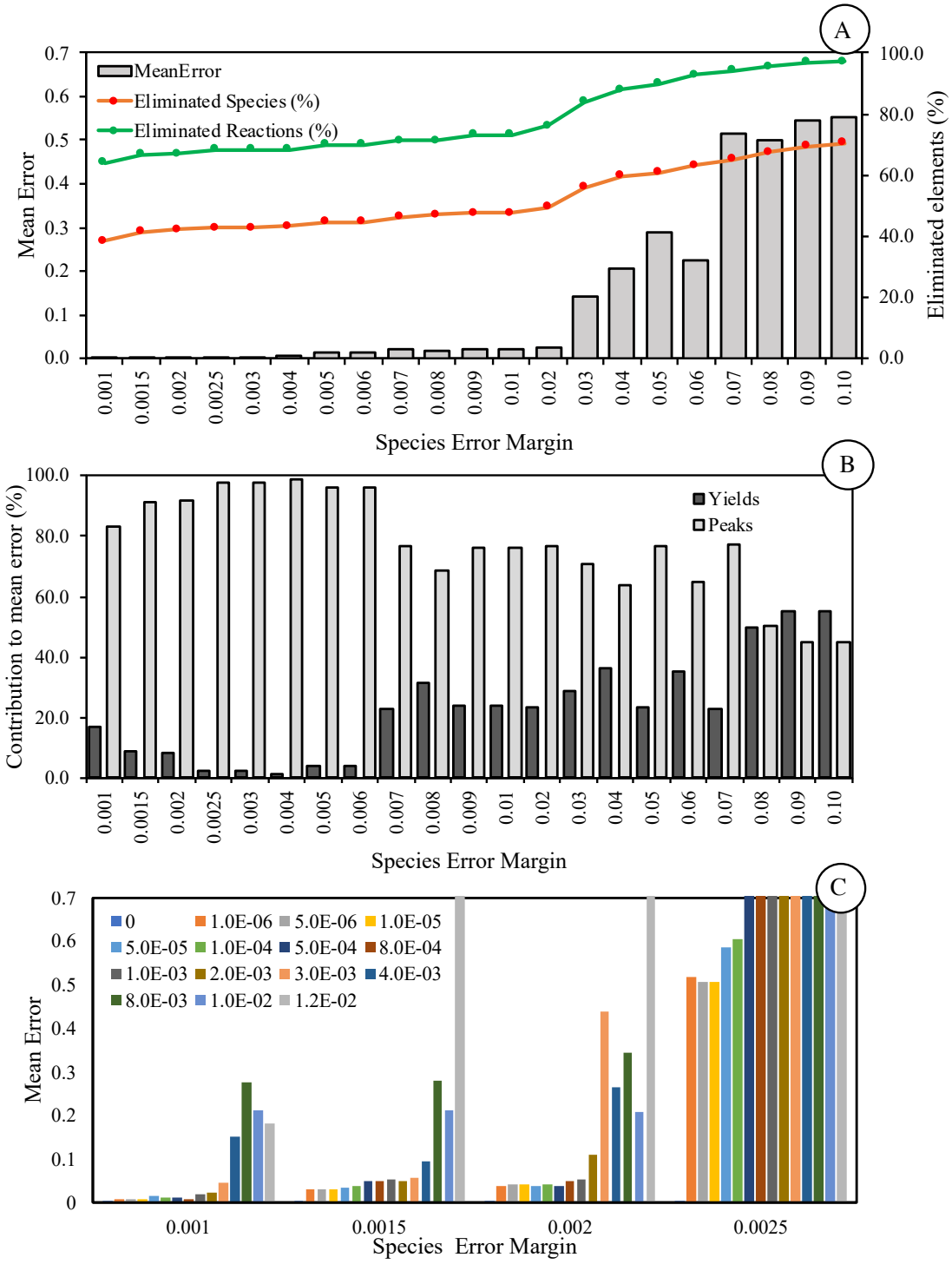

Figure 4.7. a) Mean error for the mechanisms obtained from species reduction, b) Contribution of the peaks and yields errors to the mean error (%) and c) Mean error for mechanisms originated from species and reactions reduction for a temperature of 1200 ºC and S/B of1.7.

Mechanisms that present mean error values higher than approximately 30% were found not to retain the characteristic features (in this work considered the value of the yields and the position of the release rate peaks along the length of the reactor) of the reference mechanism and can therefore be discarded as possible solutions in this present work. However, in Figures 4.3 to 4.7, these mechanisms are nevertheless shown with the purpose of illustrating the variation of the mean error value for the different error margins. The maximum presented value of the mean error is 0.7, although a few mechanisms present higher values. The reason the limit is established in 70% is to enable a better visual inspection of the results for mechanisms associated with error margins that present low mean error values, ensuring at the same time that the variation of the mean error with respect to the species error margin can also be analyzed. Figures A and B from Figures 4.3 to 4.7, show the results obtained for the species reduction step. It was selected a range of 21 different species error margins. For each margin, species with lower mean error values than that margin are eliminated, and a new reduced mechanism is obtained. From the inspection of Figure A from Figures 4.3 to 4.7, it is possible to see that the magnitude of the mean error presents a clear growing tendency with respect to the raise of the value of the species error margin. This result is expected since the higher the value of the species error margin, the higher is the number of eliminated species. It is also possible to identify that the zone corresponding to the interval of error margins [0.01, 0.05] is the range of error margins for which the percentage of eliminated species and reactions tends to present the higher slope, meaning that for these specific operating conditions, this interval is where the elimination of species and their associated reactions is more significant.

As previously shown, the mean error is calculated considering a mean of seven error contributions, four of which are related to the product yields, with the remaining three being associated with release rate peaks. Figure B from Figures 4.3 to 4.7 show the contribution of the release rate peaks and the yields for the mean error. The results show that generally, for significantly high values of the mean error, the contribution of the errors associated with the peaks is lower and the contribution of the errors associated with the yields is higher when compared to mechanisms that present low mean error values. In the area of interest, where the mechanisms that present mean error values lower than 15% (mechanisms that are found to retain the characteristic features of the reference mechanism) are situated, the contribution of the errors associated with the yields of the final products are very low in magnitude and much smaller when compared to the contributions from the peak errors. For the mechanisms with mean error values approximately higher than 30%, the contributions of the yields and peaks errors are generally similar, with the yields error even surpassing the peaks error in some cases (Figures 4.3B and 4.7B)

Figure C from Figures 4.3 to 4.7 show the mean error and the percentage of eliminated reactions for the reactions reduction step. It is worth to emphasize that the reactions reduction step is implemented for mechanisms already reduced in the species reduction step. Each group of columns is associated with a single species error margin. The four groups of bars presented these figures are associated with the first four (lower values) species error margins selected from the species reduction step. This specific selection is due to the fact that the higher the value of the species error margin (higher number of eliminated species), the more sensitive the mechanisms get to the elimination of reactions. This high

sensitivity is demonstrated through the mean error values shown in Figure C from Figures 4.3 to 4.7, which are generally higher for species error margins with higher magnitude, reinforcing the idea that species error margins much higher than 0.0025 do not present meaningful results for the purpose of this work. For the four mechanisms associated with the four species error margins, a range of 14 reactions error margins was selected and analyzed. With the raise of the value of the reactions error margin, a growing tendency of the mean error value is again identified in general. A black line corresponding to the percentage of eliminated reactions is also shown in Figure 4.6C for the species error margin 0.001 and, through its inspection, an initial significant jump can be identified between the mechanism obtained only through species reduction and the mechanism obtained through species and reactions reduction, followed by small increments of eliminated reactions with the increase of the reaction error margin. The percentage of eliminated reactions trends corresponding to the remaining species error margins and for the different operating conditions are similar to the one shown for the species error margin of 0.001 in Figure 4.6C, hence, these are not shown.

The selection process for the mechanisms to be used un the merging step is based on the post-processing analysis of the results obtained in the reduction step. The selection criteria used in this work was chosen through a preliminary analysis of the results of the reduction process and the characteristics of the mechanisms obtained in that process. The value 15% was identified, in a preliminary analysis, as the value below which the mechanisms would keep the core characteristics of the initial detailed mechanism. The criteria, which is based on the mean error and the yields error obtained for each mechanism, is shown in Table 4.1**.** The mechanism selected from each operating condition will be the one with lower number of reactions that matches the selection criteria.

Table 4.1. Selection criteria for mechanisms to undergo the merging step

Criteria Name / Limit variables	Yields error (%)	Mean error (%)
Regular	**< 2**	**< 15**
Conservative	**< 1**	**< 5**
Super Conservative	**< 1**	**< 1**

The super conservative approach was not considered on the mechanisms obtained through the reduction of both species and reactions since none of the mechanisms presents mean error values lower than 1%. Therefore, taking into consideration the previous statement and the fact that were considered three different selection criteria, two different reduction processes (species and species plus reactions) and two different merging approaches (with and without the central point), ten final reduced mechanisms were obtained.

4.3. VALIDATION

The mechanisms originated from the merging step are analyzed in this section and compared with the data obtained from the original mechanism. The analysis is focused on four different parameters: mean

error, number of secondary gas phase reactions, number of species and the computational time. The results obtained through the error calculation for the selected ten mechanisms are shown in Figure 4.8 and the number of reactions, species, the average error and the computational time of each mechanism are shown in Table 4.2. The error scale upper limit is 12% to enable a clear vizualization of the differences between small error values. The computational time associated with the detailed mechanism is 86.9 seconds using the computer with the specifications of table 4.3.

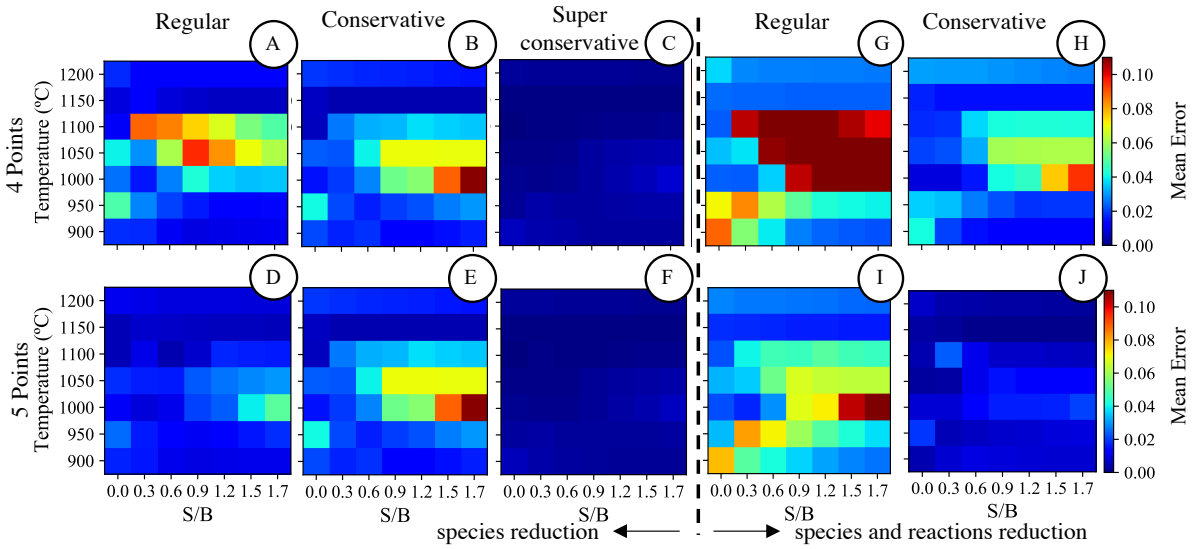

Figure 4.8. Mechanisms originated from species reduction with 4 points A) regular, B) conservative, C) super conservative; and 5 points D) regular, E) conservative; F) super conservative. Mechanisms from species and reactions reduction with 4 points G) regular, H) conservative; and 5 points I) regular, J) conservative.

Table 4.2. Characteristics of the reduced mechanisms obtained in the merging step.

Mechanism /Properties	Reduction Type	N of used points	Criteria Name	N reactions	N Species	Average error (%)	Computational time reduction (%)
A	**Species**	**4**	**Regular**	**1182**	**95**	**3.1**	**49.6**
B			**Conservative**	**1423**	**99**	**2.9**	**46.0**
C			**Super Cons.**	**1776**	**109**	**0.3**	**38.3**
D		**5**	**Regular**	**1202**	**96**	**1.5**	**49.0**
E			**Conservative**	**1423**	**99**	**2.9**	**46.3**
F			**Super Cons.**	**1778**	**109**	**0.2**	**38.1**
G	**Species + Reactions**	**4**	**Regular**	**298**	**111**	**6.7**	**55.7**
H			**Conservative**	**362**	**116**	**3.0**	**42.1**
I		**5**	**Regular**	**322**	**113**	**4.3**	**55.2**
J			**Conservative**	**476**	**116**	**0.8**	**52.9**
Reference	**-**	**-**	**-**	**4533**	**166**	**-**	**-**

Table 4.3. Work computer specifications.

CPU	Intel® core™ i7 quad-core CPU @ 2.60GHz
RAM	16.00 GB LPDDR3 2133 MHz

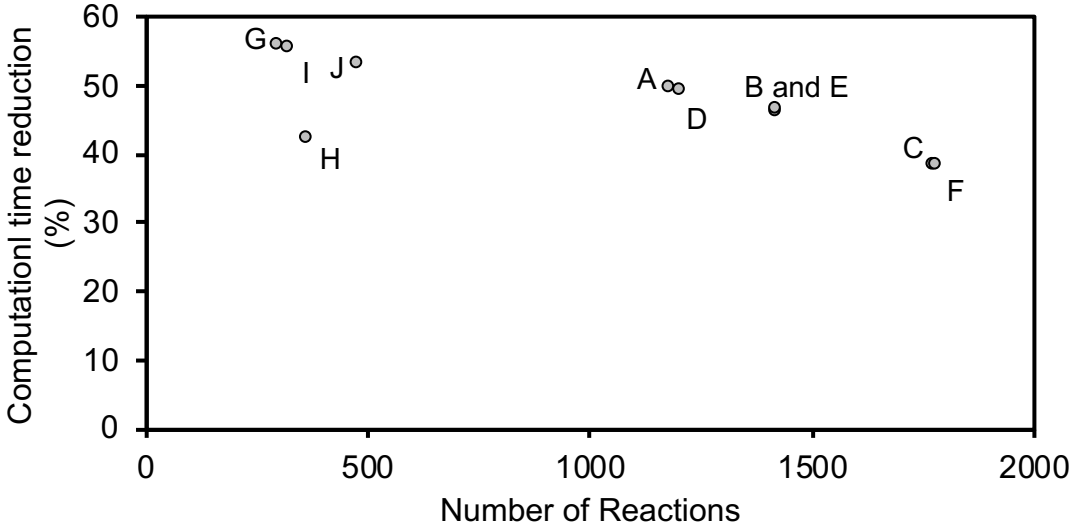

Figure 4.9. Computation time (%) as a function of the number of reactions.

Analyzing the error heatmaps of the mechanisms built from the merging of only the reduced mechanisms associated with the four conditions set as the boundaries (Figures 4.8A-C, 4.8G,H), it is found that the more conservative the selection criteria is, the lower is the error. For the mechanisms originated from the merge of all five sets of operating points considered (Figures 4.8D-F, 4.8I,J), the same tendency is verified except for mechanism E, for which the error actually increases when compared to mechanism D. This fact, together with the phenomena of reduced mechanisms that have more reactions, but still present higher errors shown in Figures 4.3 to 4.7, show that, despite the tendency verified during the entire reduction process of mechanisms with lower number of reactions presenting higher errors when compared to the original mechanism, it is clear that this relation does not present a full linearity when using the reduction methodology used in this work. Analyzing the influence of the inclusion of the central point of operating conditions, it is clear that for the regular approach using both reduction techniques and for the conservative approach in the species and reactions reduction side, the error is significantly lower for the case where mechanisms from all five operating points are considered. It is also clear that for the cases where the central operating condition is not considered, the higher values of the error are located for operating conditions close to the ones associated with that point, with the error generally decreasing when approaching minimum or maximum boundaries of both temperature and steam to biomass ratio.

From the general analysis of all six mechanisms resulting from species reduction (Figures 4.8A-F), it can be concluded that when using more conservative approaches, which originates the merge of the mechanisms with higher number of reactions, the mechanisms obtained with or without the inclusion

of the central operating point tend to be very similar or even equal. The previous conclusion is supported by the similarity of the remaining studied parameters (number of reactions, number of species and computational time) for the mechanisms obtained through the conservative and super conservative approaches, listed in Table 4.2. Therefore, the influence of the central point is only significant and visible in Figure 4.8 for the mechanisms with lower number of reactions (Figure 4.8A,D, Figure 4.8G,I, Figure 4.8H,J). It can be identified a higher influence of the central point in the behavior of the final reduced mechanisms obtained through species and reactions reduction when compared to the mechanism obtained through the reduction of species exclusively, as the mechanisms obtained using the same selection criteria present values of error and numbers of reactions significantly different for the results with and without the consideration of the central point. This fact sustains the conclusion previously stated that the central point of the operating conditions has more influence on the results when there are less reactions in the merged mechanisms. This is due to not considering some reaction paths when eliminating reactions.

It should be noted that the two mechanisms obtained from the species reduction process using the super conservative approach have the same number of species and a different number of reactions. That is due to the fact that for both the reduction of species and the reduction of both species and reactions, the merged mechanisms are built from joining all reactions that belong to the reduced mechanisms, with the species taking part in the reduction step but not in the merging step. Another important result worth noticing is that mechanisms obtained with the reduction of both species and reactions have a significantly lower number of reactions and present a higher number of species, when compared to the mechanisms obtained only with the reduction of species. The reason of such results is due to the species and reactions reduction process, i.e., the species error margins selected have a very low magnitude, which implies a lower number of species eliminated.

In Table 4.2 it is shown the reduction of the computational time obtained when using the reduced mechanisms compared to the original mechanism. It can be identified reductions up to 55.71 % on the computational time. The computer used to obtain these times has the specifications presented in Table 4.3. Due to the low error values associated with mechanisms D, C, F and J shown in Figure 4.8 and consequent low average errors shown in Table 4.2, it is possible to consider these mechanisms the most viable alternatives to the initial detailed mechanism when predicting the secondary gas-phase reactions that occur during biomass gasification, using a composition similar to the one shown in Table 3.2. Analyzing Figure 4.9, it can be concluded that the reduction of computational time increases as the number of reactions decrease, which is what it was expected, with the exception being mechanism H. This exception may be due to different reaction paths that occur during the gasification process in this mechanism, which leads to a higher time for the CVODE solver [44] implemented in the numerical tool used in this work to conclude its calculations. Another conclusion that can be withdrawn from Figure 4.5 is that the decrease of computational time with the decrease of the number of reactions presents a continuously lower slope with the decreasing number of reactions. This slope decrease can be visually identified between the reduced mechanisms in Figure 4.9. A very good result was found for mechanism J which presents not only a very low number of reactions and a very low error values for all sets of

operating conditions, but also a very high percentage of computational time reduction (52.91%). Mechanism J is provided in the supplementary material.

Figure 4.1 presented the results for the syngas LHV, the final gas yield in volume percentage, the hydrogen to carbon monoxide ratio (H_2/CO ratio), the carbon conversion efficiency and the amount of unconverted tars for the selected operating conditions, using the reference mechanism and the reactions from the soot formation and char reduction. After an identical study using the obtained reduced mechanisms and adding the same soot formation and char reduction reactions, it was concluded that the results obtained regarding the parameters presented in Figure 4.1 with all reduced mechanisms are the same as the ones obtained using the initial detailed mechanism. The reason such phenomena is possible is because the mean errors obtained between the reduced and the reference mechanisms is almost exclusively due to the peak errors, with the errors associated with the yields being close to zero as discussed in the next section. Since the gasification parameters (gas yield, carbon conversion efficiency, syngas LHV, H_2/CO ratio and unconverted tars) are directly related only with final product yields, and since the yields errors are significantly small, these parameters will present equal or very close values to the ones of the reference mechanism, obtaining heatmaps identical or even qual with the heatmaps associated with the gasification parameters obtained with the reference mechanism presented in Figure 4.1

4.4. ANALYSIS OF OPERATING CONDITIONS WITH HIGH MEAN ERROR VALUES

The inspection of Figure 4.8 allowed the identification of specific operating conditions that present high mean error values when compared with the remaining studied operating condition. The conditions that better corroborate the previous statement are the one with temperature of 1000 ºC and 1.7 of steam to biomass ratio and the one with temperature of 1050 ºC and steam to biomass ratio of 0.9, which is the condition closest to the central operating point presented in Figure 4.2. A deep study of the behavior of the reference mechanism and the six mechanisms with higher average error values (shown in Table 4.2: A, B, E, G, H and I) in the previously mentioned operating conditions,is presented in Figures 4.10 and 4.11.

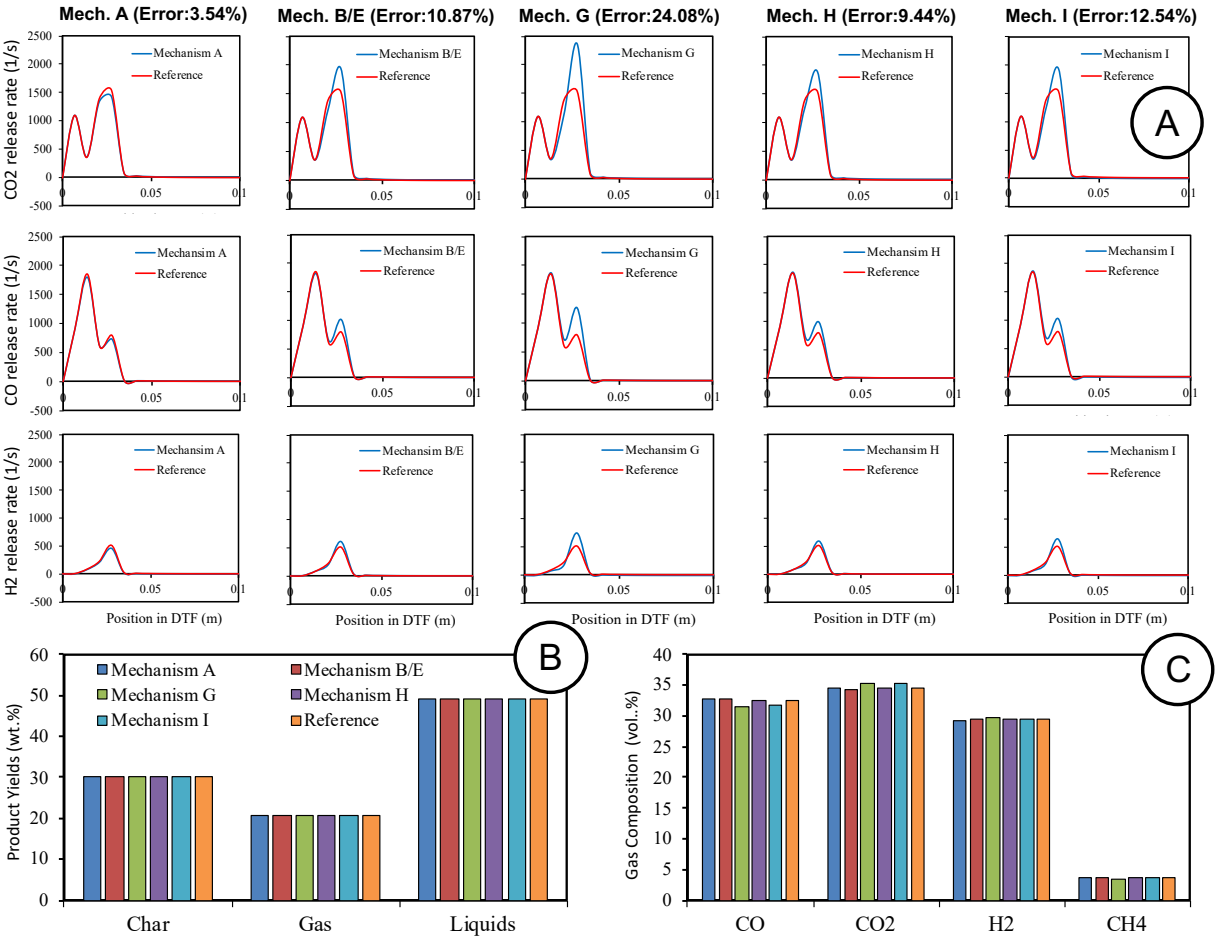

Figure 4.10. a) CO_2 release rate (1/s), CO release rate (1/s) and H_2 release rate (1/s) as function of position in the DTF (m); b) product yields (wt.%) and c) gas composition (vol.%) for mechanism A, B, D, G, H, and I and the reference mechanisms for an operating temperature of 1000ºC and S/B of 1.7.

Analyzing Figure 4.10A and 4.11A, it is possible to verify that the errors associated with the peaks of the H_2, CO and CO_2 release rates are the only significant contributions to the mean error, as Figures 4.10B, 4.10C, 4.11B and 4.11C show identical values of the yields for both operating conditions. As previously discussed, mean error values lower than approximately 15% present contributions of the error of the release rate peaks significantly higher than the ones from the errors of the yields. The results shown in Figures 4.10 and 4.11 support this statement, showing also that some mechanisms that present errors between approximately 15~30 % can also retain the characteristic features of the reference mechanism, although it is not the case for a significant majority of mechanisms that present this error values. The higher mean error values obtained for the operating condition studied in Figure 4.10 suggests significantly different reaction paths when compared to the remaining operating conditions. The same possible conclusion can be applied to the operating condition with temperature 900 ºC and S/B of 0 (and the surrounding operating conditions area), which although being considered in the reduction process, also presents higher error values when compared with the average error from the remaining operating conditions for three of the four mechanisms obtained through reduction of both species and reactions. The difference in the release rate curves between the reduced and the reference

mechanisms shown in Figures 4.10 and 4.11 are exclusively obtained due to the peaks magnitude. Therefore, since the release rate peaks occur approximately for the same time, position (in the DTF) and temperature of the values of the yields are very approximate with the ones from the reference mechanism, it is possible to state that mechanisms A, B, E, G, H and I are considered to keep the core characteristic features of the reference mechanism, although presenting poor results with respect to the magnitude of the release rate peaks.

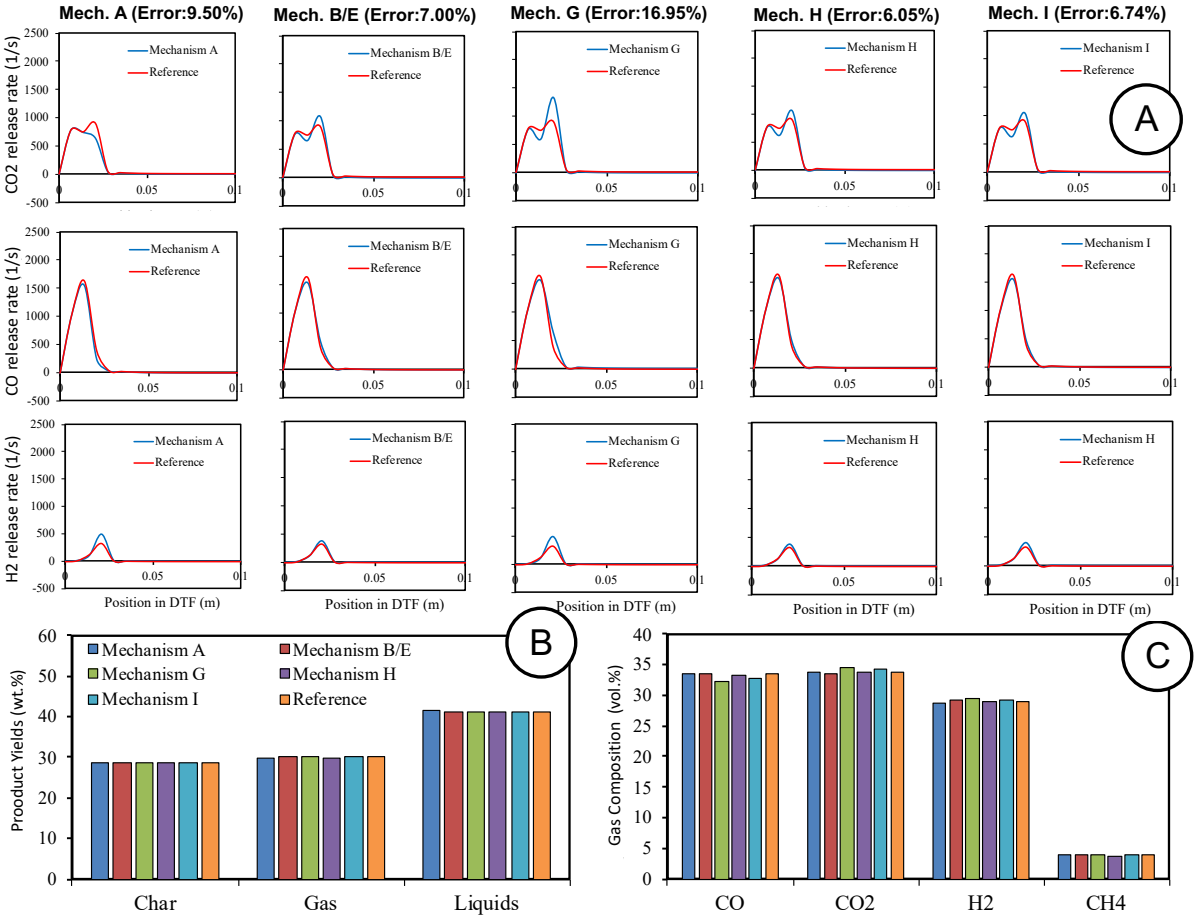

Figure 4.11. a) CO_2 release rate (1/s), CO release rate (1/s) and H_2 release rate (1/s) as function of position in the DTF (m); b) product yields (wt.%) and c) gas composition (vol.%) for mechanism A, B, D, G, H, and I and the reference mechanisms for an operating temperature of 1050ºC and S/B of 0.9.

4.5 REDUCED MECHANISM PERFORMANCE FOR BIOMASS COMPONENTS

The reference mechanism has been validated for a wide range of fuels, nevertheless the methodology developed in this work considered only the sample of wheat straw. Hence, to verify if the obtained reduced mechanism J is able to keep the characteristic features of the reference mechanism for a wide range of fuels, a sensitivity analysis on biomass components was carried out. Therefore, this mechanism was evaluated separately for each reference component of biomass (CELL, HCE, LIGC, LIGH, LIGO, TGL and TANN). This was carried out considering the two operating condition with the

higher mean error values: T = 1000 ºC with S/B =1.7 and T = 1050 ºC with S/B =0.9, with the results (errors of each considered characteristic for each reference component) shown in Table 4.4 and Table 4.5, respectively.

Table 4.4. Errors of each considered characteristic for each reference component for operating condition T=1000 ºC and S/B=1.7.

Component	$\delta_{gas\ yield}$	$\delta_{H_2\ yield}$	$\delta_{CO\ yield}$	$\delta_{CO_2\ yield}$	$\delta_{H_2\ peaks}$	$\delta_{CO\ peaks}$	$\delta_{CO_2\ peaks}$	Mean error
CELL	0.01%	0.10%	0.07%	0.03%	1.04%	0.85%	1.24%	0.48%
HCE	0.03%	0.16%	0.18%	0.09%	2.17%	0.71%	1.42%	0.68%
LIGC	0.04%	0.10%	0.13%	0.07%	0.84%	14.77%	16.38%	4.62%
LIGH	0.08%	0.19%	0.28%	0.35%	0.41%	1.54%	1.50%	0.62%
LIGO	0.02%	0.07%	0.12%	0.06%	0.24%	0.13%	0.14%	0.11%
TGL	0.61%	3.99%	12.32%	0.99%	23.59%	14.61%	4.77%	8.70%
TANN	0.03%	0.13%	0.16%	0.13%	1.63%	0.97%	1.51%	0.65%

Table 4.5. Errors of each considered characteristic for each reference component for operating condition T=1050 ºC and S/B=0.9.

Component	$\delta_{gas\ yield}$	$\delta_{H_2\ yield}$	$\delta_{CO\ yield}$	$\delta_{CO_2\ yield}$	$\delta_{H_2\ peaks}$	$\delta_{CO\ peaks}$	$\delta_{CO_2\ peaks}$	Mean error
CELL	0.02%	0.10%	0.08%	0.05%	0.90%	1.04%	1.04%	0.46%
HCE	0.05%	0.16%	0.26%	0.12%	1.00%	0.53%	1.37%	0.50%
LIGC	0.01%	0.08%	0.13%	0.08%	3.48%	12.23%	11.90%	3.99%
LIGH	0.08%	0.21%	0.25%	0.37%	0.35%	4.35%	0.91%	0.93%
LIGO	0.02%	0.08%	0.11%	0.06%	0.18%	0.42%	0.24%	0.16%
TGL	0.04%	0.13%	0.15%	0.13%	1.71%	1.48%	1.73%	0.77%
TANN	0.5%	2.24%	4.37%	0.78%	7.71%	10.04%	2.05%	3.96%

It is clear that generally all errors are very small, hence, it can be concluded that mechanism J is able to keep the characteristic features of the reference mechanism for a wide range of biomass fuels. The higher errors, observed for LIGC and TGL components in Table 4.4 and for LIGC and TANN in Table 5.5, are mainly due to the release rate peaks magnitude that, as established above, are not critical in a macroscopic analysis. The CO yield error for TGL for the operating condition T=1000ºC and S/B=1.7 is also relatively high. However, the CO yield is around 3% of the final gas composition for this specific case, hence a 12.36% of error corresponds to a low relevance change in the CO yield regarding the final gas composition.

5. CONCLUSIONS

5.1 SUMMARY

The objective of this work was to obtain a reduced mechanism that kept the features of the CRECK-S-BIO mechanism, while reducing the computational time. A reactor model was built and implemented in python in order to compare the reference and reduced mechanisms within typical operating conditions selected through the inspection of the available literature on biomass gasification. A reduction method was implemented and, according to the chosen selection criteria, ten reduced mechanisms were obtained. Their error results based on the product yields, gas composition and release rate peaks of CO, CO_2 and H_2 along with their characteristics (number of species, number of reactions and computational time) were compared with the ones from the reference mechanism to assess their validity and possible use in future applications. The gasification parameters such as carbon conversion efficiency, amount of unconverted tars, low heating value of the syngas and H_2/CO ratio were also taken into account in the assessment of their validity to simulate the gasification process with accuracy with respect to the original mechanism.

5.2 MAIN CONCLUSIONS

The main conclusions that can be withdrawn from this work are the following:

- The reduction methodology applied in this work is found to effectively reduce the reference mechanism, obtaining reduced mechanisms capable of accurately predicting the behavior of the reference mechanism together with significantly reducing the computational time, which are the cases of mechanisms C, D, F and J.
- The remaining mechanisms retain the essential characteristic features of the reference mechanism, but are not able to predict with a very high precision the release rate curves of the major non-condensable gases (H_2, CO and CO_2) for some operating conditions;
- The errors obtained for the reduced mechanisms in the interest region (mean error < 15%) have a near-exclusive contribution of the magnitude of the release rate peaks, with the yield values and the location of those peaks presenting very identical values to the ones obtained with the reference detailed mechanism;
- A tendency of mechanisms with lower number of reactions presenting higher errors is verified. However, the presence of a small minority of mechanisms that do not respect this tendency reveals the absence of a full linearity regarding the aforementioned relation when using this reduction method;
- The consideration of operating conditions located at the interior of the parametric domain in the merging step of the reduction process generally leads to the construction of mechanisms better suited to predict the mechanism behavior for the entire range of operating conditions when compared to the mechanism built from the merge of reduced mechanism obtained using only boundary operating conditions;

- The computational time decreases with the decrease of the number of reactions, with the reduction being more significant the higher the number of reactions of the mechanisms compared;
- Different rection paths for different operating conditions and different mechanisms can cause of a higher difficulty in the prediction of the mechanism’s behavior for those same operating conditions and the raise in computational time, respectively;
- One can highlight that in order to obtain a suitable reduced mechanism able to predict the reference mechanism's behavior, the mechanism reduction procedure strongly depends on the following main aspects: the selection criteria used to select the reduced mechanisms to be merged, the choice of the operating conditions to represent the parametric domain boundaries and the addition of operating conditions at the interior of the parametric domain;
- The sensitivity analysis carried out on the biomass components proved that mechanism J is able to keep the characteristic features of the reference mechanism for a wide range of biomass fuels.

5.3 RECOMMENDATIONS FOR FUTURE WORK

The reduction methodology presented in this work represents the base point of a complex reduction method that can be further developed. A wider range of error margins can be applied along with a larger number of selection criteria with the goal of obtaining more viable mechanisms with lower number of species and/or reactions. The parametric study can also be further developed with the study of other gasification parameters besides temperature and steam to biomass ratio such as type of gasifying agent, equivalence ratio and types of biomass. The development of the previously mentioned studies can enhance the effectiveness and range of application of the numerical tool developed in this work for mechanism reduction.

6. REFERENCES

[1] Z. Wang, Q. Bui, B. Zhan, T. L. H. Pham, "Biomass energy production and its impacts on the ecological footprint: An investigation of the G7 countries", *Science of the Total Environment*, vol.743, 140741, 2020.

[2] V. S. Vassilev, D. Baxter, L. K. Andersen, C. G. Vassileva, T. J. Morgan, "An overview of the organic and inorganic phase composition of biomass", *Fuel* , vol. 94, pp. 1–33, 2012.

[3] A. D. Sagar, S. Kartha, "Bioenergy and sustainable development?" *Annual Review of Environment and Resources*, vol. 32, pp. 31-67, 2007.

[4] IEA Bioenergy 2021, Forest management and market responses, IEA Bionenergy, viewed in 22 March 2021, <https://www.ieabioenergy.com/ieapublications/faq/woodybiomass/market-responses>.

[5] P.Basu, "Biomass gasification and pyrolysis: Practical Design and Theory", Elsevier Inc., Oxford, UK, 2010.

[6] E. Ranzi, P. E. A. Debiagi, A. Frassoldati, "Mathematical Modeling of Fast Biomass Pyrolysis and Bio-Oil Formation. Note I: Kinetic Mechanism of Biomass Pyrolysis", *ACS Sustainable Chemistry and* Engineering, vol. 5, pp. 2867-2881, 2017.

[7] A. I. Ferreiro, R. Segurado, M. Costa, "Modelling soot formation during biomass gasification", *Renweable and Sustainable Energy Review*, vol. 134, 110380, 2020.

[8] S. Safarian, R. Unnþórsson, C. Richter, "A review of biomass gasification modelling", *Renweable and Sustainable Energy Reviews*, vol. 110, pp. 378-391, 2019.

[9] WBC Laboratory 2021, Gasification- poly-generation from biomass, WBC Laboratory, viewed 22 March 2021, <https://wbc-lab.com/gasification>.

[10] A. Anca-Couce, "Reaction mechanisms and multi-scale modelling of lignocellulosic biomass pyrolysis", *Progress in Energy and Combustion Science*, vol. 53, pp. 41-79, 2016.

[11] P. E. A. Debiagi, G. Gentile, M. Pelucchi, A. Frassoldati, A. Cuoci, T. Faravelli, E. Ranzi, "Detailed kinetic mechanism of gas-phase reactions of volatiles released from biomass pyrolysis", *Biomass and Bioenergy*, vol.93, pp. 60-71, 2016.

[12] P. Debiagi, G. Gentile, A. Cuoci, A. Frassoldati, E. Ranzi, T. Faravelli. "A predictive model of biochar formation and characterization", *Journal of Analytical and Applied Pyrolysis*, vol. 134, pp. 326-335, 2018.

[13] E. Ranzi, P. E. A. Debiagi, A. Frassoldati, "Mathematical Modeling of Fast Biomass Pyrolysis and Bio-Oil Formation. Note II: Secondary Gas-Phase Reactions and Bio-Oil Formation", *ACS Sustainable Chemistry and* Engineering, vol. 5, pp. 2882-2896, 2017.

[14] C. Netzer, T. Li, L. Seidel, F. Mauß, T. Løvås, "Stochastic reactor-based fuel bed model for grate furnaces", *Energy and Fuels*, vol. 34, pp. 16599-16612, 2020.

[15] H. Goyal, P. Pepiot, "A Compact Kinetic Model for Biomass Pyrolysis at Gasification Conditions", *Energy and Fuels*, vol. 31, pp. 12120-12132, 2017.

[16] Y. Chang, M. Jia, B. Niu, X. Dong, P. Wang, "Reduction of large-scale chemical mechanisms

using global sensitivity analysis on reaction class/sub-mechanism", *Combustion and Flame*, vol. 212, pp. 355-366, 2020.

[17] W. Wang, X. Gou, "A Mechanism Reduction Method Integrating Path Flux Analysis with Multi Generations and Sensitivity Analysis", *Combustion Science and Technology*, vol. 189, pp. 24-42, 2017.

[18] L. Petzold, W. Zhu, "Model reduction for chemical kinetics: An optimization approach", *AIChE Journal*, vol. 45, pp. 869-886, 1999.

[19] Y. Zhao, S. Sun, H. Zhou, R. Sun, H. Tian, J. Luan, J. Qian, "Experimental study on sawdust air gasification in an entrained-flow reactor", *Fuel Processing Technology*, vol. 91, pp. 910-914, 2010.

[20] J. J. Hernández, G. Aranda-Almansa, A. Bula, "Gasification of biomass wastes in an entrained flow gasifier: Effect of the particle size and the residence time", *Fuel Processing Technology*, vol. 91, pp. 681-692, 2010.

[21] K. Qin, P. A. Jensen, W. Lin, A. D. Jensen, "Biomass gasification behavior in an entrained flow reactor: Gas product distribution and soot formation", *Energy and Fuels*, vol. 26, pp. 5992-6002, 2012.

[22] J. J. Hernández, G. Aranda, J. Barba, J. M. Mendoza, "Effect of steam content in the air-steam flow on biomass entrained flow gasification", *Fuel Processing Technology*, vol. 99, pp. 43-55, 2012.

[23] J. Billaud, S. Valin, M. Peyrot, S. Salvador, "Influence of H2O, CO2 and O2 addition on biomass gasification in entrained flow reactor conditions: Experiments and modelling", *Fuel*, vol. 166, pp. 166-178, 2016.

[24] X. Ku, J. Wang, H. Jin, J. Lin, "Effects of operating conditions and reactor structure on biomass entrained-flow gasification", *Renewable Energy*, vol. 139, pp. 781-795, 2019.

[25] W. Jangsawang, K. Laohalidanond, S. Kerdsuwan, "Optimum Equivalence Ratio of Biomass Gasification Process Based on Thermodynamic Equilibrium Model", *Energy Procedia*, vol. 79. pp. 520-527, 2015.

[26] M. J. Prins, "Thermodynamic analysis of biomass gasification and torrefaction", PhD Thesis, Technische University Eindhovent, 2005.

[27] S. V. Vassilev, D. Baxter, L. K. Andersen, C. G. Vassileva, "An overview of the chemical composition of biomass", *Fuel* , vol.89 , pp. 913-933, 2010.

[28] E. R. Widjaya, G. Chen, L. Bowtell, C. Hills, "Gasification of non-woody biomass: A literature review", *Renweable and Sustainable Energy Reviews, vol. 89,* pp.184-193, 2018.

[29] J. U. Hernández-Beltrán, I. O Hernández-De Lira, M. M. Cruz-Santos, A. Saucedo-Luevanos, F. Hernández-Terán, N. Balagurusamy, "Insight into pretreatment methods of lignocellulosic biomass to increase biogas yield: Current state, challenges, and opportunities", *Applied Sciences*, vol. 9, 18th Edition, 2019.

[30] A. I. Ferreiro, "Pyrolysis of Pine Bark , Wheat Straw and Rice Husk : Thermogravimetric Analysis and Kinetic Study", MSc Thesis, Intituto Superior Técnico, 2015.

[31] M. La Villetta, M. Costa, N. Massarotti, "Modelling approaches to biomass gasification: A review

with emphasis on the stoichiometric method", *Renweable and Sustainable Energy Reviews*, vol. 74, pp. 71-88, 2017.

[32] A. Molino, S. Chianese, D. Musmarra, "Biomass gasification technology: The state of the art overview", Journal of Energy Chemistry , vol. 25, pp.10-25, 2016.

[33] D. R. Tree, K. I. Svensson, "Soot processes in compression ignition engines", Progress in Energy and Combustion Science , vol. 33, pp. 272-309, 2007.

[34] S. Karimipour, R. Gerspacher, R. Gupta, R. J. Spiteri, "Study of factors affecting syngas quality and their interactions in fluidized bed gasification of lignite coal", *Fuel*, vol. 103, pp. 308-320, 2013.

[35] L. Wei, J. A. Thomasson, R. M. Bricka, R. Sui, J. R. Wooten, E. P. Columbus, "Syn-Gas Quality Evaluation for Biomass Gasification with a Downdraft Gasifier", Transactions of the ASABE, vol.52, pp. 21-37, 2009.

[36] V. Silva, E. Monteiro, N. Couto, P, Brito, A. Rouboa, "Analysis of syngas quality from Portuguese biomasses: An experimental and numerical study", *Energy and Fuels*, vol. 28, pp. 5766-5777, 2014.

[37] M. M. Sarafraz, M. R. Safaei, M. Jafarian, M. Goodarzi, M. Arjomandi, "High quality syngas production with supercritical biomass gasification integrated with a water–gas shift reactor", *Energies*, vol. 12, pp. 1-14, 2019.

[38] Y. Cao, Z. Gao, J. Jin, H. Zhou, M. Cohron, H. Zhao, H. Liu, W. Pan, "Synthesis gas production with an adjustable H2/CO ratio through the coal gasification process: Effects of coal ranks and methane addition", *Energy and Fuels*, vol. 22, pp. 1720-1730, 2008.

[39] L. Waldheim, T. Nilsson, "Heating value of gases from biomass gasification", IEA Bioenergy Agreement Task 20 - Thermal Gasification of Biomass, 2001.

[40] T. Rio, "Wheat Straw and Pig Manure Gasification in a Drop Tube Furnace", MSc Thesis, Instituto Superior Técnico, 2019.

[41] F.S Duarte, "Biomass Gasification in a Drop Tube Furnace", MSc Thesis, Instituto Superior Técnico, 2018.

[42] Stringel S. High temperature gasification of millimétriques de bois entre 800 ° C et 1400 ° C 2011.

[43] A. I. Ferreiro AI, P. Giudicianni, C. M. Grottola, M. Rabaçal, M. Costa, R. Ragucci, "Unresolved Issues on the Kinetic Modeling of Pyrolysis of Woody and Nonwoody Biomass Fuels", *Energy and Fuels*, vol. 31, pp. 4035-4044, 2017.

[44] D. G. Goodwin, H. K. Moffat HK, "Cantera: An object-oriented software toolkit for chemical kinetics, thermodynamics, and transport processes", https://www.cantera.org.

[45] D. F. Fletcher, B. S. Haynes, F. C. Christo, S. D. Joseph, "A CFD based combustion model of an entrained flow biomass gasifier", *Applied Mathematrical Modelling*, vol.24, pp. 165-82, 2000.

[46] W. Song, C. Deng, S. Guo, "Effect of Steam on the Tar Reforming during Circulating Fluidized Bed Char Gasification", *ACS Omega*, vol. 6, pp, 11192-11198, 2021.

[47] B. Das, "Effect of Temperature on Gasification Performance of Biomass in a Bubbling Fluidized Bed Gasifier", *International Asian Congress on Contemporary Science - IV*, pp. 588-596, 2020.

7. APPENDIX

The reactions of reduced mechanism J (very accurate reduced mechanism) are here presented in the format they are introduced in the python software along with three parameters of the Arrhenius equation with the first number being the pre-exponential factor, the second the temperature exponent and the third the activation energy (cal/mol):

```
reaction('H + O2 <=> O + OH', [9.600000e+14, -0.2, 16625.0])
reaction('H2 + O <=> H + OH', [4.330000e+13, 0.0, 10000.0])
falloff_reaction('H + O2 (+M) <=> HO2 (+M)',
                 kf=[5.580000e+12, 0.4, 0.0],
                 kf0=[8.400000e+17, -0.8, 0.0],
                 efficiencies='AR:0.8 CO:1.2 CO2:2.4 H2:2.5 H2O:18.0 HE:0.8 N2:1.26 ',
                 falloff=Troe(A=0.5, T3=1e-30, T1=1.0000000000000002e+30, T2=0.0))
reaction('HO2 + OH <=> H2O + O2', [5.000000e+13, 0.0, 1000.0])
reaction('H + HO2 <=> 2 OH', [2.500000e+14, 0.0, 1900.0])
reaction('HO2 + O <=> O2 + OH', [3.250000e+13, 0.0, 0.0])
reaction('2 OH <=> H2O + O', [3.570000e+04, 2.4, -2110.0])
reaction('H + HO2 <=> H2 + O2', [2.500000e+13, 0.0, 700.0])
reaction('2 HO2 <=> H2O2 + O2', [2.110000e+12, 0.0, 0.0])
falloff_reaction('2 OH (+M) <=> H2O2 (+M)',
                 kf=[7.400000e+13, -0.37, 0.0],
                 kf0=[1.300000e+18, -0.9, -1700.0],
                 efficiencies='AR:0.7 C2H6:3.0 CH4:2.0 CO:1.5 CO2:2.0 H2:2.0 H2O:6.0 HE:0.7 N2:0.9 ',
                 falloff=Troe(A=0.7346, T3=94.0, T1=1756.0, T2=5182.0))
reaction('HCO + O2 <=> CO + HO2', [3.000000e+12, 0.0, 0.0])
falloff_reaction('CO + O (+M) <=> CO2 (+M)',
                 kf=[9.640000e+10, 0.0, 3800.0],
                 kf0=[2.070000e+26, -3.34, 7610.0],
                 efficiencies='AR:0.5 CO:1.5 CO2:2.0 H2:2.0 H2O:12.0 ')
reaction('CO + OH <=> CO2 + H', [9.600000e+11, 0.14, 7352.0])
reaction('CO + OH <=> CO2 + H', [7.320000e+10, 0.03, -16.0])
reaction('CO + HO2 <=> CO2 + OH', [3.000000e+13, 0.0, 23000.0])
reaction('CO + H2O <=> CO2 + H2', [2.000000e+11, 0.0, 38000.0])
falloff_reaction('CH3 + H (+M) <=> CH4 (+M)',
                 kf=[1.200000e+15, -0.4, 0.0],
                 kf0=[6.400000e+23, -1.8, 0.0],
                 efficiencies='CO:2.0 CO2:3.0 H2:2.0 H2O:5.0 ',
                 falloff=SRI(A=0.45, B=797.0, C=979.0, D=1.0, E=0.0))
falloff_reaction('2 CH3 (+M) <=> C2H6 (+M)',
                 kf=[2.500000e+13, 0.0, 0.0],
                 kf0=[2.330000e+34, -5.03, -1200.0],
                 efficiencies='CO:2.0 CO2:3.0 H2:2.0 H2O:5.0 ',
                 falloff=Troe(A=0.38, T3=73.0, T1=1180.0, T2=0.0))
falloff_reaction('C2H5 + H (+M) <=> C2H6 (+M)',
                 kf=[5.210000e+17, -0.99, 1580.0],
                 kf0=[1.990000e+41, -7.08, 6685.0],
                 efficiencies='AR:0.7 C2H6:3.0 CH4:2.0 CO:1.5 H2O:6.0 ',
                 falloff=Troe(A=0.8422, T3=125.0, T1=2219.0, T2=6882.0))
reaction('CH2CHCH2 + H <=> AC3H4 + H2', [1.810000e+13, 0.0, 0.0])
falloff_reaction('CH2CHCH2 + H (+M) <=> C3H6 (+M)',
                 kf=[1.000000e+14, 0.0, 0.0],
                 kf0=[1.330000e+60, -12.0, 5967.8],
                 efficiencies='AR:0.7 C2H6:3.0 CH4:2.0 CO:1.5 CO2:2.0 H2:2.0 H2O:6.0 ',
                 falloff=Troe(A=0.02, T3=1097.0, T1=10970.0, T2=6860.0))
```

```
falloff_reaction('C2H5 + CH3 (+M) <=> C3H8 (+M)',
        kf=[9.600000e+14, -0.5, 0.0],
        kf0=[6.800000e+61, -13.42, 6000.0],
        falloff=Troe(A=1.0, T3=1000.0, T1=1434.0, T2=5329.0))
falloff_reaction('C3H3 + H (+M) <=> AC3H4 (+M)',
        kf=[1.000000e+17, -0.8, 315.0],
        kf0=[3.500000e+33, -4.9, 2225.0],
        efficiencies='C2H6:4.3 CH4:2.9 CO:2.1 CO2:2.9 H2:2.9 H2O:8.6 ',
        falloff=Troe(A=0.709, T3=134.0, T1=1784.0, T2=5740.0))
falloff_reaction('C3H3 + H (+M) <=> PC3H4 (+M)',
        kf=[1.000000e+17, -0.8, 315.0],
        kf0=[3.500000e+33, -4.9, 2225.0],
        efficiencies='C2H6:4.3 CH4:2.9 CO:2.1 CO2:2.9 H2:2.9 H2O:8.6 ',
        falloff=Troe(A=0.709, T3=134.0, T1=1784.0, T2=5740.0))
falloff_reaction('C2H3 + CH3 (+M) <=> C3H6 (+M)',
        kf=[2.500000e+13, 0.0, 0.0],
        kf0=[4.270000e+58, -11.94, 9770.0],
        efficiencies='AR:0.7 C2H6:3.0 CH4:2.0 CO:1.5 CO2:2.0 H2:2.0 H2O:6.0 ',
        falloff=Troe(A=0.175, T3=1341.0, T1=60000.0, T2=10140.0))
reaction('C4H4 <=> C2H + C2H3', [1.000000e+16, 0.0, 105000.0])
reaction('NC4H8 <=> CH2CHCH2 + CH3', [2.000000e+16, 0.0, 78000.0])
falloff_reaction('H + SC4H7 (+M) <=> NC4H8 (+M)',
        kf=[5.000000e+13, 0.0, 0.0],
        kf0=[1.330000e+60, -12.0, 5967.8],
        efficiencies='AR:0.7 C2H6:3.0 CH4:2.0 CO:1.5 CO2:2.0 H2:2.0 H2O:6.0 ',
        falloff=Troe(A=0.02, T3=1097.0, T1=10970.0, T2=6860.0))
reaction('C2H2 + C2H3 <=> C4H4 + H', [2.500000e+14, -0.71, 6700.0])
reaction('C4H5 <=> C2H2 + C2H3', [7.500000e+12, 0.0, 40000.0])
reaction('C2H3 + H <=> C2H2 + H2', [3.000000e+13, 0.0, 0.0])
reaction('C2H4 + H2 <=> C2H5 + H', [1.000000e+14, 0.0, 65000.0])
reaction('C2H3 + CH3 <=> C2H2 + CH4', [1.333000e+13, 0.0, 0.0])
reaction('C3H3 + CH2CHCH2 => C2H2 + C4H6', [5.000000e+11, 0.0, 0.0])
falloff_reaction('C2H2 + H (+M) <=> C2H3 (+M)',
        kf=[1.000000e+13, 0.0, 2770.0],
        kf0=[3.900000e+16, 0.0, -560.0],
        efficiencies='CO:2.0 CO2:3.0 H2:2.0 H2O:5.0 ')
falloff_reaction('C2H4 + H (+M) <=> C2H5 (+M)',
        kf=[1.770000e+13, 0.0, 2110.0],
        kf0=[4.600000e+18, 0.0, 1070.0],
        efficiencies='CO:2.0 CO2:3.0 H2:2.0 H2O:5.0 ',
        falloff=Troe(A=1.0, T3=1e-15, T1=95.0, T2=200.0))
falloff_reaction('AC3H4 + H (+M) <=> CH2CHCH2 (+M)',
        kf=[1.200000e+11, 0.69, 3007.0],
        kf0=[5.660000e+33, -5.0, 4448.0])
falloff_reaction('AC3H4 + H (+M) <=> CH2CCH3 (+M)',
        kf=[8.490000e+12, 0.0, 2000.0],
        kf0=[1.110000e+34, -5.0, 4448.0])
reaction('H + PC3H4 <=> CH2CCH3', [5.000000e+13, 0.0, 4000.0])
reaction('CH2CCH3 <=> C2H2 + CH3', [2.000000e+13, 0.0, 38000.0])
reaction('IC3H7 <=> NC3H7', [2.000000e+12, 0.0, 42000.0])
reaction('NC3H7 <=> C2H4 + CH3', [1.000000e+13, 0.0, 32000.0])
reaction('NC3H7 <=> C3H6 + H', [1.000000e+13, 0.0, 39500.0])
reaction('C4H2 + H <=> C4H3', [2.500000e+14, 0.0, 3016.0])
reaction('C4H5 <=> C4H4 + H', [5.000000e+12, 0.0, 44000.0])
reaction('C4H4 + H <=> C2H + C2H4', [2.000000e+13, 0.0, 2000.0])
reaction('CH2C3H5 <=> C2H3 + C2H4', [2.500000e+13, 0.0, 38000.0])
reaction('2 CH3 <=> C2H5 + H', [1.400000e+14, 0.0, 14000.0])
reaction('H + PC3H4 <=> C2H2 + CH3', [2.000000e+05, 2.5, 1000.0])
reaction('C2H6 <=> C2H4 + H2', [3.000000e+13, 0.0, 71000.0])
falloff_reaction('CH3OH (+M) <=> CH3 + OH (+M)',
```

```
            kf=[7.000000e+20, -1.3, 92000.0],
            kf0=[1.250000e+14, 0.85, 67000.0])
reaction('CH3CHO <=> CH3 + HCO', [1.500000e+16, 0.0, 85000.0])
reaction('C3H6 + OH => CH3 + CH3CHO', [2.000000e+12, 0.0, 0.0])
reaction('C2H2 + O2 <=> HCCO + OH', [2.000000e+07, 1.5, 30000.0])
reaction('CH4 + O2 <=> CH3 + HO2', [9.000000e+13, 0.0, 56000.0])
reaction('CH2O + O2 <=> HCO + HO2', [1.300000e+14, 0.0, 41000.0])
three_body_reaction('HCO + M <=> CO + H + M', [1.200000e+17, -1.0, 17000.0],
              efficiencies='CH4:2.8 CO:1.9 CO2:3.0 H2:1.9 H2O:5.0 ')
falloff_reaction('CH3O (+M) <=> CH2O + H (+M)',
            kf=[6.000000e+11, 0.0, 18000.0],
            kf0=[1.200000e+25, -2.7, 30600.0])
three_body_reaction('CH2OH + M <=> CH2O + H + M', [3.750000e+14, 0.0, 25000.0])
reaction('CH3CO <=> CH2CO + H', [1.000000e+14, 0.0, 49000.0])
three_body_reaction('CH3CO + M <=> CH3 + CO + M', [2.500000e+15, 0.0, 14400.0])
reaction('CH2CO + H => CH3 + CO', [1.000000e+06, 2.0, 2000.0])
reaction('CH2CO + H <=> H2 + HCCO', [3.600000e+14, 0.0, 8600.0])
reaction('CH3OH + H => CH3 + H2O', [6.500000e+11, 0.0, 5300.0])
reaction('C2H4 + O <=> CH3 + HCO', [5.000000e+06, 1.88, 200.0])
reaction('AC3H4 + O => C2H4 + CO', [2.000000e+13, 0.0, 0.0])
reaction('C3H6 + O => C2H5 + HCO', [1.000000e+13, 0.0, 3000.0])
reaction('CH2O + O => CO2 + 2 H', [2.000000e+13, 0.0, 5000.0])
reaction('CH3CHO + O => CH3 + CO2 + H', [2.000000e+13, 0.0, 3000.0])
reaction('CH2CO + O => 2 HCO', [2.000000e+13, 0.0, 2300.0])
reaction('C2H2 + OH => CH3 + CO', [1.500000e+11, 0.0, 0.0])
reaction('CH2CO + OH => CH3 + CO2', [1.000000e+13, 0.0, 0.0])
reaction('CH2CO + OH => CH2O + HCO', [1.000000e+13, 0.0, 0.0])
reaction('C4H4 + OH => CH2CHCH2 + CO', [3.000000e+13, 0.0, 0.0])
reaction('C2H2 + HO2 => CH2O + HCO', [5.000000e+12, 0.0, 15000.0])
reaction('C2H2 + O2 => CH2O + CO', [3.000000e+11, 0.0, 26000.0])
reaction('CH2CO + O2 => CH2O + CO2', [1.000000e+14, 0.0, 37000.0])
reaction('C2H2 + O2 => 2 HCO', [3.000000e+11, 0.0, 27000.0])
reaction('C2H4 + O2 => CH3O + HCO', [1.000000e+14, 0.0, 43000.0])
reaction('CH2OH + O2 <=> CH2O + HO2', [6.000000e+12, 0.0, 0.0])
reaction('C2H5 + O2 => C2H4 + HO2', [1.000000e+12, 0.0, 3000.0])
reaction('C2H3 + O2 <=> CH2CHO + O', [7.500000e+14, -0.61, 5260.0])
reaction('C2H3 + O2 => CH2O + HCO', [1.000000e+12, 0.0, 4000.0])
reaction('C2H3 + O2 => CH2CO + OH', [6.000000e+11, 0.0, 1000.0])
three_body_reaction('CH3 + O + M => CH3O + M', [5.000000e+16, 0.0, 0.0])
reaction('C2H5 + O => 0.3 C2H4 + 0.35 CH2O + 0.35 CH3 + 0.35 CH3CHO + 0.35 H + 0.3 OH',
[5.000000e+13, 0.0, 0.0])
reaction('CH2CHCH2 + O => C2H3 + CH2O', [3.250000e+13, 0.0, 0.0])
reaction('CH3 + OH <=> CH2OH + H', [1.100000e+13, 0.0, 6300.0])
reaction('CH3 + OH <=> CH2O + H2', [6.000000e+12, 0.0, 0.0])
reaction('CH3 + OH <=> CH4 + O', [2.000000e+12, 0.0, 8000.0])
reaction('CH3 + HO2 <=> CH3O + OH', [6.000000e+12, 0.0, 0.0])
reaction('C2H5 + HO2 => CH2O + CH3 + OH', [5.000000e+12, 0.0, 0.0])
reaction('CH2CHCH2 + HO2 => C2H3 + CH2O + OH', [3.500000e+11, 0.0, 0.0])
reaction('H + HCO <=> CO + H2', [5.000000e+13, 0.0, 0.0])
reaction('HCO + OH <=> CO + H2O', [5.000000e+13, 0.0, 0.0])
reaction('HCO + HO2 => CO2 + H + OH', [3.000000e+13, 0.0, 0.0])
reaction('CH3 + HCO <=> CH4 + CO', [1.000000e+13, 0.0, 0.0])
reaction('CH2OH + CH3 => CH2O + CH4', [1.500000e+13, 0.0, 0.0])
reaction('CH2CHO <=> CH3CO', [2.000000e+11, 0.0, 32000.0])
reaction('CH2CHO <=> CH2CO + H', [6.000000e+13, 0.0, 41000.0])
reaction('C2H4 + O => CH2CHO + H', [1.000000e+13, 0.0, 3000.0])
reaction('C2H2 + OH => CH2CHO', [5.000000e+11, 0.0, 0.0])
reaction('C4H6 + OH => 0.2 C2H3 + 0.25 C2H4 + 0.25 CH2CHO + 0.55 CH2O + 0.2 CH3CHO + 0.55
CHCHCH3', [5.000000e+12, 0.0, 0.0])
reaction('CH2S + H2 <=> CH3 + H', [7.200000e+13, 0.0, 0.0])
```

```
reaction('CH3 + OH <=> CH2S + H2O', [2.000000e+13, 0.0, 0.0])
reaction('CH2O + CH3 <=> CH3CHO + H', [2.000000e+11, 0.0, 7600.0])
reaction('CH2 + O2 <=> CH2O + O', [5.000000e+13, 0.0, 9000.0])
reaction('CH2 + O2 <=> CO + H2O', [1.600000e+13, 0.0, 1500.0])
reaction('CH2 + O2 <=> CO + H + OH', [1.700000e+13, 0.0, 1500.0])
reaction('CH2 + O2 <=> CO2 + 2 H', [1.320000e+13, 0.0, 1500.0])
three_body_reaction('CH2S + M <=> CH2 + M', [1.000000e+13, 0.0, 0.0],
                efficiencies='C2H2:4.0 H:20.0 H2O:3.0 ')
reaction('C2H2 + O <=> CH2 + CO', [3.500000e+03, 2.8, 500.0])
reaction('C2H2 + O <=> H + HCCO', [5.000000e+06, 2.0, 1900.0])
falloff_reaction('CH2CO (+M) <=> CH2 + CO (+M)',
              kf=[1.500000e+14, 0.0, 76000.0],
              kf0=[5.500000e+15, 0.0, 59270.0])
reaction('CH2CO + O <=> CH2 + CO2', [1.500000e+12, 0.0, 1350.0])
reaction('HCCO <=> CH + CO', [6.500000e+12, 0.0, 59000.0])
reaction('H + HCCO <=> CH2S + CO', [1.500000e+14, 0.0, 0.0])
reaction('HCCO + O <=> 2 CO + H', [9.600000e+13, 0.0, 600.0])
reaction('HCCO + O2 <=> 2 CO + OH', [1.600000e+12, 0.0, 830.0])
reaction('HCCO + O2 <=> CO2 + HCO', [2.400000e+11, 0.0, -854.0])
reaction('C2H + O2 <=> HCCO + O', [2.300000e+13, 0.0, 0.0])
reaction('C4H2 + O <=> C3H2 + CO', [2.700000e+13, 0.0, 1660.0])
reaction('C4H2 + OH <=> C3H2 + HCO', [3.000000e+12, 0.0, 0.0])
reaction('C3H3 + H <=> C3H2 + H2', [1.500000e+13, 0.0, 3000.0])
reaction('C3H3 + O <=> C2H + CH2O', [3.000000e+13, 0.0, 0.0])
reaction('C3H3 + OH <=> C3H2 + H2O', [1.500000e+13, 0.0, 3000.0])
reaction('C3H3 + O2 <=> CH2CO + HCO', [2.000000e+10, 0.0, 2840.0])
reaction('C3H3 + HCO <=> CO + PC3H4', [2.500000e+13, 0.0, 0.0])
reaction('C3H2 + O2 <=> HCCO + HCO', [4.000000e+13, 0.0, 0.0])
reaction('C3H6 + H <=> CH2CHCH2 + H2', [1.000000e+07, 2.0, 4200.0])
reaction('C2H4 + OH <=> C2H3 + H2O', [2.000000e+13, 0.0, 6000.0])
reaction('CH3OH + H <=> CH3O + H2', [9.000000e+12, 0.0, 6100.0])
reaction('CH3OH + H <=> CH2OH + H2', [3.200000e+13, 0.0, 6100.0])
reaction('CH2O + H <=> H2 + HCO', [4.500000e+14, 0.0, 7500.0])
reaction('CH3CHO + H <=> CH3CO + H2', [4.500000e+14, 0.0, 7500.0])
reaction('AC3H4 + H <=> C3H3 + H2', [5.000000e+07, 2.0, 5000.0])
reaction('H + PC3H4 <=> C3H3 + H2', [1.000000e+07, 2.0, 5000.0])
reaction('OH + PC3H4 <=> C3H3 + H2O', [8.000000e+06, 2.0, 1000.0])
reaction('H + H2O <=> H2 + OH', [4.800000e+10, 1.0, 19000.0])
reaction('H + H2O2 <=> H2O + OH', [2.410000e+13, 0.0, 3970.0])
reaction('H + H2O2 <=> H2 + HO2', [6.025000e+13, 0.0, 7950.0])
reaction('CH4 + H <=> CH3 + H2', [3.000000e+07, 2.0, 10000.0])
reaction('C2H6 + H <=> C2H5 + H2', [1.430000e+14, 0.0, 10500.0])
reaction('C3H8 + H <=> H2 + NC3H7', [1.270000e+14, 0.0, 10500.0])
reaction('C3H8 + H <=> H2 + IC3H7', [3.200000e+13, 0.0, 7900.0])
reaction('CH2O + HO2 => H2O2 + HCO', [5.200000e+12, 0.0, 13000.0])
reaction('CH3OH + OH => CH2OH + H2O', [9.200000e+04, 2.53, -1000.0])
reaction('CH3OH + HO2 => CH2OH + H2O2', [8.000000e+13, 0.0, 19400.0])
reaction('C3H6 + OH => CH2CHCH2 + H2O', [1.680000e+06, 2.0, -432.1])
reaction('C2H2 + OH <=> C2H + H2O', [3.370000e+07, 2.0, 14000.0])
reaction('CYC5H6 <=> CYC5H5 + H', [1.500000e+15, 0.0, 81500.0])
reaction('CYC5H6 + OH => C4H6 + HCO', [8.000000e+12, 0.0, 0.0])
reaction('CYC5H6 + OH => C2H2 + C2H4 + HCO', [2.000000e+12, 0.0, 0.0])
reaction('CYC5H6 + OH => C2H2 + CH2CO + CH3', [2.000000e+13, 0.0, 0.0])
reaction('CYC5H6 + O => C4H6 + CO', [1.000000e+13, 0.0, 0.0])
reaction('CYC5H6 + O => C4H5 + HCO', [1.500000e+13, 0.0, 0.0])
reaction('CYC5H6 + O => AC3H4 + CH2CO', [3.000000e+12, 0.0, 0.0])
reaction('CYC5H6 + O => CH2CO + PC3H4', [3.000000e+12, 0.0, 0.0])
reaction('CYC5H5 + HO2 => C4H5 + CO + OH', [3.300000e+13, 0.0, 0.0])
reaction('CYC5H5 + HO2 => C2H + C2H4 + CO + OH', [1.500000e+13, 0.0, 0.0])
reaction('CYC5H5 + HO2 => C4H4 + HCO + OH', [3.000000e+12, 0.0, 0.0])
```

```
reaction('CYC5H5 + OH => C2H2 + C2H4 + CO', [2.000000e+14, 0.25, 4350.0])
reaction('CYC5H5 + OH => C3H3 + CH2CO + H', [3.500000e+13, 0.25, 4350.0])
reaction('CYC5H5 + OH => C4H6 + CO', [1.250000e+13, 0.25, 4350.0])
reaction('CYC5H5 + O => C4H5 + CO', [1.000000e+14, 0.0, 0.0])
reaction('CYC5H5 + O2 => C5H5O + O', [1.500000e+11, 0.0, 16000.0])
reaction('C5H5O => CYC5H4O + H', [1.000000e+13, 0.0, 52000.0])
reaction('CYC5H6 + H => CYC5H5 + H2', [1.600000e+15, 0.0, 7925.0])
reaction('CYC5H5 + H2 => CYC5H6 + H', [1.800000e+14, 0.0, 30000.0])
reaction('CYC5H6 + OH => CYC5H5 + H2O', [1.000000e+14, 0.0, 1714.0])
reaction('CYC5H5 => C2H2 + C3H3', [2.000000e+12, 0.0, 68000.0])
reaction('CH3 + CYC5H5 => C2H3 + C4H5', [1.000000e+12, 0.0, 3000.0])
reaction('CH3 + CYC5H5 => C2H2 + C4H6', [1.500000e+12, 0.0, 3000.0])
reaction('2 CYC5H5 => C10H8 + 2 H', [1.000000e+12, 0.0, 6000.0])
reaction('CH3 + CYC5H5 => MCPTD', [1.000000e+13, 0.0, 3000.0])
reaction('H + MCPTD => CH3 + CYC5H6', [1.500000e+13, 0.0, 2000.0])
reaction('C6H6 <=> C6H5 + H', [1.500000e+17, 0.0, 114000.0])
reaction('C6H6 + OH => CO + CYC5H6 + H', [1.000000e+13, 0.0, 7000.0])
falloff_reaction('2 C3H3 (+M) <=> C6H6 (+M)',
                 kf=[3.000000e+12, 0.0, 0.0],
                 kf0=[5.000000e+17, 0.0, 0.0])
reaction('2 C3H3 <=> C6H5 + H', [3.000000e+12, 0.0, 0.0])
reaction('C6H5 + O => CO + CYC5H5', [1.000000e+14, 0.0, 0.0])
reaction('C6H6 + H <=> C6H5 + H2', [1.500000e+14, 0.0, 10000.0])
reaction('C10H8 + H => C4H4 + C6H5', [5.000000e+12, 0.0, 2500.0])
reaction('CH3 + O2 <=> CH3OO', [2.000000e+12, 0.0, 0.0])
reaction('CH3OO <=> CH2O + OH', [1.500000e+13, 0.0, 47000.0])
reaction('CH3 + CH3OO => 2 CH3O', [3.000000e+13, 0.0, -1200.0])
three_body_reaction('CH3CHOH + M <=> CH3CHO + H + M', [1.800000e+24, -2.5, 34200.0])
falloff_reaction('C2H4 + OH (+M) <=> C2H4OH (+M)',
                 kf=[2.000000e+12, 0.0, 0.0],
                 kf0=[2.000000e+15, 0.0, -10000.0],
                 falloff=Troe(A=0.25, T3=1e-30, T1=1.0000000000000002e+30, T2=0.0))
reaction('CH3CHOH + O2 <=> CH3CHO + HO2', [2.000000e+12, 0.0, 3000.0])
reaction('C3H6O => CH2CHO + CH3', [5.000000e+16, 0.0, 73000.0])
reaction('C3H6O => C2H4 + CH2O', [1.000000e+16, 0.0, 64000.0])
reaction('C3H6 + O => C3H6O', [7.000000e+12, 0.0, 5000.0])
reaction('C2H4O2 <=> CH2OH + HCO', [1.000000e+16, 0.0, 82000.0])
reaction('C2H4O2 <=> 2 CH2O', [5.000000e+12, 0.0, 60000.0])
reaction('C2H4O2 <=> CH2CO + H2O', [1.000000e+14, 0.0, 70000.0])
reaction('C2H2O2 <=> 2 HCO', [3.000000e+16, 0.0, 71000.0])
reaction('C4H6O2 <=> 2 CH3CO', [1.000000e+16, 0.0, 72000.0])
reaction('C6H6O3 => C5H4O2 + H + HCO', [2.000000e+16, 0.0, 79000.0])
reaction('C6H6O3 <=> C5H4O2 + CH2O', [5.000000e+12, 0.0, 59000.0])
reaction('C4H3O => C3H3 + CO', [1.500000e+12, 0.0, 38000.0])
reaction('C4H3O => C2H2 + HCCO', [1.500000e+12, 0.0, 38000.0])
reaction('C4H3O => C2H + CH2CO', [1.500000e+12, 0.0, 38000.0])
reaction('C6H10O5 => C6H6O3 + 2 H2O', [1.000000e+14, 0.0, 65000.0])
reaction('C6H10O5 => C6H8O4 + H2O', [1.000000e+14, 0.0, 65000.0])
reaction('C6H8O4 => C6H6O3 + H2O', [1.000000e+14, 0.0, 65000.0])
reaction('C5H8O4 => C2H4O2 + CH2CHO + HCO', [1.700000e+16, 0.0, 82000.0])
reaction('C5H8O4 => C5H4O2 + 2 H2O', [1.000000e+14, 0.0, 65000.0])
reaction('C9H10O2 => 0.5 C10H8 + 2 CH2CHO', [3.300000e+15, 0.0, 72000.0])
reaction('C9H10O2 + H => 0.5 C2H4 + 0.5 C2H5 + C6H5OH + 0.5 CO + 0.5 HCO', [1.000000e+13, 0.0,
5000.0])
reaction('C11H12O4 + H => C2H3 + C8H10O3 + CO', [1.000000e+13, 0.0, 5000.0])
reaction('C3H3 + OH <=> C2H3CHO', [3.000000e+13, 0.0, 0.0])
reaction('C2H3CHO + OH => CH3CHO + HCO', [4.000000e+12, 0.0, 0.0])
reaction('C2H3CHO + OH => C2H4 + CO2 + H', [1.100000e+13, 0.0, 0.0])
reaction('CHCHCH3 + O2 => 0.2 C2H3CHO + 0.4 CH2O + 0.4 CH3CHO + 0.4 CH3CO + 0.4 HCO +
0.2 OH', [6.000000e+12, 0.0, 0.0])
```

```
reaction('C2H3CHO + H => C2H3 + CH2O', [3.000000e+13, 0.0, 5000.0])
reaction('C2H3CHO + H => C2H4 + HCO', [1.000000e+13, 0.0, 5000.0])
reaction('C6H5OCH3 <=> C6H5O + CH3', [1.500000e+15, 0.0, 63000.0])
falloff_reaction('C6H5O + H (+M) <=> C6H5OH (+M)',
                 kf=[4.000000e+14, 0.0, 0.0],
                 kf0=[3.000000e+20, 0.0, 0.0],
                 efficiencies='AR:0.7 C2H6:3.0 CH4:2.0 CO:1.5 CO2:2.0 H2:2.0 H2O:6.0 ',
                 falloff=Troe(A=0.2, T3=1e-30, T1=1.0000000000000002e+30, T2=1e-10))
reaction('C6H5OH <=> CO + CYC5H6', [2.500000e+13, 0.0, 72400.0])
reaction('C6H5OH + O2 => C2H2 + CH2CO + CO + H + HCO', [1.000000e+17, 0.0, 53000.0])
reaction('C6H5OH + O2 => C4H6 + CO + CO2', [2.000000e+17, 0.0, 55500.0])
reaction('C6H5OH + H <=> C6H6 + OH', [1.200000e+13, 0.0, 6000.0])
reaction('C6H5OH + OH => CO + CYC5H6 + OH', [4.000000e+12, 0.0, 0.0])
reaction('C6H5O => CO + CYC5H5', [2.000000e+11, 0.0, 43920.0])
reaction('C6H5O + H <=> CO + CYC5H6', [2.000000e+14, 0.0, 0.0])
reaction('C6H5O + O => C4H5 + 2 CO', [1.000000e+14, 0.0, 0.0])
reaction('C6H5 + O2 <=> C6H5O + O', [2.600000e+13, 0.0, 6120.0])
reaction('C6H6 + O <=> C6H5O + H', [1.500000e+13, 0.0, 4000.0])
reaction('C7H8 <=> C7H7 + H', [4.500000e+15, 0.0, 89200.0])
reaction('C7H7 + O2 => C6H5 + CH2O + O', [6.000000e+11, 0.0, 14500.0])
reaction('C7H8 + H <=> C6H6 + CH3', [1.200000e+13, 0.0, 5100.0])
reaction('C7H8 + CH3 <=> C7H7 + CH4', [4.000000e-05, 5.62, 9000.0])
reaction('C7H7 <=> C2H2 + CYC5H5', [5.000000e+13, 0.0, 70000.0])
reaction('C6H5O + CH3 => CRESOL', [3.300000e+12, 0.0, 0.0])
reaction('CRESOL + H <=> C6H5OH + CH3', [5.000000e+13, 0.0, 5000.0])
reaction('RCRESOLC <=> RCRESOLO', [1.000000e+11, 0.0, 30000.0])
reaction('HCOOH <=> CO + H2O', [9.000000e+13, 0.0, 65300.0])
reaction('C3H6O2 <=> C2H3CHO + H2O', [4.000000e+13, 0.0, 51000.0])
reaction('C3H6O2 <=> CH2O + CH3CHO', [4.000000e+13, 0.0, 54000.0])
reaction('CH2CO + OH => H2O + HCCO', [1.198000e+06, 2.0, -3529.84])
reaction('CH2CO + O => HCCO + OH', [4.060000e+06, 2.0, 1356.53])
reaction('CH4 + OH => CH3 + H2O', [2.796000e+06, 2.0, 1566.11])
reaction('C2H2 + O => C2H + OH', [2.707000e+06, 2.0, 8781.96])
reaction('C2H4 + H => C2H3 + H2', [1.925000e+07, 2.0, 10409.77])
reaction('C2H4 + O => C2H3 + OH', [1.083000e+07, 2.0, 8781.96])
reaction('C2H4 + CH3 => C2H3 + CH4', [3.122000e+05, 2.0, 11393.6])
reaction('C2H6 + OH => C2H5 + H2O', [3.595000e+06, 2.0, -238.2])
reaction('C2H6 + O => C2H5 + OH', [1.218000e+07, 2.0, 5025.57])
reaction('C3H6 + O => CH2CHCH2 + OH', [4.060000e+06, 2.0, 2579.54])
reaction('C3H6 + H => CHCHCH3 + H2', [1.053000e+07, 2.0, 10122.65])
reaction('C3H6 + OH => CHCHCH3 + H2O', [1.747000e+06, 2.0, 1484.61])
reaction('C4H4 + H => C4H3 + H2', [3.369000e+07, 2.0, 10152.16])
reaction('C4H4 + OH => C4H3 + H2O', [5.592000e+06, 2.0, 1698.84])
reaction('C4H6 + H => C4H5 + H2', [5.776000e+07, 2.0, 10398.54])
reaction('C4H6 + OH => C4H5 + H2O', [9.586000e+06, 2.0, 1675.91])
reaction('H + NC4H8 => H2 + SC4H7', [1.203000e+07, 2.0, 4202.36])
reaction('CH3 + H2O => CH4 + OH', [3.903000e+05, 2.0, 15366.11])
reaction('H2O2 + OH => H2O + HO2', [3.195000e+05, 2.0, -4169.95])
reaction('CH3OH + OH => CH3O + H2O', [1.997000e+05, 2.0, -2715.03])
reaction('CH2O + OH => H2O + HCO', [3.195000e+06, 2.0, -2065.87])
reaction('CH2O + O => HCO + OH', [1.083000e+07, 2.0, 1094.46])
reaction('CH2O + CH3 => CH4 + HCO', [3.122000e+05, 2.0, 3781.38])
reaction('CH3CHO + OH => CH3CO + H2O', [2.396000e+06, 2.0, -1734.99])
reaction('H + MCPTD => C6H6 + H + H2', [2.407000e+07, 2.0, 2663.07])
reaction('C6H6 + O => C6H5 + OH', [2.165000e+07, 2.0, 8781.96])
reaction('C2H5OH + OH => C2H4OH + H2O', [1.198000e+06, 2.0, -474.43])
reaction('C2H5OH + H => CH3CHOH + H2', [6.257000e+06, 2.0, 3950.57])
reaction('C2H5OH + OH => CH3CHOH + H2O', [1.038000e+06, 2.0, -2259.83])
reaction('C2H4O2 + H => CH2OH + CO + H2', [9.627000e+06, 2.0, 2387.18])
reaction('C2H4O2 + OH => CH2OH + CO + H2O', [1.598000e+06, 2.0, -3343.83])
```

```
reaction('C2H4O2 + CH3 => CH2OH + CH4 + CO', [1.561000e+05, 2.0, 3259.77])
reaction('C2H4O2 + H => C2H2O2 + H + H2', [2.407000e+06, 2.0, 3950.57])
reaction('C2H4O2 + OH => C2H2O2 + H + H2O', [3.994000e+05, 2.0, -2259.83])
reaction('C2H2O2 + H => CO + H2 + HCO', [1.925000e+07, 2.0, 2387.18])
reaction('C2H2O2 + OH => CO + H2O + HCO', [3.195000e+06, 2.0, -3343.83])
reaction('C2H2O2 + O => CO + HCO + OH', [1.083000e+07, 2.0, 1094.46])
reaction('C2H2O2 + CH3 => CH4 + CO + HCO', [3.122000e+05, 2.0, 3259.77])
reaction('C3H4O3 + H => C2H2O2 + CO + H + H2', [1.925000e+07, 2.0, 2387.18])
reaction('C3H4O3 + OH => C2H2O2 + CO + H + H2O', [3.195000e+06, 2.0, -3343.83])
reaction('C6H6O3 + H => C5H4O2 + CO + H + H2', [9.627000e+06, 2.0, 2387.18])
reaction('C6H6O3 + OH => C5H4O2 + CO + H + H2O', [1.598000e+06, 2.0, -3343.83])
reaction('C5H4O2 + H => C3H3 + 2 CO + H2', [9.627000e+06, 2.0, 2387.18])
reaction('C5H4O2 + OH => C3H3 + 2 CO + H2O', [1.598000e+06, 2.0, -3343.83])
reaction('C5H4O2 + H => C4H3O + CO + H2', [9.627000e+06, 2.0, 2387.18])
reaction('C5H4O2 + OH => C4H3O + CO + H2O', [1.598000e+06, 2.0, -3343.83])
reaction('C5H4O2 + O => C4H3O + CO + OH', [5.413000e+06, 2.0, 1094.46])
reaction('C6H10O5 + H => C3H4O3 + CH2CHO + CH2O + H2', [9.627000e+06, 2.0, 3950.57])
reaction('C6H10O5 + OH => C3H4O3 + CH2CHO + CH2O + H2O', [1.598000e+06, 2.0, -2259.83])
reaction('C6H10O5 + H => C6H8O4 + H2 + OH', [1.203000e+06, 2.0, 3950.57])
reaction('C6H10O5 + OH => C6H8O4 + H2O + OH', [1.997000e+05, 2.0, -2259.83])
reaction('C5H8O4 + H => C5H4O2 + H2 + H2O + OH', [4.813000e+06, 2.0, 3950.57])
reaction('C5H8O4 + OH => C5H4O2 + 2 H2O + OH', [7.988000e+05, 2.0, -2259.83])
reaction('C5H8O4 + H => C2H4O2 + CH2CHO + CO + H2', [4.813000e+06, 2.0, 3950.57])
reaction('C5H8O4 + OH => C2H4O2 + CH2CHO + CO + H2O', [7.988000e+05, 2.0, -2259.83])
reaction('C5H8O4 + H => C2H2O2 + 0.5 C2H3CHO + 0.5 CH3CHO + H2 + 0.5 HCO + 0.5 OH',
[4.813000e+06, 2.0, 3950.57])
reaction('C5H8O4 + OH => C2H2O2 + 0.5 C2H3CHO + 0.5 CH3CHO + H2O + 0.5 HCO + 0.5 OH',
[7.988000e+05, 2.0, -2259.83])
reaction('C5H8O4 + O => C2H2O2 + 0.5 C2H3CHO + 0.5 CH3CHO + 0.5 HCO + 1.5 OH',
[2.707000e+06, 2.0, 2579.54])
reaction('C9H10O2 + H => 0.5 C10H8 + CH2CHO + CH2CO + H2', [9.627000e+06, 2.0, 2387.18])
reaction('C9H10O2 + OH => 0.5 C10H8 + CH2CHO + CH2CO + H2O', [1.598000e+06, 2.0, -3343.83])
reaction('C8H10O3 + H => 0.5 AC3H4 + C2H2 + CH3O + 2 CO + H2 + 0.5 PC3H4', [1.203000e+07,
2.0, 6525.57])
reaction('C8H10O3 + H => C2H2 + 0.5 C4H4 + CH2CO + CH3O + CO + H2', [1.203000e+07, 2.0,
6525.57])
reaction('C2H3CHO + H => 0.1 C2H2 + 0.9 C2H3 + 0.9 CO + H2 + 0.1 HCO', [1.444000e+07, 2.0,
2387.18])
reaction('C2H3CHO + OH => 0.1 C2H2 + 0.9 C2H3 + 0.9 CO + H2O + 0.1 HCO', [2.396000e+06, 2.0,
-3343.83])
reaction('C6H5OH + H => C6H5O + H2', [1.203000e+07, 2.0, 6706.81])
reaction('C6H5OH + OH => C6H5O + H2O', [1.997000e+06, 2.0, 841.27])
reaction('C6H5OH + O => C6H5O + OH', [6.767000e+06, 2.0, 5025.57])
reaction('CRESOL + H => H2 + 0.75 RCRESOLC + 0.25 RCRESOLO', [1.925000e+07, 2.0, 3950.57])
reaction('CH3COOH + H => CH2CO + H2 + OH', [7.220000e+06, 2.0, 6525.57])
reaction('CH3COOH + OH => CH2CO + H2O + OH', [1.198000e+06, 2.0, -474.43])
reaction('CH3COOH + H => CH3 + CO2 + H2', [2.407000e+06, 2.0, 6525.57])
reaction('CH3COOH + OH => CH3 + CO2 + H2O', [3.994000e+05, 2.0, -474.43])
three_body_reaction('H + OH + M <=> H2O + M', [4.500000e+22, -2.0, 0.0],
                    efficiencies='CO2:1.9 H2:2.0 H2O:16.0 ')
falloff_reaction('C2H3 + H (+M) <=> C2H4 (+M)',
                 kf=[6.080000e+12, 0.27, 280.0],
                 kf0=[1.400000e+30, -3.86, 3320.0],
                 efficiencies='AR:0.7 C2H6:3.0 CH4:2.0 CO:1.5 CO2:2.0 H2:2.0 H2O:6.0 ',
                 falloff=Troe(A=0.782, T3=207.49999999999997, T1=2663.0, T2=6095.0))
reaction('CHCHCH3 <=> C2H2 + CH3', [2.000000e+13, 0.0, 38000.0])
reaction('C2H3 + CH3 <=> CH2CHCH2 + H', [5.000000e+01, 3.7, 5677.0])
falloff_reaction('CH3OH (+M) <=> CH2OH + H (+M)',
                 kf=[1.540000e+16, 0.0, 96800.0],
                 kf0=[7.200000e+46, -7.93, 107700.0])
```

```
reaction('C4H2 + OH <=> C2H2 + HCCO', [5.000000e+12, 0.0, 0.0])
reaction('CH2CO + O2 => CO + HCO + OH', [3.000000e+14, 0.0, 40000.0])
reaction('CH2OH + H => CH2O + H2', [2.000000e+13, 0.0, 0.0])
reaction('CH2CHO + H => CH3CHO', [6.000000e+13, 0.0, 0.0])
reaction('CYC5H6 + O2 => CH2CHCH2 + CO + HCO', [8.000000e+13, 0.0, 39000.0])
reaction('C8H10O3 + H => 0.5 C6H5OH + 0.5 C8H10O3 + CH3O', [1.000000e+13, 0.0, 5000.0])
reaction('CH3COOH <=> CH4 + CO2', [1.500000e+13, 0.0, 70000.0])
reaction('C2H3 + H2 => C2H4 + H', [9.496000e+05, 2.0, 8459.77])
reaction('C7H7 + H2 => C7H8 + H', [3.780000e+05, 2.0, 19839.23])
reaction('C3H8 + OH => H2O + NC3H7', [3.195000e+06, 2.0, -498.69])
reaction('CH3CHO + HO2 => CH3CO + H2O2', [3.233000e+05, 2.0, 8726.73])
reaction('C2H4O2 + O => CH2OH + CO + OH', [5.413000e+06, 2.0, 1094.46])
reaction('C2H4O2 + HO2 => CH2OH + CO + H2O2', [2.155000e+05, 2.0, 9982.61])
reaction('C6H6O3 + CH3 => C5H4O2 + CH4 + CO + H', [1.561000e+05, 2.0, 3259.77])
reaction('C5H4O2 + O => C3H3 + 2 CO + OH', [5.413000e+06, 2.0, 1094.46])
reaction('C5H4O2 + CH3 => C3H3 + CH4 + 2 CO', [1.561000e+05, 2.0, 3259.77])
reaction('C5H8O4 + O => C5H4O2 + H2O + 2 OH', [2.707000e+06, 2.0, 2579.54])
three_body_reaction('H2 + M <=> 2 H + M', [1.115000e+14, 0.0, 96081.0],
                efficiencies='AR:0.5 CO:1.9 CO2:3.8 H2:2.5 H2O:12.0 ')
reaction('C3H3 <=> C3H2 + H', [1.000000e+13, 0.0, 79000.0])
reaction('2 C2H2 <=> C4H4', [1.500000e+12, 0.0, 37400.0])
reaction('C4H4 <=> C4H2 + H2', [3.500000e+11, 0.0, 66000.0])
reaction('C2H3 + O => CH2CHO', [2.500000e+13, 0.0, 0.0])
reaction('HCO + O <=> CO2 + H', [3.000000e+13, 0.0, 0.0])
reaction('CH2OH + OH => CH2O + H2O', [1.500000e+13, 0.0, 0.0])
reaction('CH2 + CH3 <=> C2H4 + H', [4.200000e+13, 0.0, 0.0])
reaction('CH2 + H <=> CH + H2', [1.750000e+14, 0.0, -165.0])
reaction('CH2 + O <=> CO + 2 H', [7.000000e+13, 0.0, 0.0])
reaction('CH2 + CO2 <=> CH2O + CO', [1.100000e+11, 0.0, 1000.0])
reaction('CH2S + CO2 <=> CH2O + CO', [3.000000e+12, 0.0, 0.0])
reaction('CH + H <=> C + H2', [1.500000e+14, 0.0, 0.0])
reaction('CH + O2 <=> HCO + O', [3.300000e+13, 0.0, 0.0])
reaction('CH + H2O <=> CH2O + H', [5.700000e+12, 0.0, -760.0])
reaction('C2H3 + HCCO <=> CO + PC3H4', [4.000000e+13, 0.0, 0.0])
reaction('C3H2 + OH <=> C2H2 + HCO', [5.000000e+13, 0.0, 0.0])
reaction('AC3H4 + C2H2 <=> CYC5H6', [4.000000e+11, 0.0, 22000.0])
reaction('C2H2 + PC3H4 <=> CYC5H6', [5.000000e+10, 0.0, 22000.0])
reaction('C3H4O3 => C2H2O2 + H + HCO', [1.000000e+16, 0.0, 77000.0])
reaction('C2H3CHO => C2H3 + HCO', [3.000000e+16, 0.0, 90000.0])
reaction('C7H8 <=> C6H5 + CH3', [1.200000e+16, 0.0, 99800.0])
reaction('CH3COOH <=> CH2CO + H2O', [1.400000e+12, 0.0, 65000.0])
reaction('C3H4O3 + O => C2H2O2 + CO + H + OH', [1.083000e+07, 2.0, 1094.46])
reaction('C6H6O3 + O => C5H4O2 + CO + H + OH', [5.413000e+06, 2.0, 1094.46])
reaction('C6H8O4 + H => C6H6O3 + H2 + OH', [2.407000e+06, 2.0, 3950.57])
reaction('C6H8O4 + OH => C6H6O3 + H2O + OH', [3.994000e+05, 2.0, -2259.83])
reaction('AC3H4 + OH <=> C3H3 + H2O', [2.000000e+07, 2.0, 1000.0])
reaction('C6H10O5 => C3H4O3 + C3H6O2', [1.700000e+13, 0.0, 65000.0])
three_body_reaction('O + OH + M <=> HO2 + M', [1.000000e+16, 0.0, 0.0])
falloff_reaction('C2H4 (+M) <=> C2H2 + H2 (+M)',
            kf=[8.000000e+12, 0.44, 88770.0],
            kf0=[1.580000e+51, -9.3, 97800.0],
            efficiencies='AR:0.7 C2H6:3.0 CH4:2.0 CO:1.5 CO2:2.0 H2:2.0 H2O:6.0 ',
            falloff=Troe(A=0.7345, T3=180.0, T1=1035.0, T2=5417.0))
reaction('2 C2H2 <=> C4H3 + H', [2.000000e+16, 0.0, 81500.0])
reaction('C4H3 + H <=> C4H4', [1.000000e+14, 0.0, 0.0])
reaction('2 C3H3 => C2H2 + C4H4', [1.000000e+11, 0.0, 0.0])
reaction('AC3H4 <=> PC3H4', [6.026000e+53, -12.18, 84276.0])
reaction('CH3 + CH4 => C2H6 + H', [2.500000e+13, 0.0, 31000.0])
reaction('NC4H8 <=> C4H6 + H2', [5.000000e+13, 0.0, 70000.0])
reaction('AC3H4 + O2 => CH2CO + CH2O', [1.000000e+15, 0.0, 41000.0])
```

```
reaction('C2H2 + O => CH2CO', [1.000000e+13, 0.0, 15000.0])
reaction('C4H4 + O <=> C3H3 + HCO', [3.200000e+08, 1.44, 525.0])
reaction('C4H6 + O => C3H6 + CO', [1.500000e+12, 0.0, 0.0])
reaction('CH2O + OH => CO2 + H + H2', [1.000000e+11, 0.0, 0.0])
reaction('AC3H4 + OH => 0.5 C2H3 + 0.5 CH2CO + 0.5 CH2O + 0.5 CH3', [5.000000e+11, 0.0, 1000.0])
reaction('NC4H8 + OH => 0.5 C2H5 + 0.5 CH2O + 0.5 CH3CHO + 0.5 NC3H7', [1.500000e+12, 0.0,
0.0])
reaction('CH2O + HCO <=> CH3 + CO2', [5.000000e+11, 0.0, 6000.0])
reaction('C3H6 + O2 => CH2O + CH3CHO', [1.000000e+14, 0.0, 39000.0])
reaction('CH3 + O2 <=> CH3O + O', [4.000000e+12, 0.0, 27000.0])
reaction('C2H + O2 <=> CO + HCO', [2.000000e+14, 0.0, 7000.0])
reaction('C2H5 + O2 => CH2O + CH3O', [1.000000e+14, 0.0, 24000.0])
reaction('CH2CHO + O2 => CH2O + CO + OH', [6.000000e+10, 0.0, 0.0])
reaction('C2H3 + OH => CH3CHO', [5.000000e+12, 0.0, 0.0])
reaction('C2H3 + OH <=> C2H2 + H2O', [4.000000e+12, 0.0, 0.0])
reaction('CH3 + CH3O => CH2O + CH4', [1.000000e+13, 0.0, 0.0])
reaction('CH2CHO + O2 => CH2CO + HO2', [5.000000e+11, 0.0, 3000.0])
three_body_reaction('CH3 + M <=> CH2 + H + M', [1.000000e+16, 0.0, 90600.0])
reaction('CH2 + O <=> CO + H2', [5.000000e+13, 0.0, 0.0])
reaction('CH2 + OH <=> CH2O + H', [3.000000e+13, 0.0, 0.0])
reaction('CH2S + O2 <=> CO + H + OH', [3.100000e+13, 0.0, 0.0])
reaction('CH + CO2 <=> CO + HCO', [3.400000e+12, 0.0, 705.0])
reaction('C2H2 + CH2 <=> C3H3 + H', [1.200000e+13, 0.0, 6600.0])
reaction('C2H2 + CH2S <=> C3H3 + H', [6.000000e+13, 0.0, 0.0])
reaction('C2H2 + CH <=> C3H2 + H', [8.400000e+13, 0.0, 0.0])
reaction('CH2CO + CH3 <=> C2H5 + CO', [1.500000e+11, 0.0, 7600.0])
reaction('CH2CO + CH3 <=> AC3H4 + OH', [1.500000e+11, 0.0, 32300.0])
reaction('HCCO + OH <=> CO + H + HCO', [1.000000e+13, 0.0, 0.0])
reaction('C3H3 + HCCO <=> C4H4 + CO', [1.000000e+12, 0.0, 0.0])
reaction('CH2CHCH2 + HCCO <=> C4H6 + CO', [1.000000e+12, 0.0, 0.0])
reaction('CYC5H5 + O => HCCO + PC3H4', [5.000000e+12, 0.0, 0.0])
three_body_reaction('C2H5 + OH + M <=> C2H5OH + M', [1.000000e+16, 0.0, -10000.0])
falloff_reaction('C2H5OH (+M) <=> C2H4 + H2O (+M)',
                 kf=[8.000000e+13, 0.0, 67900.0],
                 kf0=[1.000000e+17, 0.0, 53918.0],
                 efficiencies='AR:0.7 CH4:2.0 CO:1.5 CO2:2.0 H2:2.0 H2O:6.0 HE:0.7 ',
                 falloff=Troe(A=0.5, T3=1e-30, T1=1.0000000000000002e+30, T2=0.0))
reaction('C2H5OH + HO2 => 0.33 C2H4OH + 0.67 CH3CHOH + H2O2', [1.000000e+13, 0.0, 16000.0])
reaction('CH2CHCH2 + OH => 0.5 C2H4 + 0.5 C3H6O + 0.5 CH2O', [3.000000e+12, 0.0, 0.0])
reaction('C2H3CHO + OH => C2H2O2 + CH3', [1.000000e+12, 0.0, 0.0])
reaction('C6H10O5 => C2H3CHO + C2H4O2 + HCO + OH', [2.500000e+16, 0.0, 85000.0])
reaction('OH + PC3H4 => C2H3CHO + H', [6.000000e+11, 0.0, 1000.0])
reaction('CH2CHCH2 + O2 => 0.2 C2H2 + 0.8 C2H3CHO + 0.2 CH2O + OH', [1.000000e+10, 0.0,
8000.0])
reaction('C6H5O + OH => C4H5 + CO + HCO', [5.000000e+12, 0.0, 0.0])
reaction('C6H5O + OH => C6H5 + HO2', [5.000000e+12, 0.0, 0.0])
reaction('C6H5O + HO2 => 2 C2H2 + CO + HCO + OH', [1.000000e+12, 0.0, 6000.0])
reaction('C6H5O + OH => CYC5H4O + H + HCO', [3.000000e+12, 0.0, 0.0])
reaction('C7H7 + HO2 => C6H5 + CH2O + OH', [5.000000e+12, 0.0, 0.0])
reaction('C7H7 + O <=> C6H5 + CH2O', [8.000000e+13, 0.0, 0.0])
reaction('C7H7 => C3H3 + C4H4', [1.000000e+14, 0.0, 83600.0])
reaction('C3H3 + C4H4 => C7H7', [2.000000e+13, 0.0, 16000.0])
reaction('H + RCRESOLO <=> CRESOL', [1.500000e+14, 0.0, 0.0])
reaction('H + RCRESOLC <=> CRESOL', [1.500000e+14, 0.0, 0.0])
reaction('RCRESOLO => C6H6 + CO + H', [2.500000e+11, 0.0, 44000.0])
reaction('RCRESOLO => 0.5 C2H4 + CO + CYC5H5', [2.500000e+11, 0.0, 44000.0])
reaction('CH3COOH => CH3 + CO + OH', [7.500000e+15, 0.0, 91600.0])
reaction('CH3COOH => CH3 + CO2 + H', [2.500000e+14, 0.0, 88000.0])
reaction('CH2CO + HO2 => H2O2 + HCCO', [1.616000e+05, 2.0, 10613.33])
reaction('C2H2 + CH3 => C2H + CH4', [7.806000e+04, 2.0, 11601.78])
```

reaction('C2H4 + HO2 => C2H3 + H2O2', [4.310000e+05, 2.0, 20242.54])
reaction('C2H6 + HO2 => C2H5 + H2O2', [4.849000e+05, 2.0, 14841.16])
reaction('C2H6 + CH3 => C2H5 + CH4', [3.513000e+05, 2.0, 7621.99])
reaction('C3H6 + CH3 => CH2CHCH2 + CH4', [1.171000e+05, 2.0, 5617.33])
reaction('C3H6 + O => CHCHCH3 + OH', [5.921000e+06, 2.0, 8519.89])
reaction('C3H6 + CH3 => CH4 + CHCHCH3', [1.708000e+05, 2.0, 11075.95])
reaction('C4H4 + O => C4H3 + OH', [1.895000e+07, 2.0, 8519.89])
reaction('C4H4 + CH3 => C4H3 + CH4', [5.464000e+05, 2.0, 11163.39])
reaction('H + NC4H8 => CH2C3H5 + H2', [7.220000e+06, 2.0, 6525.57])
reaction('NC4H8 + OH => CH2C3H5 + H2O', [1.198000e+06, 2.0, -474.43])
reaction('NC4H8 + O => CH2C3H5 + OH', [4.060000e+06, 2.0, 5025.57])
reaction('H2O + HO2 => H2O2 + OH', [5.388000e+05, 2.0, 28780.05])
reaction('C7H7 + H2O => C7H8 + OH', [2.700000e+05, 2.0, 30572.64])
reaction('CH3OH + O => CH3O + OH', [6.767000e+05, 2.0, 4151.99])
reaction('CH3 + CH3OH => CH3O + CH4', [1.952000e+04, 2.0, 5923.34])
reaction('CH3CHO + O => CH3CO + OH', [8.120000e+06, 2.0, 1094.46])
reaction('CH3 + CH3CHO => CH3CO + CH4', [2.342000e+05, 2.0, 3916.44])
reaction('CH3CHO + H => CH2CHO + H2', [7.220000e+06, 2.0, 6675.07])
reaction('CH3CHO + OH => CH2CHO + H2O', [1.198000e+06, 2.0, 610.83])
reaction('CH3CHO + O => CH2CHO + OH', [4.060000e+06, 2.0, 5025.57])
reaction('O + PC3H4 => C3H3 + OH', [8.120000e+07, 2.0, 8781.96])
reaction('MCPTD + OH => C6H6 + H + H2O', [3.994000e+06, 2.0, -3152.53])
reaction('C2H5OH + OH => 0.67 CH2O + 0.67 CH3 + 0.33 CH3CHO + 0.33 H + H2O', [3.994000e+05, 2.0, -474.43])
reaction('C2H5OH + H => C2H4OH + H2', [7.220000e+06, 2.0, 6525.57])
reaction('C2H5OH + O => C2H4OH + OH', [4.060000e+06, 2.0, 5025.57])
reaction('C2H4O2 + O => C2H2O2 + H + OH', [1.353000e+06, 2.0, 2579.54])
reaction('C2H4O2 + HO2 => C2H2O2 + H + H2O2', [5.388000e+04, 2.0, 11887.73])
reaction('C2H4O2 + CH3 => C2H2O2 + CH4 + H', [3.903000e+04, 2.0, 4871.29])
reaction('C3H4O3 + CH3 => C2H2O2 + CH4 + CO + H', [3.122000e+05, 2.0, 3259.77])
reaction('C6H6O3 + HO2 => C5H4O2 + CO + H + H2O2', [2.155000e+05, 2.0, 9982.61])
reaction('C5H4O2 + HO2 => C3H3 + 2 CO + H2O2', [2.155000e+05, 2.0, 9982.61])
reaction('C5H4O2 + HO2 => C4H3O + CO + H2O2', [2.155000e+05, 2.0, 9982.61])
reaction('C5H4O2 + CH3 => C4H3O + CH4 + CO', [1.561000e+05, 2.0, 3259.77])
reaction('C6H10O5 + O => C3H4O3 + CH2CHO + CH2O + OH', [5.413000e+06, 2.0, 2579.54])
reaction('C6H10O5 + HO2 => C3H4O3 + CH2CHO + CH2O + H2O2', [2.155000e+05, 2.0, 11887.73])
reaction('C6H10O5 + CH3 => C3H4O3 + CH2CHO + CH2O + CH4', [1.561000e+05, 2.0, 4871.29])
reaction('C5H8O4 + O => C2H4O2 + CH2CHO + CO + OH', [2.707000e+06, 2.0, 2579.54])
reaction('C5H8O4 + CH3 => C2H4O2 + CH2CHO + CH4 + CO', [7.806000e+04, 2.0, 4871.29])
reaction('C5H8O4 + CH3 => C2H2O2 + 0.5 C2H3CHO + 0.5 CH3CHO + CH4 + 0.5 HCO + 0.5 OH', [7.806000e+04, 2.0, 4871.29])
reaction('C8H10O3 + OH => C2H2 + 0.5 C4H4 + CH2CO + CH3O + CO + H2O', [1.997000e+06, 2.0, -474.43])
reaction('C2H3CHO + O => 0.1 C2H2 + 0.9 C2H3 + 0.9 CO + 0.1 HCO + OH', [8.120000e+06, 2.0, 1094.46])
reaction('C2H3CHO + HO2 => 0.1 C2H2 + 0.9 C2H3 + 0.9 CO + H2O2 + 0.1 HCO', [3.233000e+05, 2.0, 9982.61])
reaction('C3H6O + H => C2H3CHO + H + H2', [3.610000e+06, 2.0, 3950.57])
reaction('C6H5OH + CH3 => C6H5O + CH4', [1.952000e+05, 2.0, 8062.59])
reaction('C7H8 + H => C7H7 + H2', [7.220000e+06, 2.0, 4189.23])
reaction('CRESOL + OH => H2O + 0.75 RCRESOLC + 0.25 RCRESOLO', [3.195000e+06, 2.0, -2259.83])
reaction('CH3COOH + O => CH2CO + 2 OH', [4.060000e+06, 2.0, 5025.57])
reaction('CH3COOH + HO2 => CH2CO + H2O2 + OH', [1.616000e+05, 2.0, 15025.57])
reaction('CH3 + CH3COOH => CH2CO + CH4 + OH', [1.171000e+05, 2.0, 7525.57])
reaction('CH3COOH + O => CH3 + CO2 + OH', [1.353000e+06, 2.0, 5025.57])
reaction('C3H6O2 + H => C2H4OH + CO + H2', [6.739000e+06, 2.0, 2387.18])